

Engineering

107

UNIVERSITY OF HAWAII
LIBRARY

NO. HY1
FEBRUARY 1957

MAR 5 '57

JOURNAL of the

Hydraulics

Division

PROCEEDINGS OF THE



AMERICAN SOCIETY
OF CIVIL ENGINEERS

VOLUME 83

TC1
A39

BASIC REQUIREMENTS FOR MANUSCRIPTS

This Journal represents an effort by the Society to deliver information to the reader with the greatest possible speed. To this end the material herein has none of the usual editing required in more formal publications.

Original papers and discussions of current papers should be submitted to the Manager of Technical Publications, ASCE. The final date on which a discussion should reach the Society is given as a footnote with each paper. Those who are planning to submit material will expedite the review and publication procedure by complying with the following basic requirements:

1. Titles should have a length not exceeding 50 characters and spaces.
2. A 50-word summary should accompany the paper.
3. The manuscript (a ribbon copy and two copies) should be double-spaced on one side of 8½-in. by 11-in. paper. Papers that were originally prepared for oral presentation must be rewritten into the third person before being submitted.
4. The author's full name, Society membership grade, and footnote reference stating present employment should appear on the first page of the paper.
5. Mathematics are reproduced directly from the copy that is submitted. Because of this, it is necessary that capital letters be drawn, in black ink, 3/16-in. high (with all other symbols and characters in the proportions dictated by standard drafting practice) and that no line of mathematics be longer than 6½-in. Ribbon copies of typed equations may be used but they will be proportionately smaller in the printed version.
6. Tables should be typed (ribbon copies) on one side of 8½-in. by 11-in. paper within a 6½-in. by 10½-in. invisible frame. Small tables should be grouped within this frame. Specific reference and explanation should be made in the text for each table.
7. Illustrations should be drawn in black ink on one side of 8½-in. by 11-in. paper within an invisible frame that measures 6½-in. by 10½-in.; the caption should also be included within the frame. Because illustrations will be reduced to 69% of the original size, the capital letters should be 3/16-in. high. Photographs should be submitted as glossy prints in a size that is less than 6½-in. by 10½-in. Explanations and descriptions should be made within the text for each illustration.
8. Papers should average about 12,000 words in length and should be no longer than 18,000 words. As an approximation, each full page of typed text, table, or illustration is the equivalent of 300 words.

Further information concerning the preparation of technical papers is contained in the "Technical Publications Handbook" which can be obtained from the Society.

Reprints from this Journal may be made on condition that the full title of the paper, name of author, page reference (or paper number), and date of publication by the Society are given. The Society is not responsible for any statement made or opinion expressed in its publications.

This Journal is published bi-monthly by the American Society of Civil Engineers. Publication office is at 2500 South State Street, Ann Arbor, Michigan. Editorial and General Offices are at 33 West 39 Street, New York 18, New York. \$4.00 of a member's dues are applied as a subscription to this Journal. Second-class mail privileges are authorized at Ann Arbor, Michigan.

Journal of the
HYDRAULICS DIVISION
Proceedings of the American Society of Civil Engineers

HYDRAULICS DIVISION
COMMITTEE ON PUBLICATIONS
Haywood G. Dewey, Jr., Chairman; Wallace M. Lansford,
Joseph B. Tiffany

CONTENTS

February, 1957

Papers

| | Number |
|---|--------|
| Measuring Streamflow Under Ice Conditions by A. M. Moore | 1162 |
| Pipe Friction Loss at High Pressures by J. G. Slater, J. R. Villemonte, and H. J. Day | 1163 |
| Some Physical Problems Related to Flood Insurance by A. Arthur Koch | 1164 |
| Technical Problems of Flood Insurance by H. Alden Foster | 1165 |
| Frequency Analysis of Streamflow Data by David K. Todd | 1166 |
| Butterfly Valve Flow Characteristics by M. B. McPherson, H. S. Strausser, and J. C. Williams | 1167 |
| Discussion | 1177 |

Journal of the
HYDRAULICS DIVISION
Proceedings of the American Society of Civil Engineers

MEASURING STREAMFLOW UNDER ICE CONDITIONS^{a,1}

A. M. Moore,² A.M., ASCE
(Proc. Paper 1162)

ABSTRACT

Effects of ice formation on stage-discharge relation are explained briefly. Occurrence and effect of surface, frazil, and anchor ice is described and recorder graphs registering these effects are shown. One investigation of "siphon action" is detailed. Factors affecting the accuracy of ice-affected records are listed and general appraisal made of accuracy of such records.

INTRODUCTION

Engineering literature contains few references concerning the effect of ice on streamflow measurements. In 1922, J. C. Stevens presented his paper "Winter Overflow from Ice Gorging in Shallow Streams",³ and in 1931 the Society published the final report of the Committee of Power Division under the title "Ice as Affecting Power Plants",⁴ At the Western Interstate Snow Survey Conference in Seattle in 1940, Walter J. Parsons, Jr., presented a paper on "Ice in the Northern Streams of the United States".^{5,6} Those papers describe or discuss the formation of ice in streams but do not discuss how it affects the measurement of streamflow.

The water-resources investigations of the Geological Survey necessarily include measurements of streamflow throughout the United States under all

Note: Discussion open until July 1, 1957. Paper 1162 is part of the copyrighted Journal of the Hydraulics Division of the American Society of Civil Engineers, Vol. 83, No. HY 1, February, 1957.

- Presented before the Hydraulics Division of the ASCE, August 22, 1956, Madison, Wisc.
- Publication authorized by the Director, U. S. Geological Survey.
- Hydr. Engr., U. S. G.S., U. S. Dept. of the Interior, Portland, Ore.
- ASCE Transactions 85:677
- ASCE Transactions 95:1134.
- A.G.U. Transactions of 1940, 970.
- Grover, Harrington, Streamflow, pp 164-166, John Wiley, N. Y., 1943.

conditions of weather. Thus it was logical for the Survey to study the effect of ice in open channels. Water-Supply Paper 337, "The Effects of Ice on Stream Flow", by W. G. Hoyt in 1913, describes methods and techniques developed up to that time for determining stream discharge under ice conditions. Since then there has, of course, been advancement in our knowledge of behaviour of streams during periods of ice effect. This paper summarizes current practices of the Survey, several manuals prepared for use within the Survey, and personal experience.

Statement of Problem

The problem of determining streamflow under ice conditions is to achieve a procedure for determining the daily discharge even though the stage-discharge relation is ineffective owing to ice at the control section.

For those who may be unfamiliar with the principles involved it may be explained that, when ice on the stream is not a factor, most stream-flow records are derived from a simple correlation between stage and discharge at each gaging station. A water-stage recorder provides a continuous graph of stage, which is converted to discharge by means of a stage-discharge relation known as a rating curve. Such a curve is developed for each station from discharge measurements made by current meter at various rates of flow.

So far as is practicable, gaging stations are established at points where the stage-discharge relation will remain stable. The first riffle, or steepening of water-surface profile, downstream from the gaging station is known as the control section. At this point the cross-sectional area of the stream is constricted; causing a tendency for the water upstream from the control to be ponded. Therefore, the control is the determining factor in the stage-discharge relation. Boulders, gravel, or sand washing onto or from the control may cause changes in the stage-discharge relation. Ice forming on the control may cause further ponding, or backwater.

At some stations, particularly on large streams, the controlling feature is the bed and banks of the river for a considerable distance downstream from the gage. That is known as channel control. Here, too, the formation of ice can cause backwater. Ice may clog the channel, or surface ice may increase the frictional resistance to flow with a decrease in velocity that results in a compensating increase in stage. Sometimes when there is a combination of channel control and section control, surface ice can cause backwater even though ice has not formed on the section control.

Although the control may be permanent under open water conditions, ice forming at the control causes a temporary change in the stage-discharge relation usually by raising the gage height needed to pass a given quantity of water. Figure 1 compares a stage-discharge relation defined by open-water current-meter measurements with the plotting of measurements affected by backwater from ice.

Types of Ice Formation in Streams

Surface Ice

Of the three types of ice that form in streams, the most familiar and obvious is surface ice. As the name implies, it forms on the surface, either as

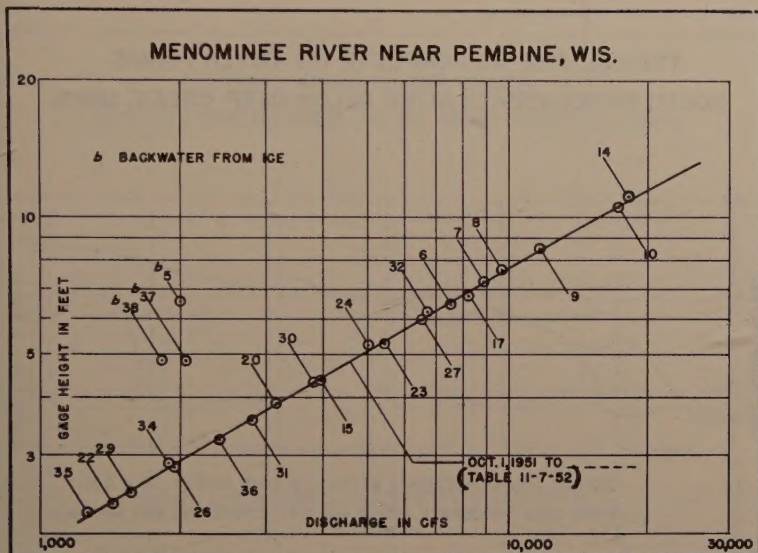


Fig. 1. Rating curve for Menominee River near Pembine, Wis.

fringe of "shore ice" or as a continuous cover spanning the stream from bank to bank. Surface ice that completely covers a small stream may be firmly anchored at either shore. Then the amount of backwater can vary greatly with stage—for example, there may be no backwater effect if the stage falls and the ice forms a bridge above the water. On large streams, surface ice usually floats so that the backwater effect is relatively constant with stage but changes as the ice thickens or thins.

Figure 2 shows the water-stage-recorder chart for a gaging station as a formation of surface ice begins to cause a backwater effect. In this example, daily mean discharge remained about the same as before the freeze-up, but undoubtedly the momentary discharge fluctuated somewhat during each day.

Surface ice can cause "siphon action" also. This effect, which is opposite that of backwater, will be covered more fully later in this paper.

Frazil Ice

"Frazil" is a French-Canadian term for finely spicular ice particles which, owing to wind or turbulence, do not unite to form surface ice and which, therefore, float downstream. Commonly the spicules or needles of ice group together into a slushy mass which moves downstream until it lodges on cold rocks or shores or freezes to the underside of surface ice, causing backwater. These floating masses also frequently interfere with the operation of a current meter.

Anchor Ice

The third type of ice formation, "anchor ice," usually is an accumulation of spongy ice on the stream bed. When this spongy ice forms at a control section it will produce characteristic "humps" or "anchor-ice rises" in the stage-height graph. Only rarely does anchor ice form as a solid ice cap on submerged rocks, and when it does the backwater effect is not large. Anchor

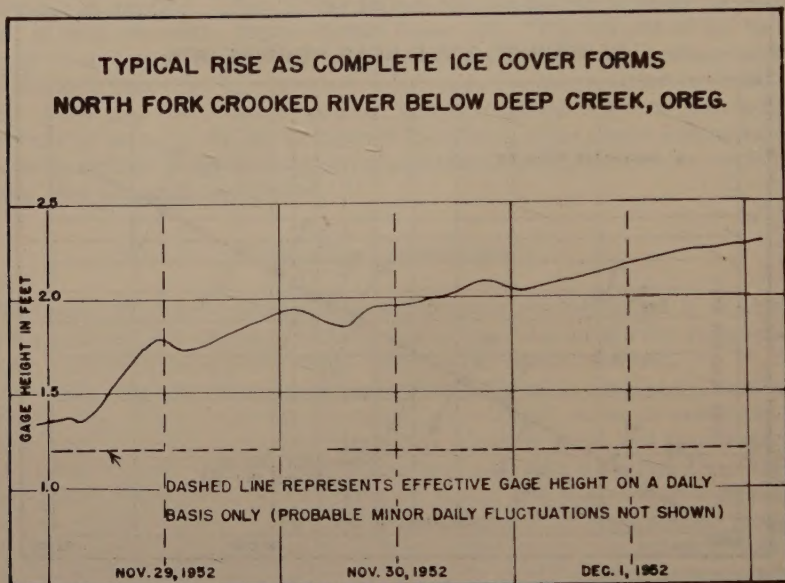


Fig. 2. Typical rise as complete ice cover forms.

ice results from loss of heat by radiation from the streambed to the atmosphere and therefore does not form when the stream is completely covered with surface ice. Generally it forms during the late evening of cold, clear nights and dissipates when the sun's rays warm the rocks the next day. The usual duration period for anchor ice is 8 to 15 hours, but if the weather is cloudy and cold the anchor ice may remain in place for a considerably longer time. Figure 3 shows a typical effect of anchor ice on a water-stage recorder record. The distinguishing feature of the "anchor-ice hump" is that the rise is slow compared to the fall, whereas an actual increase in streamflow would occur in the opposite sequence, or at least the rise would be as rapid as the fall. Therefore, simple diurnal anchor-ice rise is readily recognized and the graph can be corrected simply by "cutting out" the hump in the record.

On figure 3, the dashed line represents the estimated gage height corresponding to actual discharge. The dashed vertical lines indicate noon and the full vertical line, midnight. Note that the discharge and the effective gage height tend to diminish as the backwater increases, and then increase sharply as the anchor ice leaves the control and the detained water is released. Note, also, the small rises in the late afternoon. These probably are the result of increases in discharge from releases of anchor ice upstream combined with some melting of snow and ice during the warmer part of the day. Anchor-ice dams at successive riffles on a stream can detain a relatively large volume of water and cause sharp drops in streamflow for short periods.

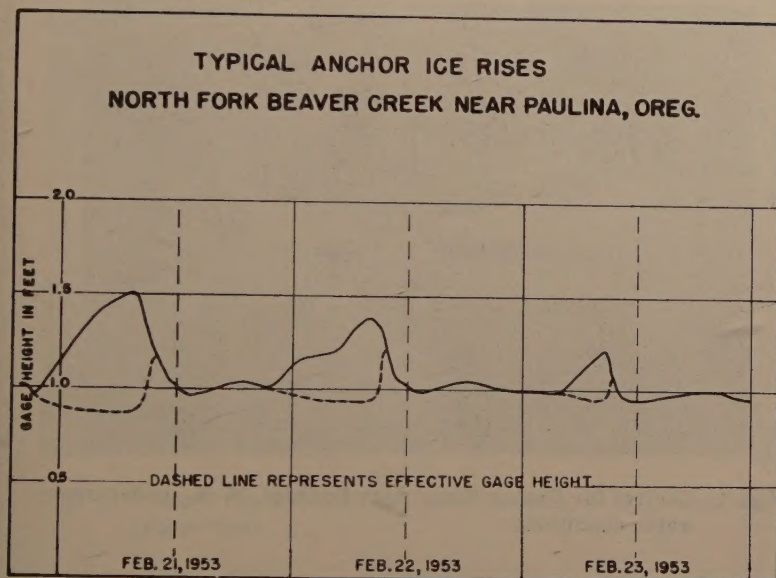


Fig. 3. Typical anchor ice rises.

Siphon Action

As has been mentioned, surface ice can cause an effect opposite to that of backwater—that is, the flow is more than would be expected for the observed gage height. This phenomenon of “siphon action” occurs infrequently, at only a few stations, and only when complete ice cover extends for some distance above and below the control section. It occurs when the hydraulic environment resembles that of a siphon spillway in that the ice cover prevents the ready entrance of air. As water siphons over the control, the stage may drop from that of an antecedent backwater condition to a level below that corresponding to discharge under an ice-free condition. Once the stage drops sufficiently so that air can enter, the siphon is broken and the stage rises until air is again prevented from entering under the ice cover and the siphon is again primed. The duration of each period of siphon action may range from about a minute to more than an hour, depending on the thickness of ice cover, amount of flow, and size of pool above the control section. Siphon action is most common on artificial controls or weirs but can occur on some natural controls.

The author and J. V. Bagley of the Boston office of the Geological Survey collaborated on a study of siphon action at Oyster River near Durham, N. H., on January 10, 1947. During that day the temperature ranged from -19°F . to 17°F . Briefly, the highlights of that study are as follows:

The control (Fig. 4) was a V-shaped concrete weir about 26 feet wide situated 30 feet downstream from the gage. Figure 5 shows this control section partly ice covered, and figure 6 shows it about as it was on the day of the

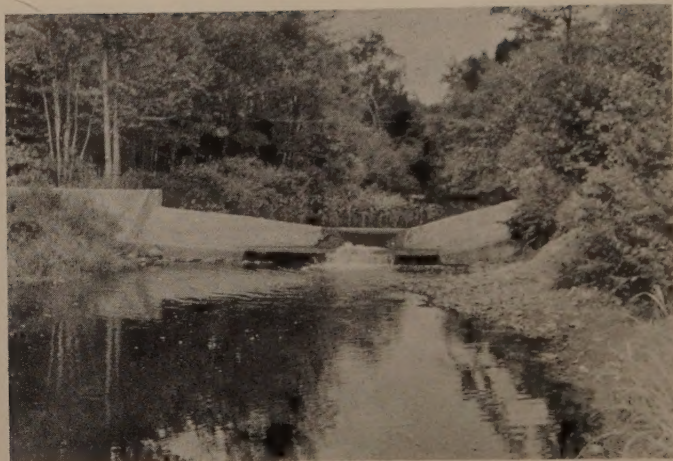


Fig. 4. Control for Oyster River near Durham, N. H., under open-water conditions.



Fig. 5. Control for Oyster River near Durham, N. H., partly frozen over.

study—that is, completely covered with ice and with siphon action occurring. Figure 7 shows the recorder graph for the study period. The slight fluctuations in the graph beginning about 11:30 a.m. on January 10 were caused by engineers clearing a measuring section about 80 feet downstream. At this time the stage was actually slightly below the point of zero flow for open-water conditions. A discharge measurement was made which showed the flow to be 7.02 cfs. The siphon was then broken by chopping a hole in the ice



Fig. 6. Control for Oyster River near Durham, N. H., completely frozen over.

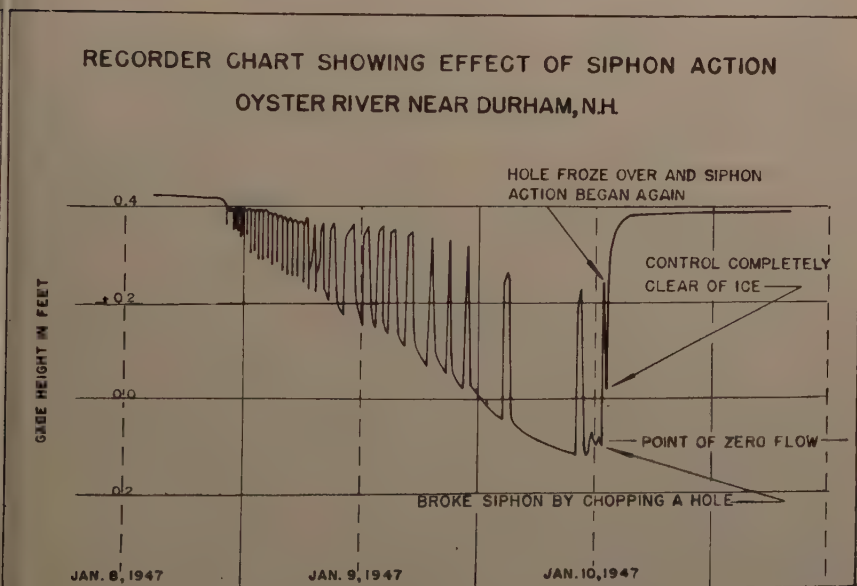


Fig. 7. Effect of siphon action.

just upstream from the weir and the stage rose to a gage height of 0.24 foot before the hole froze over. As siphon action began again the stage dropped to about 0.02 foot, at which point all ice was chopped from the control and the

stage rose and leveled off at a gage height of 0.39. The rating curve, which was well defined, showed that the discharge for that stage was 5.4 cfs. Periodically throughout these tests the velocity of the water at a fixed point in the cleared section was measured by current meter. The velocity was 0.99 fps before the siphon was broken, dropped as low as 0.30 fps after the siphon was broken, and then increased to 0.56 fps. When the hole froze over and siphon action began again the velocity jumped to 1.50 fps and then decreased to 0.83 fps just before the control was completely cleared.

From that study it was concluded that:

1. As "make and break" siphon action continues, velocity and discharge are continually changing, rising to a maximum as siphon action begins and dropping to a minimum as the siphon is broken (could be zero if the pool had been drawn below the zero-flow point).

2. A single discharge measurement is of little or no help in determining mean discharge unless it is made after the siphon is broken and flow has reached equilibrium, or is made above the gage pool.

Factors Affecting the Accuracy of Streamflow Records Under Ice Conditions

Frequency and Thoroughness of Gaging-Station Inspections

Nothing can take the place of on-the-spot determinations of actual flow and ice conditions. During open-water periods, inspections usually are made once every 4 or 5 weeks, but during the winter, inspections are made twice a month at some stations. At regulated stations, such as those below power-plants that carry a variable load, it may be necessary to make two measurements during each winter visit—one at the high stage of the regulation and another at the low stage. The backwater effects from ice may be markedly different at these two stages.

Measurements may vary widely in accuracy owing to adverse ice conditions—for example, ice floating and jamming in the stream, or even ice and water in alternating layers. Also, extremely cold temperature may cause meter trouble—for example, ice may form on the meter as it is lifted from the water to move it from one hole in the ice to another. Sometimes it is necessary to have at hand a pail of heated water in which the meter can be immersed while the engineer moves from one hole in the ice to another. Regardless of the precautions taken, some measurements are unavoidably less accurate than those made at the same site under ice-free conditions and at moderate temperature.

Accuracy of adjustments for ice effect between inspections are greatly improved if the inspecting engineer makes complete and thorough notes about ice conditions. Not only does his measurement give the flow and the amount of backwater at the time of his inspection, but his notes give dependable clues to the amount of backwater effect at lower or higher stages. Some engineers make a practice of photographing the control section and its ice cover during each inspection.

Type of Ice Formation

Surface ice can cause much uncertainty as to the discharge because its effect does not show clearly on the recorder chart. For example, it may be

evident that a backwater effect exists and even that it is increasing or decreasing, but the amount of that effect cannot be determined directly from the recorder chart. Anchor-ice rises, however, are clearly recognizable on the recorder chart, and their effect usually can be corrected directly on the chart as shown in figure 3. The shape and position of the rise just before noon is estimated on basis of similar rises at gaging stations not affected by backwater from ice. Some loss in accuracy occurs in all records affected by surface ice—particularly if siphon action occurs, but records affected by anchor ice alone are nearly as accurate as the open-water records.

Type of Gage

A water-stage recorder provides a much better winter record than a staff or wire-weight gage, because the recorder graph itself usually provides dependable clues to the discharge or at least to discharge trends. For several years the Geological Survey has operated some thermograph recorders that give a record of stream temperature, usually within 1°F. If the temperature record shows that water is more than 1° above freezing it is safe to assume that ice is not forming, although ice that had formed previously could still be causing backwater. The water-temperature record is especially useful in fixing the time that ice begins to form.

Comparison with Records for other Gaging Stations

When surface ice is present the chief basis for determining the probable discharge between discharge measurements is usually a study of runoff by comparison with records of other nearby streams. Even though the record used for comparison may be ice-affected also, it affords a different and independent set of base data—another recorder chart and a different set of current-meter measurements. Without a nearby record that compares well with the record in question, the accuracy of the computed discharge may be greatly reduced. Fortunately the network of stations is sufficiently extensive that ordinarily more than one record can be used. However, this is not always true, especially in the more sparsely settled areas. For example, in southeastern Oregon, stations are quite widely scattered and, owing to diverse hydrologic environment, the records do not compare well with one another.

Comparisons always should be used with caution, as the relationship between the flow of two streams may vary considerably during the year. Figure 8 shows the usual method of plotting discharge records with the time scale horizontal and with the discharge scale vertical and logarithmic. The solid line represents the apparent discharge obtained by applying the recorded gage height to the stage-discharge relation curve and the cross on January 26 represents the apparent discharge at the time of the measurement. The dashed line represents discharge after the effect of backwater was removed. Full basis for the adjusted graph is not shown here. Figure 9 shows the temperature graph and independent discharge record that also formed part of the basis for the adjusted record.

Useful comparison does not require that the shapes of the hydrographs be exactly alike as long as the trends are similar. On figure 9, note that the two streamflow records and the concurrent weather record respond to the effect of temperature during the winter period. The record for John Day River at Service Creek, Oreg., is unaffected by backwater from ice, and for simplicity, the adjusted record only is shown for North Fork John Day River. In actual

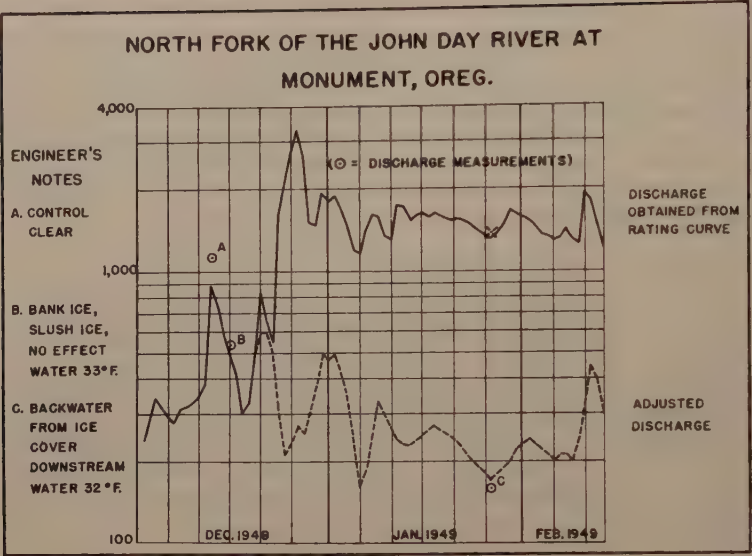


Fig. 8. Adjustment for backwater from ice.

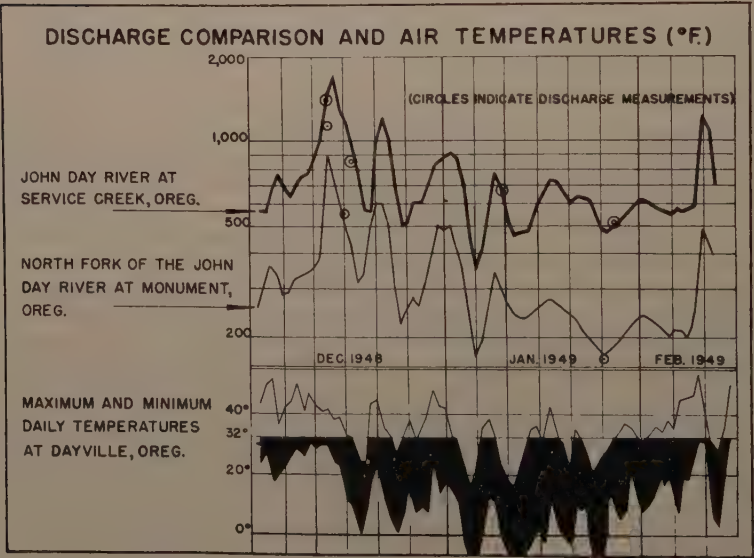


Fig. 9. Comparison of daily discharge.

practice all records are usually plotted on separate hydrographs, and, to make a comparison, one is placed over the other on a light table. At times a

streamflow record can be compared effectively with a powerplant record expressed in units of either discharge or power output. As a rule, powerplant operators maintain fairly accurate records, but even those records that may not be completely accurate quantitatively are useful in showing trends.

Comparison with Weather Records

Good records of air temperature and precipitation are an invaluable aid in making adjustments for ice effect. The temperature record helps the engineer to decide whether ice is forming, increasing, or dissipating, and whether precipitation is rain or snow.

For stations which do not have a nearby discharge record for comparison, and for which the recorder chart does not provide a dependable clue, it may be necessary to adjust for ice effect almost solely on the basis of weather records and a few measurements of discharge. Discharge usually follows remarkably well the "ups and downs" of the aid-temperature record, and occasional discharge measurements help fix the estimated rises and drops within reasonable limits.

Comparison with Ground-Water Records

During the winter, when much of the precipitation occurs as snow, a major part of streamflow is derived from ground water. A record of fluctuations in ground-water level for such an area can be very useful in estimating discharge.

Thoroughness and Skill of Office Engineer

Computation of discharge from a gage-height record affected by backwater from ice is a painstaking job that involves much detail. The experienced engineer overlooks nothing and makes the adjustments on a day-by-day basis, giving consideration to recorder charts, to all pertinent discharge measurements, to engineers' field notes and photographs, and to records of nearby streams, ground-water levels, and weather.

Accuracy of Ice-Affected Records

Accuracy Statements in Water-Supply Papers

When only diurnal anchor ice is present, the accuracy of streamflow records generally is not affected. When surface ice is present for many days the records of streamflow for those days must be rated lower in accuracy, but usually not more than 10 percent below the accuracy of the open-water records for the same station and commonly by no more than 5 percent. If the "Remarks" paragraph of the station description in a water-supply paper states "Records excellent except those for periods of ice effect which are good," the accuracy of daily discharge is considered to be, in general, within 5 percent of open-water conditions and within 10 percent for icing conditions. A qualification of "fair" indicates accuracy within 15 percent, and "poor" indicates that the errors could be more than 15 percent. A qualification of "poor" may be necessary for ice periods if the only clues to the discharge are weather records and a few measurements spaced a month or more apart. With our present knowledge concerning ice formation, and with our present

methods for adjusting records, it seems doubtful that any ice-affected record should be more than 25 percent in error. Most such records should be less than 15 percent in error, or "fair."

Present-Day Records Versus Older Records

Some surprisingly good adjustments for ice effect were made in early years but, in general, these older adjustments are less reliable than those made in recent years, as most early records were based on gage heights from nonrecording gages. The most significant advance in knowledge of stream behavior under ice conditions that has occurred since Water-Supply Paper 337 was written is a result of the development and more general use of the water-stage recorder. Also, in the early days of stream gaging, engineers did not have the time to make the detailed examinations which are commonplace today. At the present time, streamflow records the Nation over are being reviewed and compiled in summary form—specifically, all records through 1950 are being carefully scrutinized and, if necessary, revised. This should do much toward correcting any large errors in adjustments for ice effect during early years.

Journal of the
HYDRAULICS DIVISION
Proceedings of the American Society of Civil Engineers

PIPE FRICTION LOSS AT HIGH PRESSURES

J. G. Slater,¹ J. R. Villemonte,² A.M. ASCE, and H. J. Day³
(Proc. Paper 1163)

SYNOPSIS

This paper presents the results of an investigation conducted at the Hydraulics Laboratory of the University of Wisconsin on the energy loss in oil flow in straight, smooth pipes at line pressures up to 2000 psi and temperatures up to 120° F. A total of 1200 tests were completed using Klondyke light - medium hydraulic oil and fuel oil No. 2 in four seamless steel pipes, 1/4, 1/2, 1 and 2 inches in diameter. The flow was varied to produce a change in Reynolds Number of 146 to 135,000 for a range of atmospheric viscosities of 0.00003 to 0.0019 sl per ft sec. The viscosities were measured independently by two methods: (a) Stoke's Law falling--sphere, and (b) Hagen-Poiseuille laminar flow pipe. Both viscometers were operated at the pressure and temperature ranges of the tests.

There was a small consistent increase in the energy loss due to pipe friction at 2000 psi over that at atmospheric pressure. In the absence of significant experimental errors, it is concluded that the performance characteristics of the Stoke's Law and Hagen-Poiseuille Law viscometers are not identical because of the different operating conditions of boundary, velocity distribution, character of distortion rate, and body and surface forces. It is recommended, therefore, that the viscometers be matched with the flow problem, insofar as the operating conditions are concerned, and particularly so when the pressures exceed 3000 psi.

The standard pipe friction theory is valid for wide ranges in pressure and temperature, provided the appropriate effects of pressure and temperature on the fluid properties are known. For all practical purposes, the Gunaji-Villemonte viscosity correlation constants can be combined with the Hagen-Poiseuille and Blasius formulas for petroleum oil flows at Reynolds Numbers less than 150,000.

Note: Discussion open until July 1, 1957. Paper 1163 is part of the copyrighted Journal of the Hydraulics Division of the American Society of Civil Engineers, Vol. 83, No. HY 1, February, 1957.

1. Chief Engr., W. C. Heath Associates, Inc., Milwaukee, Wis.
2. Associate Prof. of Civ. Eng., Univ. of Wisconsin, Madison, Wis.
3. Senior Project Engr., Scott Paper Co., Glen Falls, N. Y.

INTRODUCTION

Modern hydraulic control circuits and servo-mechanisms use medium viscosity oils in seamless tubing under line pressures varying from a few hundred to several thousand lbs. per sq. inch. In design work it is customary to calculate the head loss due to pipe friction by solution of the Darcy-Weisbach equation

$$h_f = f \frac{L}{D} \frac{V^2}{2g} \quad (1)$$

where f is a dimensionless friction factor dependent on the Reynolds Number

$$R = \frac{DV}{\nu} \quad (2)$$

and the relative roughness, k/D , in turbulent flow. In oil hydraulics it is not unusual for the flow regimen to be laminar, in which case the head loss is defined by the Hagen-Poiseuille Law

$$h_f = \frac{32 \nu L V}{g D^2} \quad (3)$$

which can be rearranged in the form of equation 1 to give the relationship

$$f = \frac{64}{R} \quad (4)$$

In turbulent flow, as long as the pipe wall protuberances do not disturb the normal relationship between the thickness of the laminar sublayer and R , the relationship between f and R will follow that for the so-called "smooth" pipe. Most oil-hydraulics circuits are operated at $R < 150,000$, and use seamless pipes whose absolute roughnesses are substantially less than the thickness of the laminar sublayer. In general, therefore, these are smooth pipes which have friction factors independent of the relative roughness.

For turbulent flow in smooth pipes, with $R < 150,000$, the Blasius formula

$$f = 0.3164 R^{-0.25} \quad (5)$$

is quite satisfactory for low pressure flows; and for $R > 150,000$ the Karman-Prandtl formula

$$\frac{1}{\sqrt{f}} = 2 \text{ LOG } (R \sqrt{f}) - 0.8 \quad (6)$$

can be used with more confidence than ease. The Blasius formula for head loss can be obtained by solving equations 1 and 5 simultaneously to give

$$h_f = \frac{0.1582 L \nu^{0.25} V^{1.75}}{g D^{1.25}} \quad (7)$$

The hypotheses and assumptions from which these equations have been developed might be considered as the present-day standard pipe friction theory. The theory presupposes that f is a function only of R and can be evaluated for the given conditions of velocity, diameter, pressure and temperature only if the effects of pressure and temperature on the fluid properties are known. The designer of oil-hydraulics systems is confronted, therefore, with two real questions:

- (1) Does the standard pipe friction theory apply to present-day high pressures and temperatures?
- (2) What are the effects of pressure and temperature on the properties of the fluid in question?

In regard to Question 1, a search of the literature reveals that there is little or no experimental work on friction losses in pipes at high pressures that would serve to confirm the validity of the theory, except that some inconclusive tests have been made with gases at pressures up to 4,400 psi^{4,5,6}. A philosophical answer to this question, however, would be that it is logical and reasonable to expect it to be applicable, but there seems to be no prima-facie evidence one way or the other.

In regard to Question 2, a general correlation of the effects of pressure and temperature on the properties of gases is well enough defined for most engineering problems, but such a correlation for liquids is not available.

In 1947 an investigation was initiated at the Hydraulics Laboratory of the University of Wisconsin to study the answers to the above questions. The project was necessarily divided into two parts, (a) the study of the pressure-density-viscosity-temperature relations of five petroleum oils, and (b) the study of energy loss in oil flow in straight, smooth pipes at high line pressure and a modest range in temperature. V. N. Gunaji and J. R. Villemonte⁷ have completed Part (a) of the project and reported their findings, a summary of which is presented in the Appendix.

This paper describes the work and findings in connection with Part (b) of the project, which was started in 1948 and completed in 1952.

Nomenclature

The following letter symbols are adopted for use in this paper and have dimensions expressed by any compatible system of units.

A_0 = area of pipe orifice.

C = coefficient of discharge for pipe orifice.

4. Wildhagen, M., "Über den Stromungswiderstand hochverdichteter Luft in Rohrleitungen", Zeitschrift fuer Angewandte Mathematik and Mechanik, vol. 3, 1923, page 181.

5. Newitt, D.M., and Sirkar, S.K., "The Flow of Gases at High Pressures through Metal Pipes", Transactions, Institution of Chemical Engineers (London, England), vol. 9, 1931, pages 63-73.

6. Moulton, R. W., and Beuschlein, W.L., "A Study of the Flow of Air in Tubes in the Pressure Range of 1 to 300 Atmospheres", Transactions, American Institute of Chemical Engineers, vol. 36, 1940, pages 113-133.

7. Gunaji, V. N., and Villemonte, J. R., "Effect of Pressure and Temperature on the Viscosity of Petroleum Oils", Proceedings of the Third Midwestern Conference on Fluid Mechanics, 1953, pages 719-740.

- D = diameter of pipe.
 D_o = diameter of pipe orifice.
 f = pipe friction factor (Darcy-Weisbach).
 g = gravitational acceleration.
 h = pressure head differential for pipe orifice.
 h_f = head loss due to pipe friction.
 k = pipewall roughness: average height of protuberance.
 L = length of pipe.
 Q = volumetric discharge rate.
 R = Reynolds Number of orifice.
 V = mean velocity in pipe.
 ν = kinematic viscosity.

Experimental Apparatus

The test pipes were made from seamless high carbon steel tubing, ASTM Spec. A 106-48T, the dimensions of which are shown in the following table.

| Nom Dia | Sche- dule | Actual Inside Dia. | Test L | Test $\frac{L}{D}$ | Entr $\frac{L}{D}$ | Exit $\frac{L}{D}$ | Test $\frac{D}{K}$ |
|------------|---------------|--------------------------|-----------|-----------------------|-----------------------|-----------------------|-----------------------|
| In. | | In. | Ft. | | | | |
| 1/4 | 80 | 0.2988 | 3.00 | 120 | 120 | 30 | 6000 |
| 1/2 | 40 | 0.6187 | 7.00 | 136 | 116 | 29 | 5600 |
| 1 | 40 | 1.049 | 11.00 | 126 | 103 | 17 | 17500 |
| 2 | 80 | 1.952 | 19.99 | 123 | 117 | 9 | 13000 |

The average height of pipewall protuberance, k , was measured by longitudinal profilometer readings on sections of the same material that was used to make the test pipes. The flanges at either end of the test section were welded so that the flange faces were flush with the pipe ends and the pipes concentrically oriented. Four radial piezometer holes of 1/8 inch diameter were drilled in the flange immediately preceding the joint at either end of the test section. These openings (8 for the 2-inch test pipe) admitted static pressures to a common collector ring for pressure measurement.

A schematic diagram of the test circuit is shown in Fig. 1. The main loop was fabricated from 2-inch schedule 80 seamless steel tubing. Flow rates up to 100 gpm were circulated by a Northern Ordnance Company herringbone gear pump driven by a 10-HP variable speed motor. The bypass provided an additional means for controlling the discharge rate. Pressure in the line was initially created by a Denison hydraulic test stand and measured by a 0-3000 psi Bourdon gage. The stand was then disconnected because the Gree hydro-pneumatic accumulators were able to compensate for the small leakage. Fluid temperatures were observed using nickel wire resistance-bridge thermometers immersed in the fluid. The discharge rate was measured by a flange-tapped pipe orifice connected to a Statham resistance-bridge strain

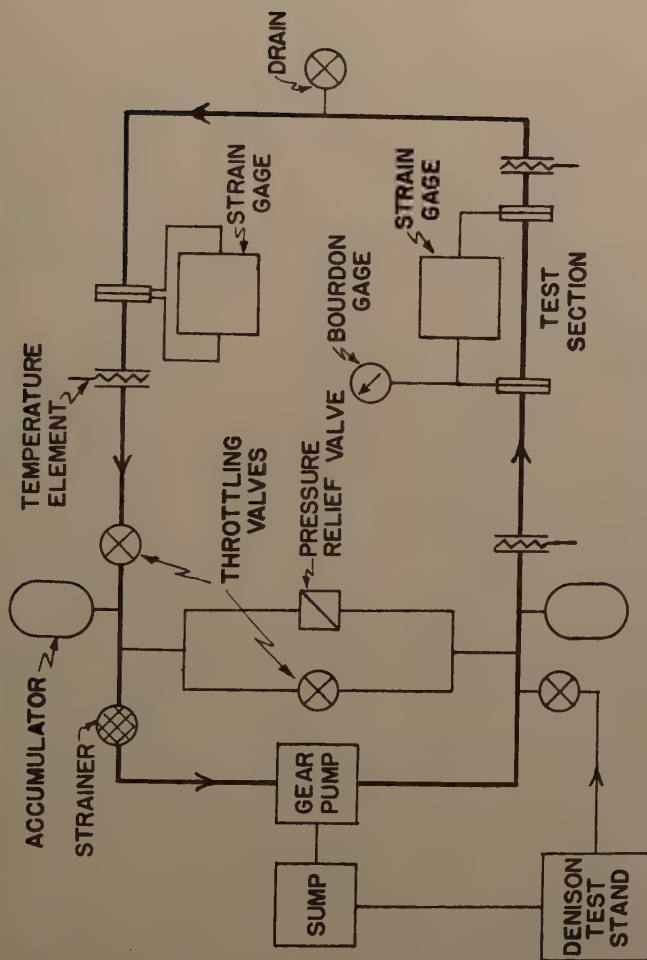


FIG. 1 - TEST CIRCUIT SCHEMATIC DIAGRAM

gage with a range of 0-40 psi. Similar gages with ranges of 0-5 and 0-100 psi were used to observe the pressure drop due to pipe friction in the test section. The resistance-bridge temperature and pressure apparatus was operated with d.c. voltages in conjunction with high-sensitivity microammeters for measuring the out-of-balance.

Laboratory Techniques

Figures 2 and 3 show the effect of temperature and pressure on the properties of the two test fluids, Klondyke light-medium hydraulic oil and No. 2 fuel oil. This information was taken from a study reported by V. N. Gunaji and J. R. Villemonte⁸, a brief summary of which is in the Appendix. The specific gravity of the oil at atmospheric pressure was measured by means of standard pycnometers. The effect of pressure was computed from the formula of Dow and Fink⁹, equation 10. Gunaji obtained the molecular viscosity of each oil by applying Stoke's Law to the motion of a falling sphere in a pressure cell and accounted for the shape and boundary factors through comparison of his atmospheric data with calibrated Cannon-Fenske-Ostwald viscosity pipettes.

The electric strain gages were calibrated at frequent intervals by dead-weight methods under atmospheric line pressure. A water column was used for the 0-5 psi gage and the others were loaded by a standard dead-weight gage tester. The latter calibrations were checked and verified dynamically by installing the gages in the circulating system in parallel with oil-mercury differential manometers for tests at low line pressures. Tests conducted by the Statham Laboratories have indicated that the gage calibrations are independent of the line pressure.

The four orifice openings were sized so that the differential strain gage connected to the pipe orifice had an output always in excess of 10 microamperes on the 0-100 microammeter. The orifices were calibrated in place by rearranging the circulating system slightly for discharge into a weighing tank. Tests were run with Klondyke light medium hydraulic oil and the coefficient of discharge was calculated from the orifice equation

$$Q = CA_o \sqrt{2gh} \quad (8)$$

and plotted as a function of Reynolds Number, defined as

$$R_o = \frac{D_o \sqrt{2gh}}{\nu} \quad (9)$$

The resistance thermometers were calibrated by immersion in a controlled temperature oil bath for comparison at temperatures of 54° to 120° F with a calibrated, precise, mercury thermometer reading to 0.1° F.

The accumulators were precharged prior to a test series for a given line pressure. The test stand was used to maintain a line pressure of approxi-

8. Ibid.

9. Dow, R. B., and Fink, C. E., "Computation of Some Physical Properties Lubricating Oils at High Pressure", I-Density, Journal of Applied Physics vol. 2, 1940, pages 353-357.

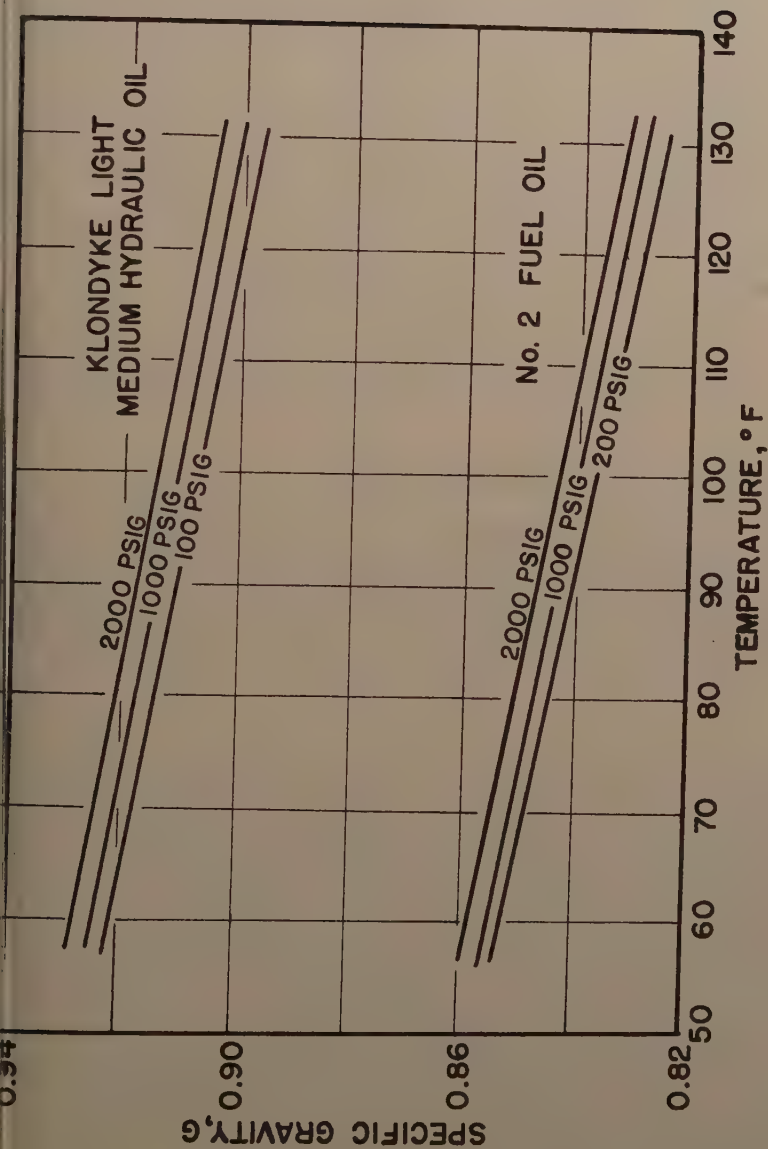


FIGURE 2. SPECIFIC GRAVITY

mately 200 psi during the initial bleeding to clear the lines and gages of air, first statically, and then with the circulating pump in operation. After building up a pressure in excess of that desired for the test series, the test stand was disconnected, and bleeding continued until the line pressure decreased to that desired for the test. The strain gages were then balanced by stopping the oil flow and adjusting the zeroizing circuit if necessary. This was repeated after each set of three runs, and the entire system was bled after every six runs. The line pressure was recorded prior to each test. Approximately 40 seconds elapsed during the observation of the data which consisted of the three simultaneous sets:

1. head loss in test section, oil temperature downstream.
2. head loss in test section, oil temperature upstream.
3. pressure drop in orifice, oil temperature downstream.

At the end of each testing period, an oil specimen was drawn from the circuit and its viscosity checked. This verified the constancy of the test fluid composition.

Scope of the Tests

A total of 1200 test runs was completed using two petroleum oils (Klondyke light-medium and fuel oil No. 2) in four pipes, 1/4, 1/2, 1 and 2 inches in diameter. The Reynolds Number, R , ranged from 146 to 135,000 in each of three pressure series of 150, 1000 and 2000 psi, for an atmospheric viscosity range of 0.00003 to 0.0019 sl per ft sec. The temperature range of the tests was about 50° to 120° F.

Results

The test data were analyzed by substitution of the observations in equations 1 and 2 in order to obtain simultaneous values of f and R . It was not necessary to correct for expansion of the pipe due to pressure because analytical studies gave a diameter increase of only 0.03 per cent under the worst combination of conditions. The pipe orifice calibrations were substantiated by the consistency of data in regions where there was an overlap of results from two different sized orifice openings. In general, there was good agreement among the pipe friction tests on all sizes of pipe at all pressures for both oils.

Figure 4 shows the variation of f with R on log-log paper for the data on all test pipes with both fluids at all pressures. The reference line in the laminar region is equation 4; in the turbulent region, the Blasius formula, equation 5. Figure 5 shows the above information for the 100-200 psi line pressure only, Figure 6 for 1000 psi, and Figure 7 for 2000 psi. It may be seen that the data are quite consistent for the Klondyke light-medium oil. There is, however, a greater scattering of the tests made with No. 2 fuel oil because for these tests simplified test procedures were used to expedite the work. A detailed study of the more consistent Klondyke data follows.

To facilitate comparison, straight lines were fitted to the log-log data by the method of averages. Figure 8 shows the ratio of the empirical equations for 100-200 psi data to those of Hagen-Poiseuille and Blasius. Figure 9 gives

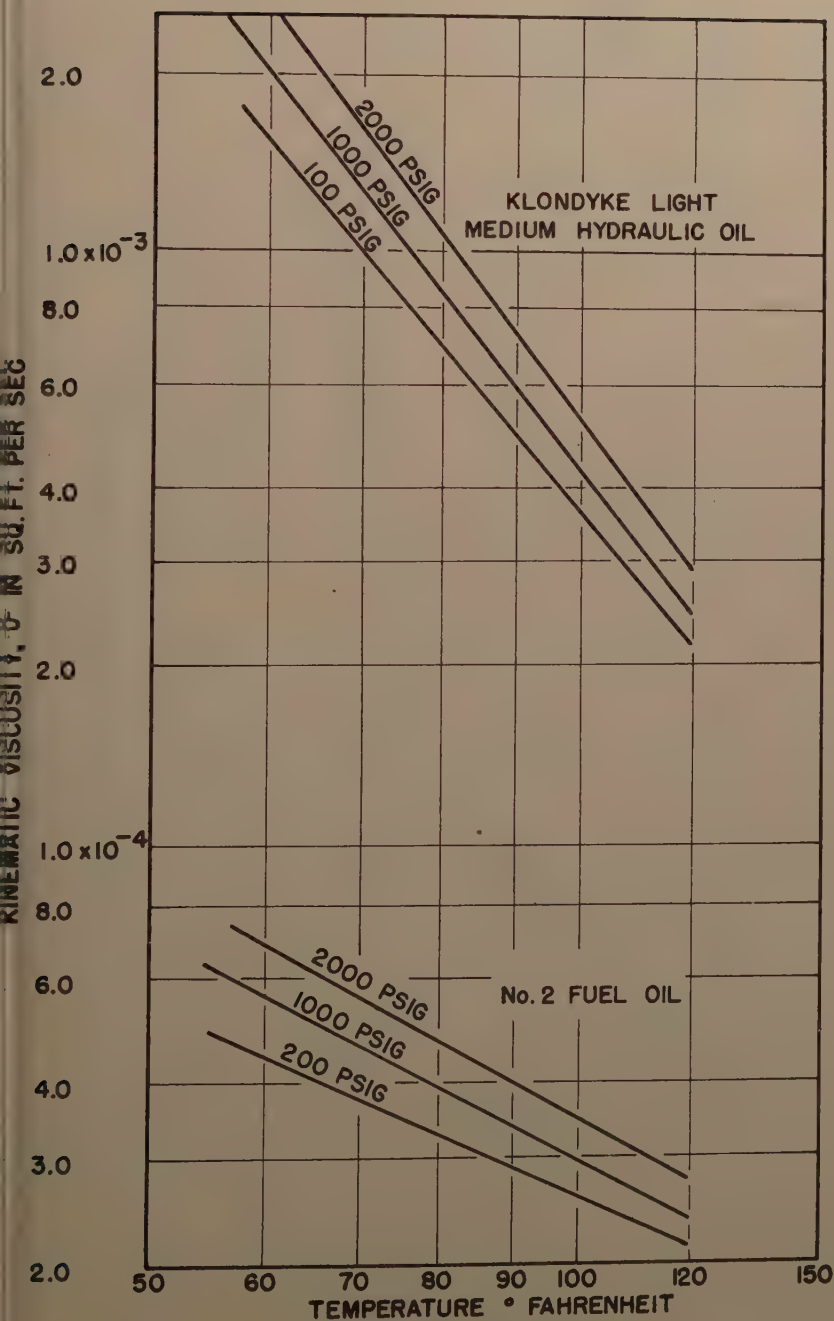


FIGURE 3. VISCOSITY

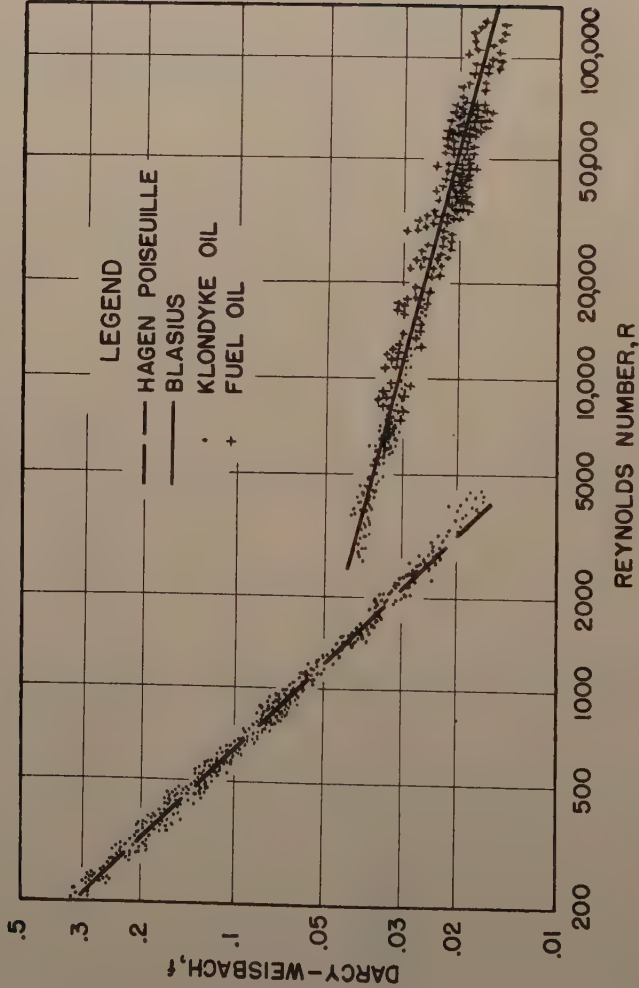


FIGURE 4. ALL PIPES AND PRESSURES

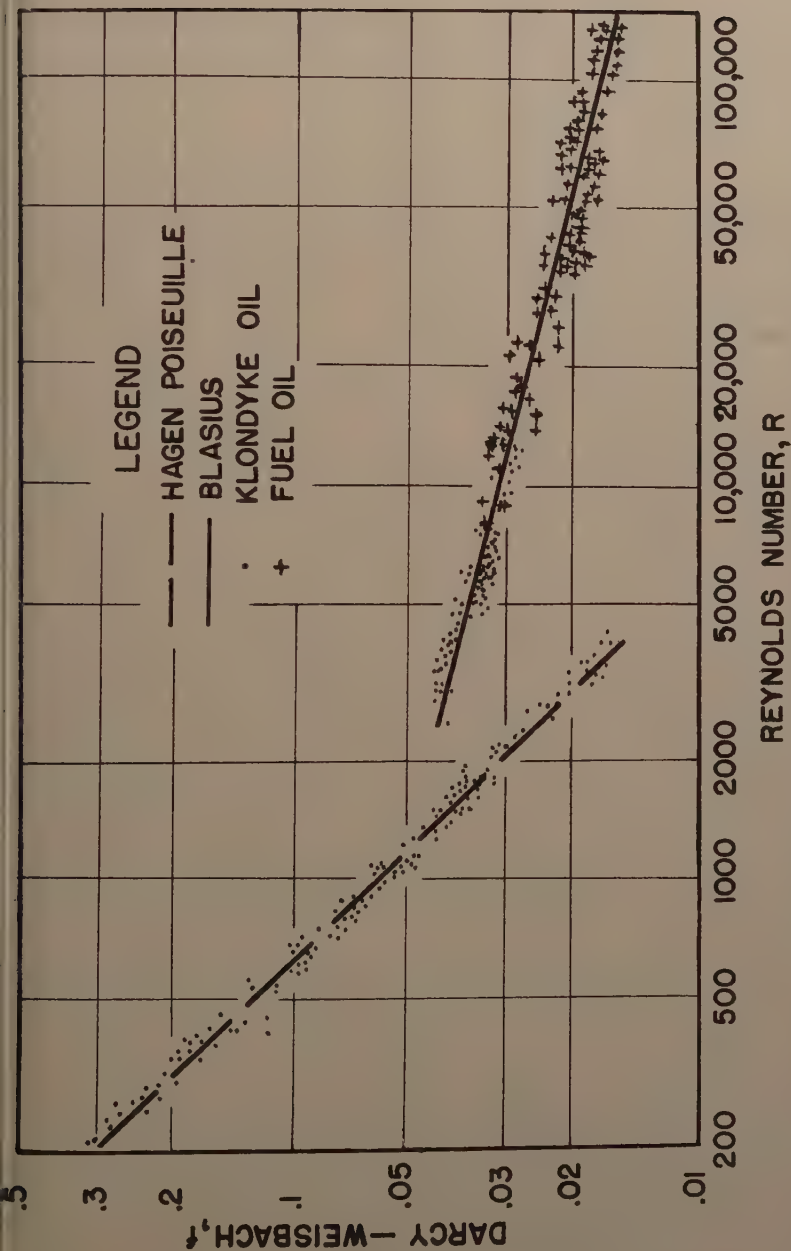


FIGURE 5. ALL PIPES — 100-200 Psi

the ratio of the 1000 and 2000 psi data to the 100-200 psi data. On the basis of the latter comparison, it is found that the 1000 psi lines check the low pressure data within the limits of accuracy for the tests. On the average, the empirical equation for laminar flow at 2000 psi is 4.6 per cent higher than the 100-200 psi data, and for turbulent flow the value of f is 1.8 per cent higher.

The above deviations must be due either to a combination of experimental errors or the inability of present-day pipe friction theory to account for all aspects of the mechanism of fluid resistance. In studying the experimental errors, the basic measurements of discharge rate, pressure difference, temperature, density, and viscosity which were observed at low pressures must be compared with those at high pressures. Errors in mass density are eliminated immediately because the total density change, by itself, is less than one per cent. Errors in the measurement of pressure differential across the orifice and in the test sections are negligible because the manufacturer conducted a most extensive series of pressure tests on their strain gages and found the pressure effect to be insignificant. The orifice was calibrated at low pressures and the results used for high pressures as well because the coefficient of discharge is a function largely of contraction rather than energy loss phenomena. A substantial change in the orifice energy loss, therefore, would produce a very small change in the discharge coefficient. The operation of the resistance-bridge thermometers is not affected by changes in pressure.

The Newtonian viscosities used in this work were measured by Gunaji¹⁰ using a new type high pressure Stoke's Law falling-sphere viscometer. It was calibrated at atmospheric pressure by comparison of its performance with those of precision Cannon-Fenske-Ostwald pipettes. The calibration should be unaffected by pressure changes within the cell, provided appropriate corrections are applied to the sphere size and elastic and density properties of the sphere and oil. Such corrections were made with great care and are believed to be accurate. The tests show, however, that the Newtonian viscosities measured by the Gunaji viscometer at 2000 psi are uniformly 4.6 per cent lower than corresponding ones computed from the laminar flow pipe friction data using the Hagen-Poiseuille Law, provided the other errors are assumed to be negligible. This is deduced from the fact that f and ν have a direct linear relation in laminar flow. It is interesting to note that a 4.6 per cent change in viscosity in turbulent flow would produce a 1.2 per cent change in f , since f and ν are related according to the Blasius formula. This shift in f compares quite favorably with the observed change of 1.8 per cent mentioned previously.

These deviations, therefore, seem to be caused by the different performance characteristics of the two types of viscometers. The assumption that they might give slightly different results seems valid since (a) the boundary structures are essentially inverted, (b) the resulting different velocity distributions would necessarily produce changes in the character of the rates of distortion, and (c) the external body force in the Gunaji viscometer is a constant, whereas in the Hagen-Poiseuille viscometer it is variable.

Within the pressure and viscosity limits of these tests, the problem under discussion is probably more academic than practical, because the deviations

10. Gunaji and Villemonte, "Effect of Pressure and Temperature on the Viscosity of Petroleum Oils".

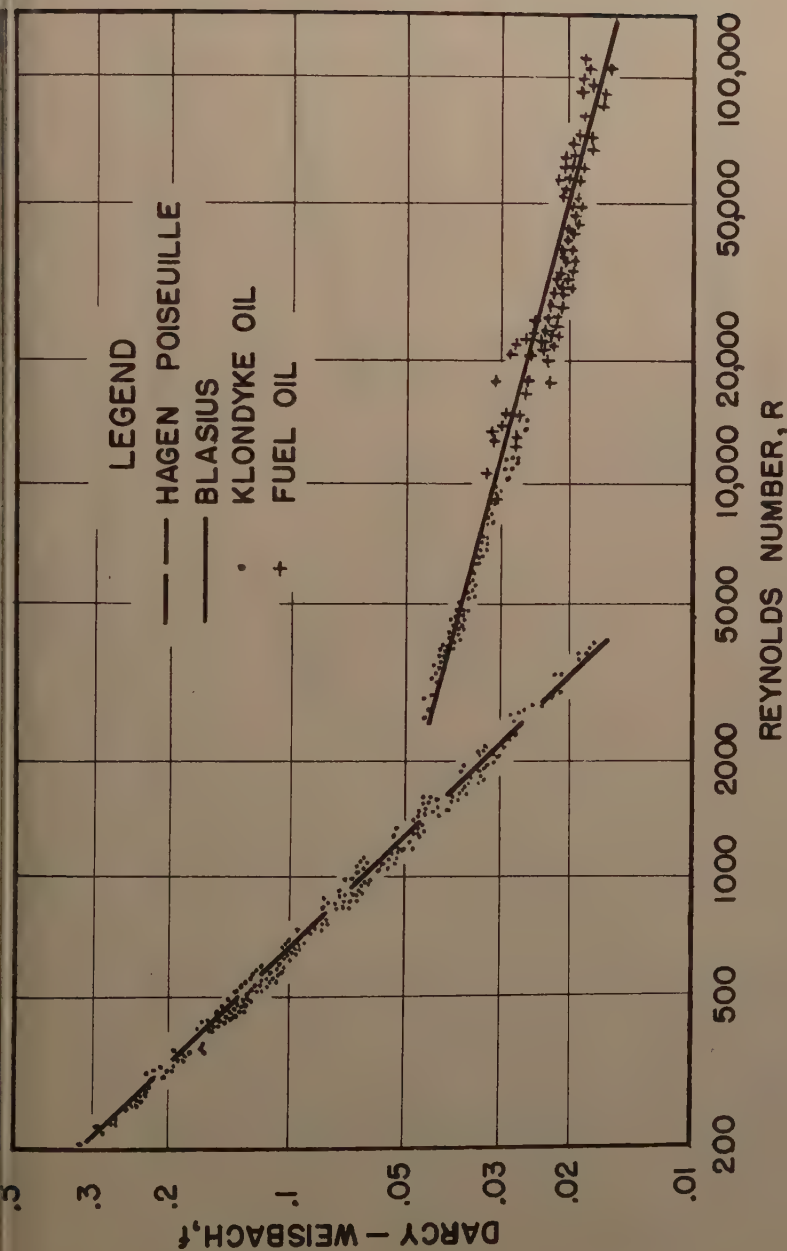


FIGURE 6. ALL PIPES — 1000 Psi

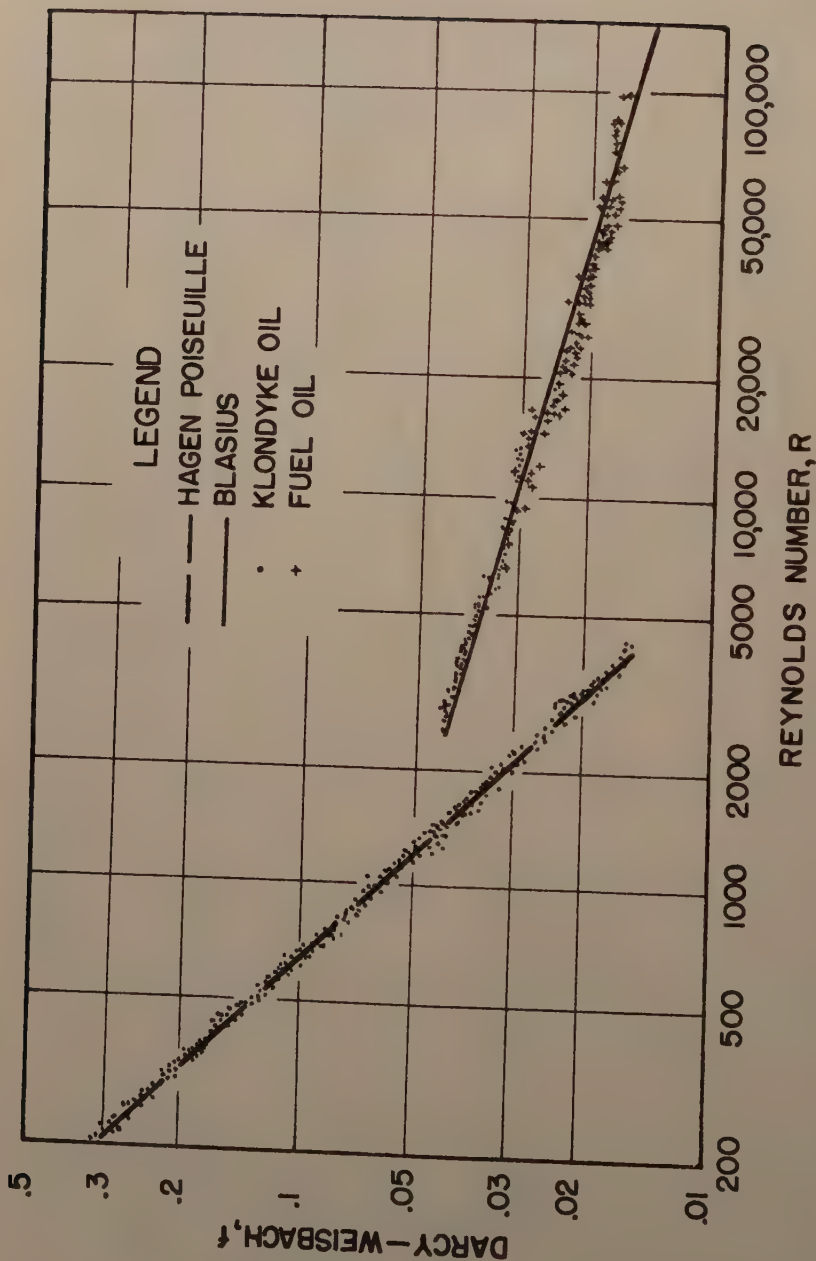


FIGURE 7. ALL PIPES - 2000 Psi

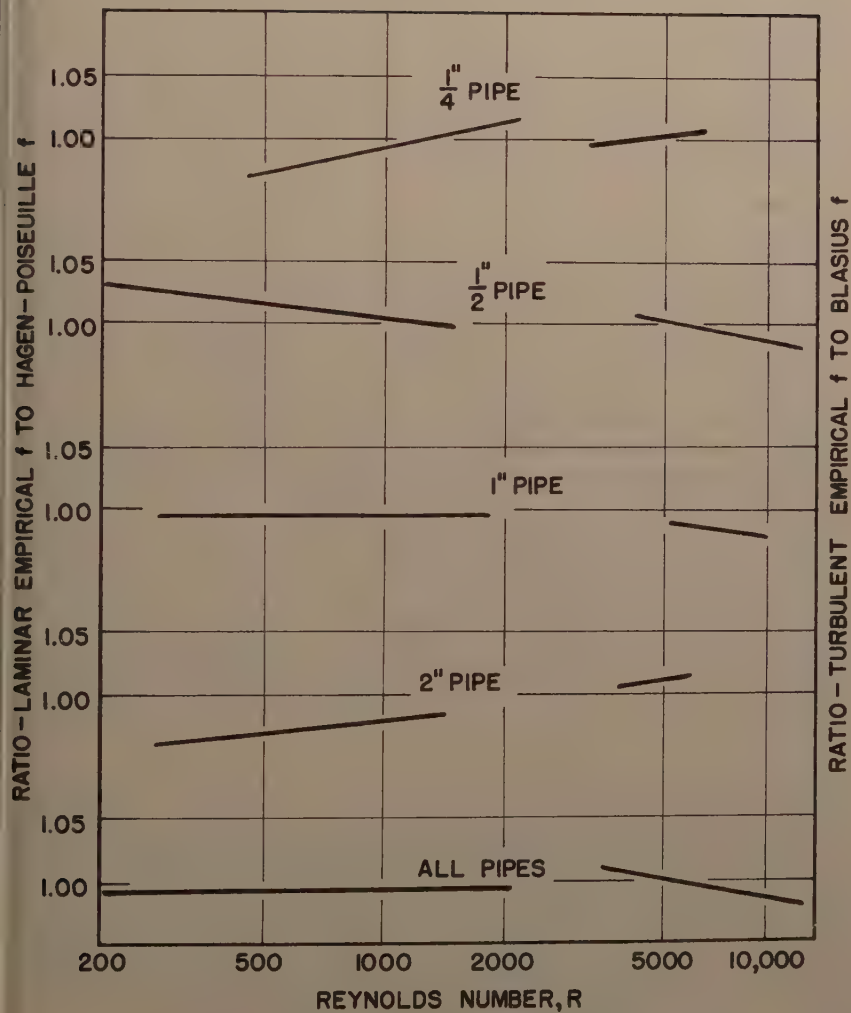


FIGURE 8. "f" COMPARISONS

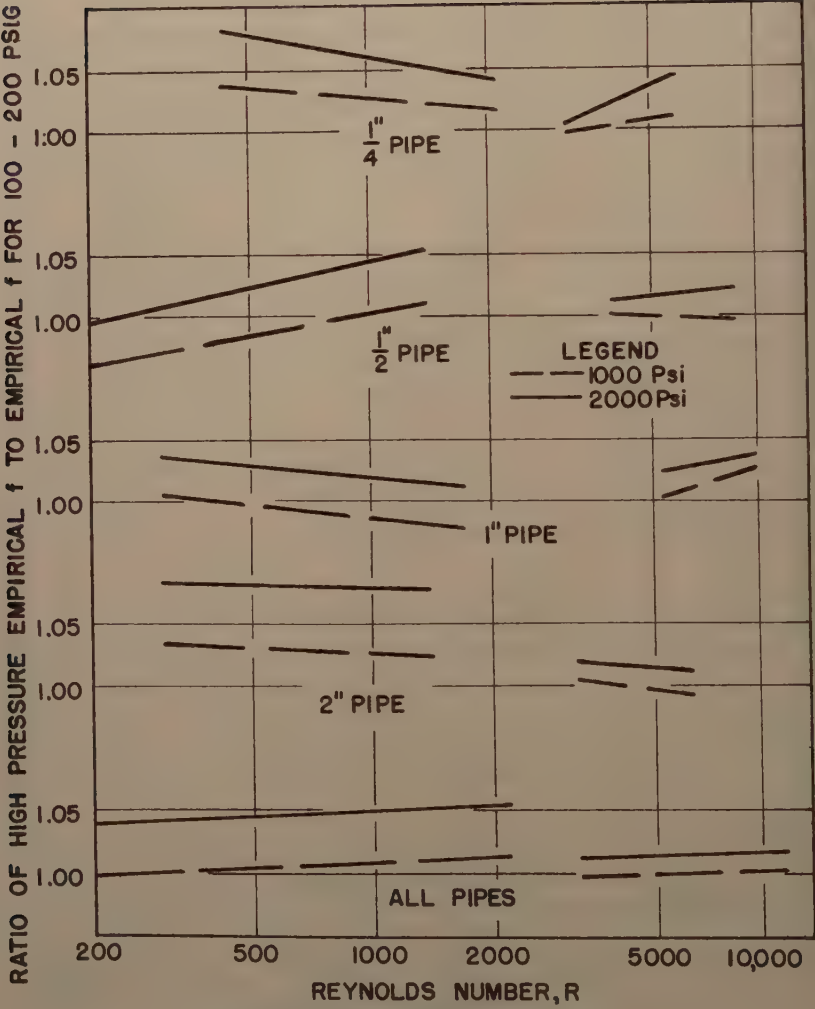


FIGURE 9. "f" COMPARISONS

involved could be neglected for all practical purposes. It may well be, however, that for higher pressures and greater viscosities, the falling-sphere viscometer does not give realistic results for pipe flow problems. The implications of this discussion are quite obvious and in line with known facts. For example, it might be concluded that the viscosities to be used for a given flow problem should be measured by an apparatus and technique that produce boundary, velocity distribution, and character of distortion rate conditions analogous to those found in the problem. This conclusion is supported by the facts that (a) results from falling-sphere, Ostwald, rotating disk and cylinder types of viscometers cannot be used for flow in micropassages where the adhesive forces become disproportionately large and entirely change the character of the resistance to motion; and (b) the viscosities required for flow in sleeve bearings seem to be some function of the rate of distortion (sometimes referred to as "shear rate" or rate of unit strain) and can be measured only with viscometers which duplicate boundary, velocity distribution, and distortion rate conditions.

The supposition that the various types of viscometry should yield different results is logical, so long as viscosity is defined as the ratio of shear stress to rate of distortion or strain. For a given shear stress and boundary the rate of distortion is a function of the molecular properties of the fluid, the basic hypotheses of which have been developed by Eyring¹¹ and others. Viscosity, therefore, is a point function and should not necessarily be a constant throughout the flow regimen. The average or apparent viscosity which a particular viscometer yields can be used, therefore, only for flow situations having analogous flow patterns. The Stoke's Law viscosities observed by Gunaji at low pressure checked the corresponding Hagen-Poiseuille Law viscosities computed from the laminar flow test section data because the Gunaji viscometer was calibrated at low pressures by comparison with Ostwald viscometers whose principle of operation is based on the Hagen-Poiseuille Law. It seems logical to conclude, therefore, that when these two different types of viscometers are operated under pressures different from those at which the calibrations were made, their performances could very well be following paths which are slightly divergent, for the reasons set forth above.

CONCLUSIONS

1. There was a small consistent increase in the energy loss due to pipe friction at 2000 psi over that at atmospheric pressure. In the absence of any significant experimental errors, it is concluded that the performance

1. Gemant, A., "Frictional Phenomena", Chemical Publishing Co., Inc., Brooklyn, N.Y., 1950.

characteristics of the Stoke's Law and Hagen-Poiseuille Law viscometers not identical because of the different conditions in boundary, velocity distribution, character of distortion rate, and external body and surface forces.

2. It is concluded that the viscosities to be used for a given flow problem should be measured by a viscometer that has boundary, velocity distribution, character of distortion rate, and external force conditions analogous to those found in the problem.

3. The standard pipe friction theory is valid for high pressures and temperatures, provided the appropriate effects of pressure and temperature on the properties of the fluid are known. For all practical purposes, the Gunaji viscosity data (based on Stoke's Law) can be used for pipe flow problems, provided the pressure and temperature ranges are reasonably close to those under which the tests were made. The Appendix presents a summary of the data.

The head loss in oil-hydraulics circuits for laminar flow can be estimated by combining the fluid property correlation equations in the Appendix with the Hagen-Poiseuille formula, equation 3, and for turbulent flow the Blasius formula, equation 7. The Blasius formula can be used, because the Reynolds Number will ordinarily be less than 150,000 for pipes that can be considered as "smooth".

APPENDIX

A. Pressure - Density Relations for Petroleum Oils.

The pressure-density relations for petroleum oils are accurately represented by the Dow-Fink¹² formula

$$\rho = \rho_0 (1 + ap - bp^2) \quad (1)$$

where ρ is the density at a gage pressure, p , in psi; ρ_0 is the density at atmospheric pressure ($p=0$) and any temperature; and a and b are empirical constants which apply for a pressure range of zero to 50,000 psi and a temperature range of 20° to 220° F. The relationship between a and b and the temperature are given in Figure 10.

B. Viscosity-Temperature-Pressure Relations for Petroleum Oils.

The viscosity-temperature-pressure relations for petroleum oils as given by Gunaji and Villemonte¹³ are represented by the formula

$$\mu = \mu_0 e^{\left[\frac{p \alpha_{100}}{\Phi (\tau - 100)} \right]} \quad (2)$$

12. Dow and Fink, "Computation of Some Physical Properties of Lubricating Oils at High Pressure".

13. Gunaji and Villemonte, "Effect of Pressure and Temperature on the Viscosity of Petroleum Oils".

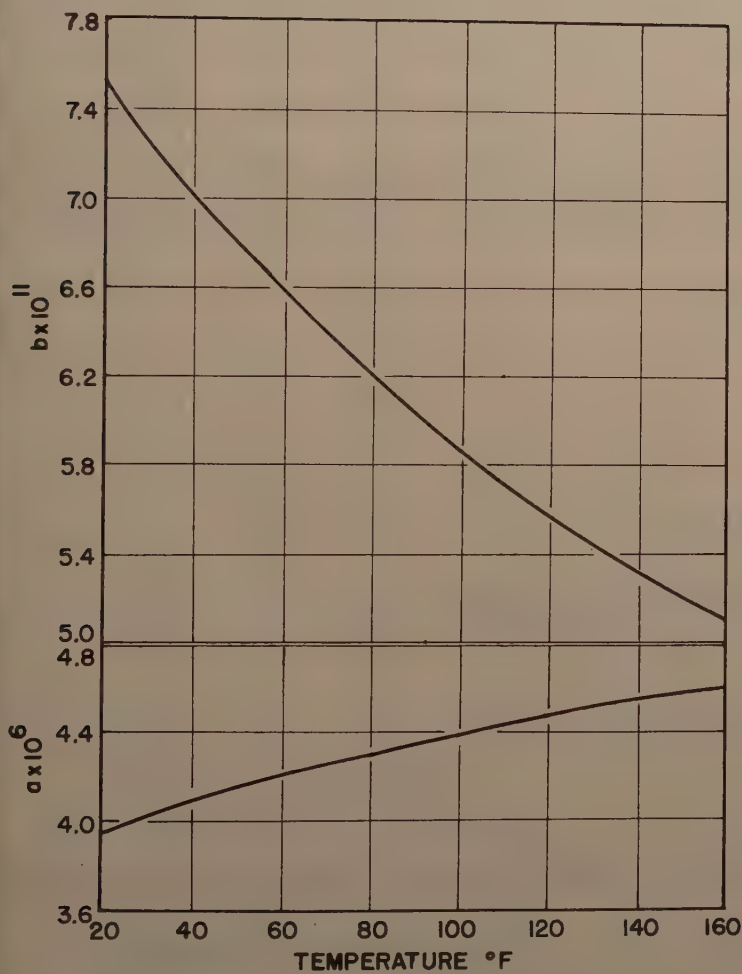
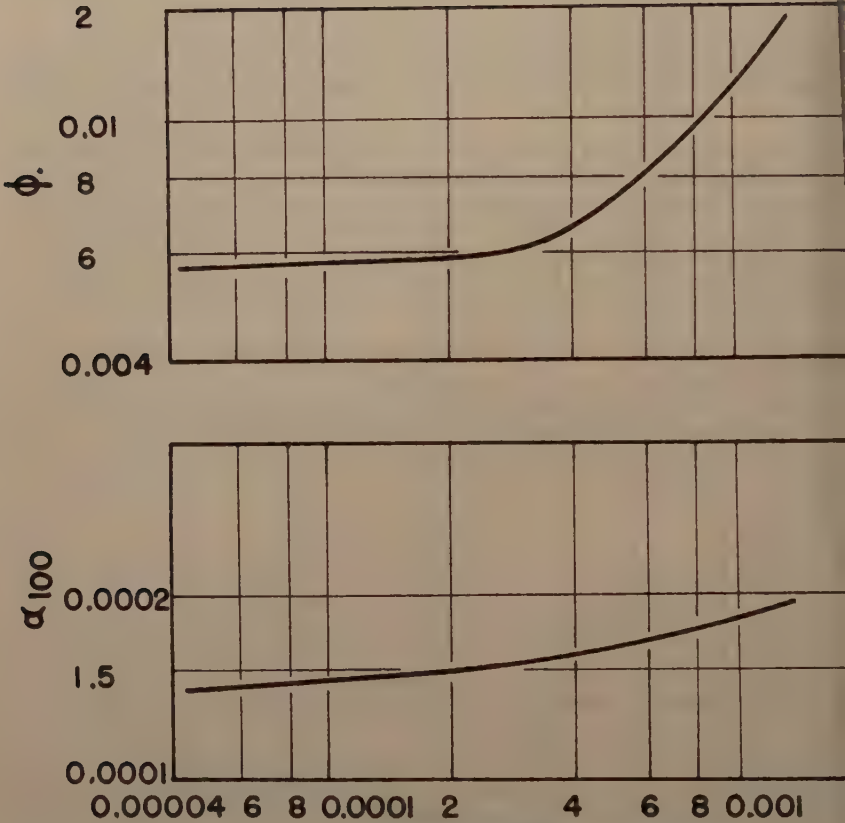


FIG 10. DENSITY CONSTANTS \underline{a} AND \underline{b}
FOR EQUATION 10



ATMOSPHERIC VISCOSITY,
 μ_s AT 100°F IN SL PER FT-SEC

FIG II. RELATION BETWEEN CORRELATION
CONSTANTS AND SPECIFIC
ATMOSPHERIC VISCOSITY
AT 100°F, μ_s FOR EQUATION II.

where μ is the viscosity at the desired pressure and temperature; μ_0 is the atmospheric viscosity at the desired temperature; p is the gage pressure in psi; t is the temperature in degrees Fahrenheit; and α_{100} and ϕ are correlation constants which apply to a specific atmospheric viscosity at 100° F., μ_s . The relationship between the correlation constants and the specific atmospheric viscosity at 100° F. is given in Figure 11. These data are applicable to pressures up to 3000 psi and temperatures up to 180° F.

ACKNOWLEDGMENTS

This study was made possible by financial support received from the Wisconsin Alumni Research Foundation, Engineering Experiment Station, and Department of Civil Engineering of the University of Wisconsin as well as the Edish Company, Cudahy, Wisconsin.

Journal of the
HYDRAULICS DIVISION
Proceedings of the American Society of Civil Engineers

SOME PHYSICAL PROBLEMS RELATED TO
FLOOD INSURANCE¹

A. Arthur Koch²
(Proc. Paper 1164)

INTRODUCTION

The adoption of any nation-wide program of flood insurance would intensify the need for solution of a large number of scientific and technical problems encompassing the fields of meteorology, hydrology, and oceanography. Fortunately within the past two decades a large body of theoretical and experimental knowledge has been accumulated that may be applied to obtain reasonable quantitative answers to some of these problems. Less fortunately, however, all three fields are handicapped by a lack of long-time observational data averaging at best less than fifty years. No attempt is made in this paper to present more than brief descriptions of some of the more important phenomena that will require the gathering of additional observations, their analysis and application.

It has been assumed that the term "flood" would imply the abnormal rising of water or water level causing inundation of land whether by a flowing stream or by an ocean, sea or lake.

Meteorology

Flood-Producing Storms

The severe floods in 1955 in New England and in the Pacific Coast States as well as those since 1950 in the Mid-western and Gulf States have emphasized the need for additional research in predicting rates of storm precipitation produced by combinations of meteorological situations and for further

¹Discussion open until July 1, 1957. Paper 1164 is part of the copyrighted Journal of the Hydraulics Division of the American Society of Civil Engineers, Vol. 83, No. HY 1, February, 1957.

²Presented at a meeting of the Hydraulics Division, ASCE, October 17, 1956, Pittsburgh, Pa.

Cons. Engr., Palo Alto, Calif.; formerly associated with Parsons, Brinckerhoff, Hall & Macdonald, Cons. Engrs., New York, N.Y.

statistical study of storm location with regard to ascertaining critical geographical flood-producing orientations of these meteorological variables.

Most regions of the continental United States are subject to precipitation produced by storms of the cyclonic type. These storms are the result of atmospheric waves developed along frontal surfaces separating cold and heavy polar air from warmer and lighter air originating in tropical regions. Cyclonic storms are characterized by the production of rainfall over extensive areas; a condition met chiefly during the winter months. Upper limits of cyclonic type rainfall rates should, as a result of extensive theoretical and statistical studies by the Weather Bureau, other agencies and individual investigators, be moderately reliable for application to regions east of the Rocky Mountains. Continued investigation will doubtless increase the reliability of estimates for extreme rainfall rates for this storm type for various physical and thermodynamic combinations of polar and tropical air characteristics.

Thunderstorms or convective storms are more or less common throughout the United States though they may locally be known by other designations as for example in the arid Southwest as the "Sonora type". They are generally responsible for the most severe floods that can occur on relatively small drainage areas (500 square miles or less). The attempt to predict precisely where they can occur and their intensity has not been too successful. Upper limits of rates of precipitation and a real extent have been investigated both theoretically and statistically for many regions. However, because of the complex internal structure much additional study will still be required before completely reliable estimates of their maximum flood-producing potential will be available for all areas of possible interest to a program of flood insurance.

Rainfall due to the lifting action of mountain ranges on the flow of warm moist air over topographic barriers (orographic action) is particularly important along the West Coast. In contrast to the relatively unpredictable occurrence of the location of cyclonic and convectional storm types, the orographic storm pattern is geographically well fixed. Also upper limits of orographic storm rainfall in the Pacific Coast region can, because of rather definitely determinable upper limits of atmospheric moisture content, be estimated with considerable accuracy. Reliable determinations of orographic storm precipitation rates for other mountainous regions of the United States are more difficult to derive.

Various combinations of the three foregoing more or less basic storm rainfall types can and do occur throughout the United States. A large amount of investigation must still be accomplished in this difficult phase of meteorological analysis to satisfy the requirements of a nation-wide flood insurance program.

Large areas of the United States are subject to hurricanes, including the states adjacent to the Gulf of Mexico and most of the Atlantic Coastal region. Recent studies of rates of precipitation produced in hurricanes indicate that maximum falls are at least comparable to those rates observed in severe thunderstorms. Possibly the rainfall of hurricanes is more intense than observations indicate due to the fact that high winds prevent gages from measuring true rates. The relative importance of the several factors producing rainfall in hurricanes are not as yet well understood. Observations indicate that the heaviest rainfall in a hurricane is produced in the right front quadrant of the storm and as a consequence for any particular watershed the flood

duced by a hurricane is dependent on the track of the storm. It is obvious that, because of the many largely undetermined inter-related meteorological and physical factors affecting hurricane floods, much additional data, study and research will yet be required to meet the technical demands of a flood insurance program.

The question concerning an increase of flood-producing storms in the United States in recent years is a subject of much controversy among meteorologists and hydrologists. At the present time no satisfactory evidence exists as to whether a temporary or permanent change has occurred.

Hydrology

The rapid development of the science of hydrology during the past thirty years has prepared an adequate background for the solution of most of the hydrologic problems that will arise in a program of flood insurance. The most pressing need will be for more extensive observations of precipitation, rates of snow-melt, temperature, soil moisture, streamflow, reservoir sedimentation, etc. For example, although the U. S. Geological Survey operates about 100 gaging stations in the principal river basins there are many small streams throughout the United States where potential flood damage exists but where the number of flow determinations are inadequate for purposes of solving the technical problems arising in a program of flood insurance. A similar situation exists with regard to the various types of precipitation measurement stations.

Oceanography

The great loss of life and property sustained by the coastal areas of New England in September 1938 and in other locations on the Atlantic Coast since that time has emphasized the importance of storm tides, currents and waves as agents of destruction. High ocean water levels acting in conjunction with rapid rates of flow from coastal streams can multiply property damages along the lower reaches of rivers adjacent to the ocean. The science of Oceanography, a relatively new field, is able to lend assistance in the solution of some of these problems.

Storm Tides

Sustained winds in the right-hand quadrants of a hurricane acting in conjunction with reduced atmospheric pressure near and at the "eye" of the storm create a rise in the level of the sea along a coast. Typical observed extreme historical storm tides are listed below.

| <u>Location</u> | <u>Date</u> | <u>Water Level Above Astronomical Tide (in feet)</u> |
|----------------------------|--------------------|--|
| New York, N.Y. | September 3, 1821 | 13 |
| Savannah-Charleston, S.C. | August 27, 1893 | Coastal islands submerged |
| Lake Erie at Buffalo, N.Y. | November 1900 | 8.5 |
| Galveston, Texas | September 14, 1919 | 16 |
| Florida Keys | September 3, 1935 | 15 to 20 |
| Martha's Vineyard, Mass. | September 21, 1938 | 15 to 20 |
| Providence, R. I. | August 31, 1954 | 15 |

A steady and sustained wind blowing over the surface of a relatively shallow body of water creates a horizontal force on the surface of the water causing both the formation of oscillatory waves and a piling up of water. Continental shelves along the coasts of the United States are particularly susceptible to this piling up of water under the action of onshore winds. In addition variations in atmospheric pressure cause water levels to rise when the barometric pressure is low. This latter action is magnified if the barometric low travels at a speed approaching that of the propagation speed of the water wave (resonance effect). The combined result of the wind tide and the barometric tide is the total storm tide.

Theoretical procedures are available for computing storm tides that should permit reasonable approximations of maximum possible water levels for any coastal location. For estuaries the total rise at any given point would be a combination of static tide and the tide due to seiches (oscillation of the body of water in the estuary).

Studies indicate that, with the possible exception of the coast of Southern New England, no portions of the coastal waters along the Atlantic seaboard and Gulf of Mexico have as yet experienced the greatest possible storm tides due to hurricanes.

Currents

Under normal circumstances reversing currents exist at the mouths of all estuaries. These currents extend their influence along the coasts on both sides of the opening to the sea.

During severe storms creating offshore or onshore winds there is a temporary variation of water surface due to the transport of surface water in the ocean and in an estuary. Frequently during violent storms the additional volume of water transported in and out of an estuary generates exceptionally strong reversing currents that are hazardous to navigation and can occasionally cause marked shoreline changes due to erosion and transport of beach material.

For many locations data concerning the magnitude of extreme current velocities created by storms is entirely lacking, a deficiency that might require rectification depending on whether the resulting damage is classified as due to floods.

Waves

Storm-generated waves superimposed on high static water levels caused by storm tides can be agents producing very severe damage to coastal improvements of all types. Forces exerted by breaking waves in particular are extremely large and until fairly recently the great magnitude of the pressures exerted on structures has often not been adequately appreciated. Past and continuing observation and research on the complex properties and action of waves on structures gives the engineer adequate tools for safe design of coastal structures.

Tsunami

Although the majority of water waves are the result of meteorological causes, mention should be made of the wave produced by submarine earthquakes and designated "tsunami". In the open sea these seismic sea waves

have small amplitude and travel at high speed. On approaching mildly sloping shores the waves rapidly increase in amplitude and are very destructive. In bays, harbors and estuaries the "tsunami" may initiate seiches whose periods of oscillation depend on the depth and shape of the body of water.

Whether the seismic sea wave is a serious threat to coastal areas of the United States is not definitely known from observation, due to the shortness of tidal records. It may be a subject worthy of investigation if "tsunami" should be classified as a flood phenomenon in any insurance program.

SUMMARY

An attempt has been made to outline in general terms some of the technical and scientific problems that would be met in a nationwide flood insurance program. Additional observational data related to meteorology, hydrology and oceanography would be a basic requirement. Although a large body of knowledge now exists that is readily available to assist in the immediate solution of some of the complex problems, an expanded program of investigation and research would be a necessity.

Journal of the
HYDRAULICS DIVISION
Proceedings of the American Society of Civil Engineers

TECHNICAL PROBLEMS OF FLOOD INSURANCE*

H. Alden Foster¹
(Proc. Paper 1165)

ABSTRACT

This paper discusses Flood Insurance from an engineering standpoint with particular emphasis on determination of flood probability from relatively short records, estimates of mean annual flood damage to particular properties for establishing self-supporting premium rates, spreading the risk of flood damage over a large number of policies, and related technical problems involved in setting up any program of flood insurance.

INTRODUCTION

The problem of bringing financial relief to property owners from the effects of damage by floods has been receiving increasing attention in recent years. The private insurance companies as well as Congress have given much study to this question. In much of the discussion that has taken place on this subject, it has been apparent that there has been considerable misunderstanding of the technical problems involved and the difficulties that would have to be overcome in establishing any program of flood insurance or indemnity, either on a private or government-sponsored basis.

The speaker proposes, therefore, to discuss this subject in a general way and to bring out the basic problems involved, without attempting to prove whether flood insurance is actually feasible. This latter question will be discussed by another speaker.

Note: Discussion open until July 1, 1957. Paper 1165 is part of the copyrighted Journal of the Hydraulics Division of the American Society of Civil Engineers, Vol. 83, No. HY 1, February, 1957.

* Presented at a meeting of the Hydraulics Division, ASCE, October 17, 1956, Pittsburgh, Pa. This paper is based largely on Proceedings Separate No. 483, "Flood Insurance," by H. Alden Foster, August, 1954.

1. Princ. Associate, Parsons, Brinckerhoff, Hall & MacDonald, New York, N. Y.

Basic Problem of Flood Insurance

When an insurance company issues a policy to indemnify the policy-holder against a certain type of loss, such as by fire, the policy provides that the owner will pay a definite annual premium to the company as compensation for the risk carried by the latter. This premium involves two parts: (1) the basic or "pure premium" which represents the average annual loss sustained by the company, and (2) a "loading charge" intended to cover the company's cost of doing business.

The basic problem in flood insurance, therefore, is to determine the Average Annual Damage that may be expected to occur to each property on which insurance is issued. This problem may be considered in three steps:

1. Estimating the average annual frequency or probability of occurrence of floods of a given magnitude at the locality under consideration.
2. Estimating the dollar value of damages caused to each property by a flood of any given intensity.
3. Determination of the Average Annual Flood Damage to the property, by combining the results of the above estimates.

Flood Frequency

Statistical Methods

Estimates of future flood occurrences must be based on past experience, modified by the anticipated effects of any changes in controlling conditions that may be expected to occur in the future. While it is impossible to forecast the actual flood intensities that will be experienced in any future year, it has been possible to make estimates of the probability of occurrence of floods of various intensities, by statistical analysis of past records.

Statistical methods of considerable refinement have been used for many years in various fields, particularly in life insurance where technical procedures of considerable value have been developed. Somewhat similar methods were introduced into the field of hydrology about forty years ago, and have received intensive study by many engineers within the past twenty years. However, there is a fundamental difference between the statistical methods used by engineers and those that have received general acceptance by statisticians.

In most statistical work, the data available for analysis run into a very large number of items or individual events, as for instance with life insurance. But in hydrology and particularly in the study of flood records where the maximum flood occurring each year is considered, the number of items available in any record is quite limited, seldom extending over more than fifty years and often being limited to twenty years or less.

Statistical methods, at best, must necessarily yield approximate results. Where the available data are limited in quantity, the degree of precision in the calculated results will become progressively smaller. This is an important consideration in evaluating any program of flood insurance.

Selecting the Curve-of-Best-Fit

Various methods have been advocated for plotting the flood-probability

curve. The purpose of all of these methods is to establish an approximate relationship between the magnitude of any particular flood and the probability of its occurrence in any future year. Some of the methods that have been advocated for this purpose are adaptations of methods extensively used in general statistical analysis; others are based on formulas developed specifically for use in hydrological investigations. It is beyond the scope of the present discussion to make a detailed comparison of these methods.

When the flood data are plotted on a diagram showing flood magnitude versus probability of occurrence, it is desirable to replace the individual items by a smooth line called the "curve-of-best-fit." While the advocates of some of the plotting methods maintain that their curves have a reliable mathematical basis for determination of this curve, it appears doubtful whether these claims can be fully substantiated. In the opinion of the speaker, the best proof of a scientific basis for a given probability curve is that it gives a reasonably good fit to the recorded data. The practical tests of reliability are: (1) which method gives the best representation of actual data; and (2) which method is most convenient to use.

The various proposed methods of curve-fitting generally produce reasonably good results with a given flood record, when used to express probabilities or recurrence-intervals within the length of the record. For example, a 20-year record could be used to obtain a reliable estimate of 10-year (10% probable) flood, regardless of which method is used for obtaining the probability curve. But when an attempt is made to extrapolate the flood-probability curve much beyond the recurrence interval covered by the record, considerable differences are revealed in the several methods. However, these differences are far outweighed in magnitude by the so-called "errors of sampling."

Errors of Sampling

In the language of statistics, a record of annual floods at a particular location is a "sample" of all floods occurring at that location over a long period of years, the long-time record being known as the "population" and the individual recorded floods being items of the population. The items of the recorded sample may be analyzed by the various probability methods previously mentioned, and a smooth probability curve may be established as giving the best representation of the sample. But there is no assurance that a sample record obtained in the future and covering the same length of time will produce the same probability curve. In a program of flood insurance, it is important to determine the extent to which the future record may differ from the available sample.

Methods have been developed in the Theory of Statistics whereby the probable errors of future samples, or the "spread" of the items in the future sample as compared with the available record, may be reasonably estimated: such methods show that the relative magnitude of the errors decreases rapidly as the number of items in the record increases. For records of less than twenty years, the possible errors may be sufficiently large to appreciably affect any estimates of mean annual flood damages.

A conspicuous example of this situation is found in the "Hurricane Floods" of August 1955 in the northeastern states. These floods in many locations greatly exceeded any that had occurred within the previous century. A probability curve obtained from a flood record in such locations prior to 1955 would be substantially different in shape from one based on a record including the 1955 floods.

Changes in River Conditions

Where regulating works have been constructed on any river and have the effect of reducing the peak discharges of floods, the probability of occurrence of floods on the river will be affected. Any studies of flood-probability on such a river based on records prior to the construction of the regulating works would have to be revised before they would be useful in a subsequent program of flood-insurance. Obviously, the amount of detailed study required for preparation of flood-probability estimates at a given location will be appreciably increased if the discharge of the river is affected by flood-control structures further upstream. Similarly, changes in watershed conditions, either in the past or anticipated in the future, which would cause increased flood discharge, such as removal of forests or the conversion of land to urban uses, must be given consideration in the determination of flood probabilities.

Conclusions as to Methods of Curve-Fitting

After studying and comparing various methods of curve-fitting that have been proposed for hydrological studies, the speaker has not been able to reach any definite conclusions regarding which one is the best for use in flood-insurance studies. Within the time limits of the actual record, the several methods seem to give substantially equivalent results. However, when the curves are extrapolated beyond the highest floods of record, there is considerable variation among the results obtained.

Since one of the principal objects in preparing a flood-probability curve for insurance purposes is to permit the extrapolation of flood frequencies beyond the time limits of the record, the question of the amount of possible error in the "sample" for less frequent floods is of particular importance. Such errors may become relatively large, especially when the record covers only a few years. In fact, these errors of sampling far outweigh in magnitude any differences between the several types of theoretical probability curves that have been mentioned. Hence the selection of the most suitable method comes down to a question of convenience in application. Fortunately, a precise determination of the magnitude of floods with very low probabilities (the floods with very long recurrence intervals) is not of great significance for computation of insurance premiums, since these rare floods have only a slight influence on the value of the "average annual flood."

Flood Damages

The second part of the problem of estimating average annual flood losses for a particular property is the computation of the probable damages to the property in question that would be caused by a flood of a given intensity. This matter must be considered in two parts:

1. To what depth will the property be inundated by the flood?
2. How much damage will be caused to the property when the water reaches that depth?

The first question involves the relation between "flood stage," or flood elevation, and flood intensity; the second involves the relation between flood stage and damages for the property in question.

Flood Stages as Related to Particular Properties

The work required for the preparation of diagrams of flood stage at a particular property, as related to the intensity of the flood, involves:

1. Preparation of necessary topographic maps showing the location and elevation of all properties under consideration at a relatively large scale.
2. Preparation of River Stage-Discharge curves, showing the elevation of the water surface at the gaging station for various intensities of discharge.

The preparation of the necessary maps and stage-discharge curves for a given locality may require a great amount of field surveying as well as office preparation, and will involve considerable time and expense for preparation of the insurance program. This must be incurred regardless of the amount of flood insurance subsequently issued in the area.

3. Determination of the MSL elevation of each property under consideration. It is important to determine the "elevation of zero damage," or the flood stage at the property that must be reached before any material damage will occur.

Classification of Flood Damages

Damages to property are classified as follows:

1. Direct losses, consisting of physical damages to property and goods, measured by present day cost of repair or the replacement in kind, and the cost of cleanup and for moving goods. The direct losses may also be subdivided according to the type of use for the structures,—such as residential, commercial, industrial, etc.
2. Indirect losses, consisting of the value of services or uses lost or made necessary by reason of flood conditions, not chargeable to direct loss. These include losses of business and wages, costs of relief and similar losses, both within and without the flood area, during the period of the flood and subsequent rehabilitation. It seems doubtful whether indirect losses of these types would be included in a program of flood insurance. On the other hand, indirect flood losses have commonly been included in determination of the benefits produced by construction of flood-control projects.
3. Depreciation losses have occasionally been included as a credit for the economic justification of flood-protection works. The total depreciation of a property that has been flooded equals the value of the property before the flood minus the value after the flood. It appears doubtful, however, whether such depreciation losses would need to be considered in connection with flood insurance if physical damage to the property has been compensated for under "direct damages."

Estimates of Damages

The determination of the amount of damage that would be caused to the property by a particular flood stage is a matter of appraisal. The most reliable estimated of damage will be for floods of record from which the owner of

the property has definite records of losses sustained. Generally the appraiser must make his own estimate, which may involve a detailed examination of the property and the installed equipment, followed by estimates of losses to be sustained by each piece of machinery or equipment, and of the cost of cleaning up.

Damage to buildings generally will be less than the total replacement cost unless the type of construction is such as to result in total destruction, such as by undermining the foundation.

Dynamic Effects of Floods

The stage-damage estimates previously described apply particularly to the inundation type of flood, where the water surface gradually rises until the property is partially or fully submerged. This type of flooding will occur where the slope of the flood-profile is moderate. However, where the surface profile of the river is relatively steep, or where the flood waters are temporarily held back by obstructions, high velocity currents may be induced that would cause serious damages. A simple inundation may cause only partial damage to a structure, whereas the dynamic effect of rapidly flowing water may bring about its complete destruction. These effects are so difficult to estimate in advance that they can only be approximated by reference to past experiences in a given locality.

The type of flood damage may be greatly influenced on a particular stream by the character of the storm producing the flood, as was conspicuously demonstrated by the "hurricane floods" of August 1955 in the northeastern states. On the larger rivers, such as the Delaware, the damage was caused largely by water transmitted from upstream at greater rates than could be handled by the natural river channel, resulting in overflow of the river banks and inundation of the adjacent flood plains. On the smaller streams there was apparently extensive sheet runoff caused by unprecedentedly high rates of rainfall resulting in "overland floods," with widespread damage and loss of life in sections that had never previously been subject to severe floods within the period of record.

Average Annual Flood Damage

The average annual flood damage experienced by the owner of a particular property is the amount which the insurer would have to collect each year merely to pay the losses that will occur during a period of years. Assuming that the property is restored after each flood experience, the total losses over a period of years divided by the number of years would be considered the average annual damage. The calculation of this quantity is made as follows:

The diagram of flood stage vs. flood discharge at the gaging station corresponding to the given property (also called the "rating curve"), is combined with the diagram of flood discharge vs. probability, for the same gaging station, to obtain a diagram of floodstage vs. probability (Fig. 1). This is applicable to all properties in the local area.

The latter curve is then combined with the diagram of floodstage vs. property damage previously described to obtain a curve of flood-damage vs. probability for the particular property (Fig. 2). This curve shows the probability of occurrence of flood damages equal to, or exceeding, various

amounts. It can be readily shown that, if the curve is plotted on a numerical scale, the total area under the damage-probability curve is a measure of the average annual damage caused by all floods which may be anticipated over a long period of years.

The value of the Average Annual Flood Damage so determined must necessarily reflect the approximations involved in preparing the several diagrams of flood stage, probability and damage. The least reliable of these is likely to be the diagram of stage vs. probability.

Test Calculations of Average Annual Flood Damage

The procedures previously described have been used to calculate the average annual flood damages to a considerable number of properties at Lowell, Mass. This location was selected because much of the basic data were available in the files of the U. S. Corps of Engineers. The ratio between the mean annual loss for each property and the maximum probable loss for the property was used as a basis of comparison, since it would be a factor in establishing the premium rate for a flood-insurance policy. Out of 54 industrial properties so investigated, the value of this ratio varied from 0.4% to a maximum of 17.5% with an average value of 4.2%. Similar results have been obtained from studies in other localities. This indicates that the cost of flood insurance to a property owner would be high if such a program were feasible.

Another important consideration is the great variation in the value of the ratio of mean annual to maximum flood losses, which would either require a great variation in the premium rates charged on different properties in the same area or would force the more favorably located properties to carry a considerable share of the insurance cost on the properties subject to greater risk.

Financial Reserves

Basing the insurance premium on average annual flood damage makes it theoretically possible for the insurance company to reimburse itself for losses over a long period of years. But this does not eliminate the possibility that the maximum possible flood may occur in any year; and unless the underwriter has set up reserve funds sufficient to pay such maximum loss at any time on all insured properties subject to flooding by a particular river, the financial stability of the insurance program would be jeopardized. Consequently, the total reserves required to assure the solvency of the underwriter for any general area would be equal to the sum of the maximum insured losses of all the insured property in that area.

Spreading the Risk

Obviously, there is no way by which the total risk may be reduced by spreading it over a large number of properties when they are all located in the same general flood area, since a major flood will cause damage to all insured properties located within the area affected by the river in question. In this respect, flood insurance differs materially from fire insurance. Under normal conditions, only a small proportion of insured properties in a particular city suffer damage by fire in any one year, so that the risk of loss can be spread over a large number of policies. It is only in the case of a

catastrophe, such as the Chicago fire of 1871, that a large number of properties are damaged by fire at one time, whereas every major flood may be considered a catastrophe since it would result in damage claims from all insured owners within the affected area.

If the insurance program were placed in operation in widely separated sections of the country, it is probable that some beneficial effect of "spreading the risk" may be realized. This is because major floods do not occur in all parts of the country in the same year. A very approximate study of flood loss statistics for the entire United States indicates that the reserve set aside to cover major flood losses in any one drainage basin might be reduced by two-thirds if the insurance program covered the entire country and was not limited to individual basins.

It is important to note that this question of spreading the risk applies only to the maximum flood losses and does not affect the mean annual loss for any property. The total flood loss for the entire country is not reduced in any year, even if the insurance program covers the whole country. The practical effect of a widespread coverage by insurance, therefore, would be only to reduce the amount of reserves required to cover large losses in particular years.

Effect of Flood Forecasting

Forecasting of floods on the more important rivers has been carried out by the U. S. Weather Bureau for many years, the extent and reliability of the forecasts having appreciably increased in recent years. If flood insurance were to be established in this country, it would doubtless be greatly benefited by an efficient forecasting service, since damages could be reduced in many cases by emergency measures taken by the property owners and based upon advanced warnings supplied by the flood-forecasting service. However, the following questions would remain to be answered:

1. If the property owner fails to take due advantage of the forecast by delaying to take the necessary precautions or neglecting them entirely, can the insurance company refuse to indemnify him for part or all of his losses?
2. How can the insurance company be sure that the flood forecast will be reliable or will be issued in time so that precautionary measures can be taken by the covered property owner?

Special Problems

Numerous special problems would have to be solved in setting up a program of flood insurance, a few of which may be mentioned:

Types of Floods

Floods are produced by numerous causes and may be classified into various types. It may be difficult in some cases to determine where damage to property has been caused by direct rainfall or by some type of flood. For example, certain areas that normally would not be considered as located in a flood-plain may be subject to damage from heavy rainfall flowing over steep ground slopes in the form of "sheet runoff." There might be some doubt whether this condition should be properly classified as a "flood," or whether

It is a case of direct damage by rainfall. Similarly, the "mud flows" or discharges of large quantities of debris carried out on the alluvial fans at the mouths of steep canyons, such as in the Los Angeles area of California, may cause widespread damage to structures, even though the discharge of water might not be sufficient to cause great damage by itself.

Some types of flood are difficult or impossible to forecast from a probability standpoint. In a flood insurance program, it would doubtless be desirable to place certain limitations on the type of flood covered by the policy issued on any property, although practical considerations might make it difficult or impossible to impose such limitations.

Effect of Insurance on Land Use

The owner of a property covered by flood insurance may be inclined to increase its use on the basis that, if a flood comes, the additional loss to which he would be subjected would be compensated to him. This condition might be taken care of by making an annual inspection of the property and, if necessary, increasing the premium charge to correspond with the increased risk.

Uneconomical development of land subject to periodic inundation may be controlled to some extent by the fact that insurance premiums on such properties would necessarily have to be relatively high, thereby having a tendency to eliminate properties of that type from the insurance program.

Effect of Protective Works

Reduction of the risk of damage by flood to properties on rivers where flood-protection works have been constructed will depend to a considerable extent on how the works are operated during a particular flood. While the works may have been designed on certain assumptions as to the manner of their operation, there is no guarantee that they always will be operated in conformance therewith. If insurance is issued on the basis of those assumptions, the additional risk involved in possible changes in the operating program would have to be assumed. Similar additional risk may have to be carried in the case of lands protected by levees that are not properly maintained.

Owners of property located downstream from flood control works may feel a false sense of security by assuming that the degree of protection from which they benefit is greater than that actually provided in the design of the works. This may result in an increased use of land that is still unprotected, and greater risk of damage from floods.

Other Applications of Probability Methods

The general methods outlined herein for determining the Average Annual Flood Damage have been extensively used to determine the Average Annual Benefits accruing to a flood control project as a result of protection furnished to various properties in the flood basin. The purpose of such estimates is to justify construction of the project on an economic basis, estimating future benefits by reference to past flood experiences. If the indicated benefits exceed the annual cost of the project, the latter is considered to be justified in accordance with law. If, in the future, greater floods occur than had been anticipated from past records, the project may still have been justified since, without the protective works, the average annual damages would doubtless

have been considerably greater. The government agency that constructs the protection works is not held liable for losses sustained by property owners if a flood occurs exceeding in magnitude that for which the project was constructed.

With flood insurance, on the other hand, the insuring agency agrees to reimburse the property owner for all losses that may occur in the future, under the terms of the policy. If the resulting average annual loss exceeds that estimated from past flood records, the insurer necessarily takes a loss. Consequently, the question of the reliability of probability estimates of future floods is of much greater significance in a program of flood insurance than in justifying a flood protection project.

SUMMARY

If a program of flood insurance were set up, the following factors require careful consideration, due to their influence on the charges required for protection on individual properties:

1. The Average Annual Loss or Damage, which is the amount of money that would have to be set aside from premium charges each year to cover losses chargeable to the policy. It equals the sum of all losses expected to occur during a considerable number of years in the future divided by the number of years, and may be estimated by a study of the probability of occurrence of floods of various magnitudes combined with estimates of the amount of damage which the various floods would cause to the property.
2. The Errors of Sampling, which are a measure of the extent to which future flood records may vary from the "sample record" on which the estimate of Average Annual Flood Damage is based. No precise estimate of future floods can be made in advance; and the shorter the available record the greater the possibility of variation in the future.
3. Sufficient Financial Reserves must be available to the insuring agency to equal the sum of all the maximum damage items on insured properties located in the same general flood area. If the insurance program covers a sufficiently large portion of the country so that maximum flood losses will not occur in all portions of the insured areas in the same year, the amount of reserve funds can be reduced to some extent. Such reduction, however, would not involve any change in the average annual flood losses for which provision must be made in establishing the premium rates.

There is no constant ratio between average annual flood loss and the amount of insurance on a property, even for similar types of properties. This ratio is an important factor in establishing the annual charge, and will vary greatly with the location of the property with respect to the river channel. In general, premium charges will have to be determined individually for the various properties. Rates for flood insurance will have to be much greater than for other types of insurance.

There are numerous other problems involved in setting up a program of flood insurance, the effects of which are difficult to assess in advance because of lack of actual experience in this field of insurance.

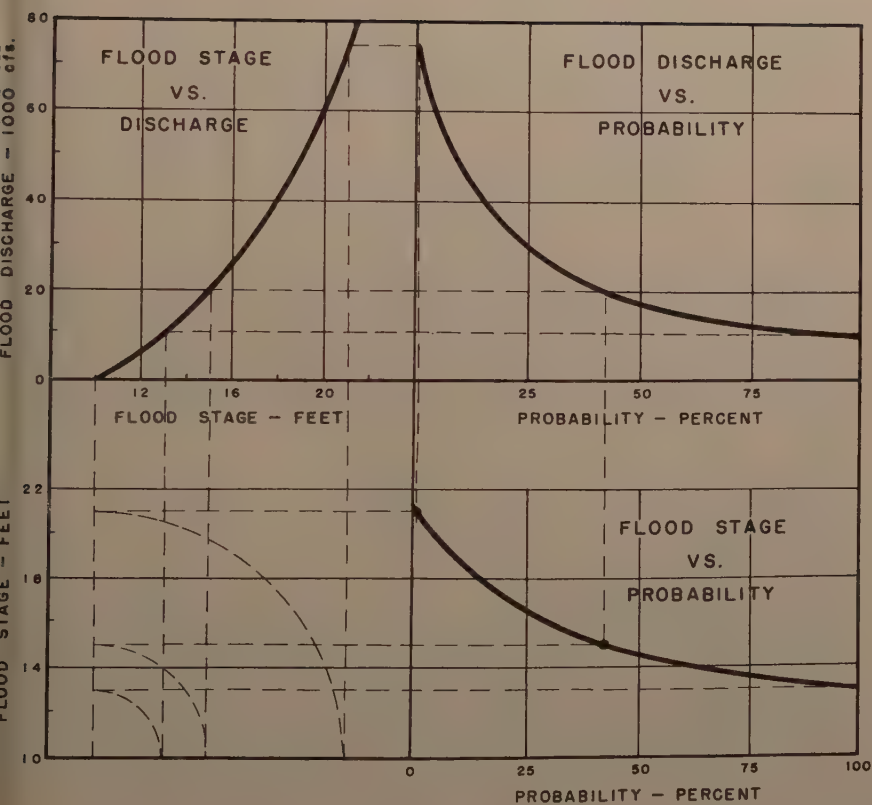


Fig.1

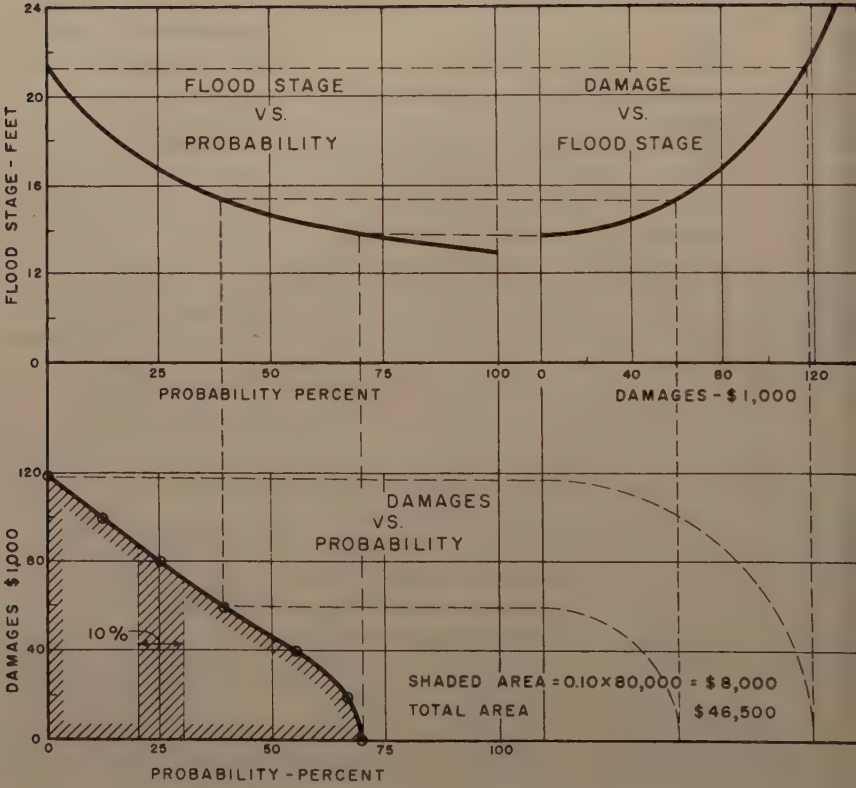


Fig.2

Journal of the
HYDRAULICS DIVISION
Proceedings of the American Society of Civil Engineers

FREQUENCY ANALYSIS OF STREAMFLOW DATA

David K. Todd,¹ J.M. ASCE
(Proc. Paper 1166)

SYNOPSIS

The basic principles of frequency analysis of streamflow data are reviewed pointing toward the advantages and applications of these simpler forms of statistical analysis. Computational procedures are only briefly outlined, but a list of references indicates where details can be found. Frequency analysis of high flows (floods), low flows (droughts), and all flows are described. A group of figures illustrates methods of expressing and interpreting streamflow data subjected to frequency analysis.

INTRODUCTION

Few civil engineers profess to be statisticians; in fact, few claim even an elementary knowledge of statistics. Lacking formal instruction in a subject, it is natural to avoid the unknown. Yet, an awareness of the advantages of statistical analysis encourages the application of such methods. Too often unnecessarily complex terminology and a variety of means of obtaining similar results prove to be the most confusing elements. Thus, a presentation of basic methods, omitting specific details and derivations but emphasizing applications, may be worthwhile.

An example of the application of simpler forms of statistics is that required for frequency analysis of streamflow data. If data are available, the civil engineer is faced with analyzing a large collection of numbers—usually mean daily discharges—to obtain information related to an engineering problem. It may involve a structure to store, pass, or divert water, or it may concern water supplies for consumption or power generation. In any event, the problem reduces to determining the frequency distribution of streamflow data. Frequency may be defined as the number of flows of a particular magnitude as compared to the total number of all such flows, whereas a frequency

Note: Discussion open until July 1, 1957. Paper 1166 is part of the copyrighted Journal of the Hydraulics Division of the American Society of Civil Engineers, Vol. 83, No. HY 1, February, 1957.

¹ Asst. Prof. of Civ. Eng., Univ. of California, Berkeley, Calif.

distribution is an arrangement by magnitude of frequencies. For example, in a given 100-year record there are 100 annual peak flows, or floods. The smallest of these flows is equalled or exceeded every year and therefore can be designated the 1-year flood. Similarly, the fifth largest flood occurs on the average every 20 years and becomes the 20-year flood; the highest flow, the 100-year flood. These recurrence intervals T_R may be defined by the familiar equation

$$T_R = \frac{n+1}{m} \quad (1)$$

where m is the order number when the values are arranged in decreasing order and n is the total number of events. It should be noted that no chronological sequence is implied but only an average interval of occurrence.

Frequency distributions can be converted to frequency curves by simple arithmetic procedures. Many plotting schemes have been devised to facilitate interpretation of frequency curves; familiarity with these is not as important as understanding the limitations of any one method.

The following three sections describe the applicability of frequency analysis to high flows, or floods; to low flows, or droughts; and to all streamflows. References at the end of the paper provide an introduction to the extensive literature available on the subject.

Frequency Analysis of Flood Flows

Flood frequencies are developed for design of culverts, bridge waterways, and spillways, for preliminary planning, and for economic studies. Available data usually consist of streamflow records published by the U. S. Geological Survey in annual Water-Supply Papers as mean daily discharges and annual peak flows. Floods may be defined either as peak or volume floods depending upon the purpose of the analysis. For floods occurring above dams having a relatively large storage capacity, the frequency of peak flows is incidental to that of flood volumes; for small dams containing minimal storage, the converse is true. A peak flood is simply the highest instantaneous discharge; whereas, a volume flood is that high rate of discharge persisting for a specified duration, such as a 1-day, 3-day or 10-day flood. Volume floods are obtained by accumulating mean daily discharges over the time interval and converting to acre-feet.

To develop a peak flood frequency curve, peak floods are selected from a streamflow record. Ordinarily a minimum of 10 to 20 years of record are necessary to approximate a frequency curve. Floods can be selected either by the highest flood in each water year (the annual flood method) or by all peak floods above the lowest annual flood (the basic flood method). If peak floods by both methods are arranged by order of magnitude, an array such as that shown in Fig. 1a for a 20-year record⁽⁷⁾ will be obtained. The 20 annual floods are indicated by dots and the 20 highest floods known as the annual exceedance floods, are designated by horizontal bars. For comparison these two sets of selected floods are replotted in Fig. 11. It can be seen that the annual exceedances form a population closely approximating the annual maxima for the higher floods but deviating positively as the lower floods are reached. It can be shown from probability theory^(7,22) that the recurrence interval obtained by the two methods differs most from the lowest floods and

least for the highest floods. Fig. 2 shows the relationship of the two methods, graphically. For a 10-year flood the recurrence interval discrepancy amounts to 5 percent and reduces to 1 percent for a 50-year flood.

For temporary or small structures where designs are based upon flood frequencies of about 10 years or less, the basic flood method should be used;(26) for large permanent structures designed for larger floods either method is satisfactory but the annual flood method is preferable because it is shorter and avoids the problem of establishing the independence of consecutive floods.

A frequency distribution for a series of floods, grouped by classes to form a bar graph, is shown in Fig. 3a. If the number of items were increased and the class size reduced, the theoretical curve would be formed. The unsymmetric shape is typical of flood frequency distributions. Now, if these values are accumulated from the highest to the lowest and divided by the total number of flood values, a cumulative frequency curve (commonly referred to simply as a frequency curve) is formed (Fig. 3b). The ordinate expresses the probability of recurrence of a flood equal or greater than that specified by the abscissa. For ease in reading and extrapolating such curves, special coordinate scales have been developed to transform the usual S-shaped curve nearer to a straight line (Fig. 3c). The particular theoretical frequency curve employed determines the type of scale required to produce a straight line. If the observed flood frequency curve differs from the theoretical one, a curved line will result.

A common problem upon developing a flood frequency curve is the need to estimate the magnitude of floods having recurrence intervals greater than that of the length of record. The extreme curvature displayed by most frequency curves plotted on rectangular coordinate paper makes extrapolation difficult; therefore plotting the curve on probability, log-probability, semi-log, or log-log paper is sometimes helpful in reducing the curvature. Most extrapolation by eye of frequencies is arbitrary, hence it does not provide a sound basis for estimating frequencies of high floods. To overcome this difficulty analytical techniques have been developed for fitting a cumulative frequency curve to specified types of frequency distributions. The contributions in this connection of men such as Foster, Hazen, Powell, Goodrich, Slade, Potter, Gumbel, Chow, and Geyer are well-known to many engineers. Essentially, these efforts have produced a variety of ways for extending a flood frequency curve from a limited length of record. Computational procedures in most cases are straight-forward—tabular forms reduce the work in many instances to almost a mechanical procedure.

With the aid of statistical parameters determined from the streamflow data and special plotting papers, it is possible to estimate say the 10,000-year flood from a record of 20 years duration. That such practices are dangerous has been well emphasized by the ASCE Subcommittee on Review of Flood Frequency Methods.(26) A short streamflow record obtained during a climatically atypical series of years is a poor sample to use for estimating large floods of infrequent occurrence. Generally speaking, the smaller the frequency required, the more accurate the estimate becomes.

Chow⁽⁶⁾ compared the equations for several of the better known analytical procedures developed for extending frequency curves. He showed that different methods based on identical data will produce different flood magnitudes for a given frequency. Nevertheless, he went on to demonstrate that the different methods are similar in structure; that is, a general formula was

applicable to all of the methods with a "frequency factor," contained in the formula, constituting the only variation.

A flood frequency curve for a Kansas river⁽¹⁹⁾ is shown in Fig. 4. This curve is plotted on Gumbel probability paper⁽²⁵⁾ and was computed from the recurrence intervals given by Eqn. 1. If the observed annual floods fitted the theory of extreme values, which is the basis for the Gumbel frequency distribution of hydrologic data, they would fall along a straight line. It can be seen that for practical purposes this does occur except for the highest flood of record which plots noticeably above the fitted straight line. Such deviations of one or more of the highest floods are quite common and, because of their confusing position, have called forth a variety of explanations for their existence. Depending upon the basin in question, one or more of three situations may apply; (a) the hydraulics of large floods, involving channel characteristics and valley storage, may differ from that of small floods; (b) the cause of the high floods may be different from that of low floods; the contrasting nature of rain floods and snow floods in mountainous basins furnishes a good example; and (c) based on the laws of probability, an unusually large flood can occur in a relatively short length of record. Causes (a) and (b) represent changes within the annual flood record at a given gaging station and suggest that two different populations are intermingled; it follows, therefore, that not one but two straight lines of differing slope should be used to fit such flood frequency curves. On the other hand, cause (c) implies that if the record were sufficiently long the unusually high flood would plot on the straight line with a much longer recurrence interval. Ignoring such floods is then an obvious recourse on the frequency curve. Yet, it is well to note that just as a 100-year flood will be outstanding in a 20-year record, so will a 1000-year flood in a 100-year record.

The recurrence interval for a given flood magnitude was defined as the average time interval within which the flood will be equaled or exceeded once. Thus, a common assumption is that in a 100-year record it is highly probable that one flood will occur representative of a 100-year recurrence interval. But, from probability theory, it can be stated that the chances of this occurring are small. To illustrate this, data from the ASCE flood frequency report⁽²⁶⁾ are plotted in Fig. 5. Here, a mythical 10,000-year record was assumed which should contain 100 floods having a recurrence interval of 100 years. Fig. 5 shows that only 37 centuries contained one 100-year flood, whereas another 37 had none and 26 others had more than one.

In hydrologically homogeneous areas frequency curves developed on gaged streams can be employed to estimate flood frequencies on ungaged areas.⁽²⁶⁾ Flood magnitudes are plotted against drainage area for equal frequencies. Lines fitting the data form a family of curves for different frequencies, thereby enabling frequency curves to be estimated for an ungaged basin within the area. Fig. 6 illustrates the result for the Atlanta, Georgia, metropolitan area.⁽⁵⁾ Flood volumes can be treated in a similar manner; Fig. 7 shows the relation among discharge, duration, frequency, and area on one set of coordinates for a California stream.⁽⁴⁾

When basins in nonhomogeneous areas are compared on a discharge-area-frequency plot, a scatter develops indicating that parameters other than area are involved. Topographic, geologic, and climatic factors cause these differences. For example, 25-year floods in Kansas,⁽¹⁹⁾ shown in Fig. 8, display definite regional patterns. If the particular factors and their interrelations were understood, it would be possible to extend the applicability of flood

frequency estimates on a more general basis. Research has indicated that a better understanding of this important problem is possible. Efforts now underway by the Soil Conservation Service, Geological Survey, and Bureau of Public Roads hold promise of better estimates of flood frequencies in the future.

An important aid for determining the reliability of a theoretical flood frequency curve is furnished by confidence limits. Gumbel⁽¹⁶⁾ developed the technique for finding confidence limits of annual floods after which Chow⁽⁷⁾ reduced the computations to a simple procedure. Confidence limits are lines constructed above and below a frequency curve such that approximately 68 percent (one standard deviation) of all observed floods will fall within the band. The confidence limits are functions of the flood frequency, the length of record, and the standard deviation of the observed flood frequency distribution. For illustration, the control curves defining the confidence limits for a peak flood frequency curve of a Utah stream are shown in Fig. 9. These indicate that from the available data there is a 68 percent probability of estimating the 100-year flood within an error of ± 20 percent.

Frequency Analysis of Low Flows

Low flows can be analyzed on a frequency basis in an identical manner of that of flood flows. Instead of selecting peak flows, the lowest recorded discharges each year are employed. If droughts are defined as the annual minima of discharges,⁽¹⁷⁾ drought frequency curves are obtained. Then too, droughts of varying durations correspond to flood volumes. Information of this type has important engineering applications for water supplies dependent upon stream-flow, for hydroelectric power developments, and for estimating storage requirements.

Because the analysis and interpretation of drought frequency curves follows that heretofore described for flood frequencies, two illustrations will suffice. Fig. 10 shows a group of drought frequency curves for the Milwaukee River at Milwaukee⁽¹³⁾ with durations varying from one day to half a year. Examples of the interpretation of the curves can be seen from the two circled points. These indicate that the mean daily discharge will fall below 27 cfs at average intervals of two years, while the average weekly discharge will fall below 27 cfs only at average intervals of five years. Another method of representing this type of data is given in Fig. 11. Here minimum flows of the West Branch Mahoning River in Ohio⁽¹¹⁾ are plotted against duration. Reading the graph, it can be seen that the minimum mean monthly discharge of record equaled 0.05 cfs/mi², but at the same time 75 percent of the years had a mean monthly discharge of at least 0.07 cfs/mi² and 50 percent had 0.095 cfs/mi².

Frequency Analysis of All Flows

Rather than developing frequency curves from only small segments of a streamflow record, analysis of the entire period of record has several engineering applications. Here, all of the mean daily flows constitute a population. Data are usually plotted on coordinates of discharge versus percent of time (of the period of record) during which any given flow rate was equaled or exceeded to form a flow-duration curve.

The flow-duration curve is familiar to many hydraulic engineers. Because it encompasses the highest flow to the lowest, it is widely employed for planning and design purposes. Studies for surface water supplies, hydroelectric power developments, dilution and disposal of sewage and industrial wastes, construction diversions, and sediment transportation are based on flow-duration curves. Then too, the hydrologic characteristics of two drainage basins can be compared by means of the flow-duration curves of each. In certain situations, it is even possible to treat the upper and lower portions of a flow-duration curve as flood and drought frequency curves.

To prepare a flow-duration curve based on mean daily discharges, the number of discharges falling within predetermined intervals are counted. Discharges are divided by the mean discharge forming a dimensionless discharge ratio which facilitates comparison with other streams. The ratios are then plotted on a logarithmic ordinate and the cumulative time percentages on a probability abscissa. The flow-duration curve is sketched between adjacent plotted points. Log-probability paper enables a wide range of discharges to be plotted on one sheet and at the same time reduces the curvature of the flow-duration curve.

Other than daily discharges can be used in developing a flow-duration curve; however, the shorter the period selected, the more definitive the curve becomes of the streamflow variations. Daily, monthly, and annual flow-duration curves are shown in Fig. 12 for an Ohio stream.⁽¹⁰⁾ Notice the greater variability of flow displayed by the curves based on the shorter time periods.

Curves based on mean daily discharges of four California streams are presented as Fig. 13. It can be seen that marked differences in flow distribution exist among these streams, particularly regarding the highest and lowest flows. An investigation by Todd⁽²⁷⁾ of these and other California streams revealed that climatic and basin differences were strongly reflected in the shape of flow-duration curves. In mountain basins, where high flows result primarily from spring snowmelt runoff, the longer duration of these flows forms a relatively flat slope (Salmon River, Fig. 13). On the other hand basins experiencing high flows from large short-duration rainfall show a relatively steep upper slope (Huasna River, Fig. 13). In a similar manner the shape of the lower portion of the curve is indicative of the ground-water storage capacity and aquifer permeability.⁽⁹⁾ Curves for Arroyo Seco, Huasna River, and Thames Creek in Fig. 13 show a pronounced steepness in the lower portions which is typical of basins containing only limited ground-water storage. In contrast, the flatter slope of Salmon River indicates a large, stable base flow.

One limitation of flow-duration curves is that small changes in slope disguise important variations in discharge distribution. Because a flow-duration curve is the integral of a frequency distribution, slope variations of a flow-duration curve appear as variations in ordinates on a frequency distribution. Three such distributions are shown in Figs. 14, 15, and 16. Fig. 16 is based upon the same Salmon River data given in Fig. 13 and points up the greater sensitivity of the frequency distribution.

Fig. 14 illustrates the common skewed distribution encountered in hydrologic data. It should be noted that logarithms of discharge appear on the abscissa; if discharges were plotted on a linear scale, the skewness would be more strongly emphasized. The dashed curve is a theoretical Pearson Type III frequency curve⁽¹⁴⁾ closely fitting the observed distribution. For

comparison Fig. 15 shows the frequency distribution of a stream located not far from that of Fig. 14. The previous curve fitting is not applicable because of the different distribution of low flows. This curve does not approach zero frequency at the lower end; instead the low flows form a secondary peak leading to periods of no flow, which create a discontinuity on the logarithmic discharge scale. The Salmon River distribution in Fig. 16 with its double maximum displays a third type of frequency distribution. From a study of the seasonal flow distribution, it was found that the lower maximum was caused by the sustained base flow of uniform magnitude occurring during the fall and that the upper maximum was associated with runoff from winter rains supplemented by spring snowmelt runoff.

CONCLUSION

The purpose of this paper is to promote an understanding of frequency analysis of streamflow data. Emphasis was placed on concepts and advantages of such procedures; illustrations were inserted wherever possible to clarify points. References provide ready access to the omitted computational procedures.

Whenever an engineering problem calls for information based on quantities of streamflow, whether they be high, low, or all flows, frequency analysis can usually be helpful. It is hoped that a greater awareness of the analytic procedures, results, and limitations will continue the trend of statistical analysis becoming a more valuable tool for the civil engineer.

ACKNOWLEDGMENT

The material presented herein is based on previous contributions of engineers, hydrologists, and statisticians. An effort has been made to acknowledge by reference the works or figures of others. The author is indebted to Mr. W. C. Ackermann and Mr. J. B. Tiffany for their encouragement in the preparation of this paper.

REFERENCES

1. Beard, L. R., 1943, Statistical analysis in hydrology, Trans. Amer. Soc. Civil Engrs., v. 108, pp. 1110-1160.
2. Beard, L. R., 1952, Statistical methods in hydrology, Office, Chief of Engineers, Dept. of the Army, Washington, D. C., 35 pp.
3. Beard, L. R., 1954, Estimation of flood probabilities, Proc. Amer. Soc. Civil Engrs., v. 80, Sep. no. 438, 21 pp.
4. California State Water Resources Board, 1951, Water resources of California, Bull. 1, Sacramento, 648 pp.
5. Carter, R. W. and S. M. Herrick, 1951, Water resources of the Atlanta metropolitan area, Circular 148, Geological Survey, Washington, D. C., 19 pp.
6. Chow, V. T., 1951, A general formula for hydrologic frequency analysis, Trans Amer. Geophys. Union, v. 32, pp. 231-237.

7. Chow, V. T., 1953, Frequency analysis of hydrologic data with special application to rainfall intensities, Univ. of Illinois Engr. Exp. Sta. Bull. 414.
8. Chow, V. T., 1954, The log-probability law and its engineering applications, Proc. Amer. Soc. Civil Engrs., v. 80, Sep. no. 563, 25 pp.
9. Cross, W. P., 1949, The relation of geology to dry-weather stream flow in Ohio, Trans. Amer. Geophys. Union, v. 30, 563-566.
10. Cross, W. P. and R. J. Bernhagen, 1949, Ohio stream-flow characteristics, Pt. 1 - Flow duration, Bull. 10, Ohio Dept. of Natural Resources, Division of Water, Columbus.
11. Cross, W. P. and E. E. Webber, 1950, Ohio stream-flow characteristics, Pt. 2 - Water supply and storage requirements, Bull. 13, Ohio Dept. of Natural Resources, Division of Water, Columbus.
12. Dalrymple, T., 1946, Use of stream-flow records in design of bridge waterways, Proceedings of the 26th Annual Meeting, Highway Research Board, Washington, D. C., pp. 163-179.
13. Drescher, W. J., F. C. Dreher, and P. N. Brown, 1953, Water Resources of the Milwaukee area, Wisconsin, Circular 247, Geological Survey, Washington, D. C. 42 pp.
14. Foster, H. A., 1924, Theoretical frequency curves and their application to engineering problems, Trans. Amer. Soc. Civil Engrs., v. 87, pp. 142-203.
15. Foster, H. A., 1934, Duration curves, Trans. Amer. Soc. Civil Engrs., v. 99, pp. 1213-1267.
16. Gumbel, E. J., 1942, Statistical control curves for flood discharges, Trans. Amer. Geophys. Union, v. 23, pt. 2, pp. 489-509.
17. Gumbel, E. J., 1954, Statistical theory of droughts, Proc. Amer. Soc. Civil Engrs., v. 80, Sept. no. 439, 19 pp.
18. Hazen, R., 1956, Economics of stream flow regulation, Jour. Amer. Water Works Assoc., v. 48, no. 7, pp. 761-767.
19. Izzard, C. F., 1953, Peak discharge for highway drainage design, Proc. Amer. Soc. of Civil Engrs., v. 79, Sep. no. 320, 10 pp.
20. Jarvis, C. S. and others, 1936, Floods in the United States, their magnitude and frequency, Water-Supply Paper 771, U. S. Geological Survey, Washington, D. C., 497 pp.
21. Lane, E. W. and Lei, K., 1950, Stream-flow variability, Trans. Amer. Soc. Civil Engrs., v. 115, pp. 1084-1134.
22. Langbein, W. B., 1949, Annual floods and the partial-duration series, Trans. Amer. Geophys. Union, v. 30, pp. 879-881.
23. Linsley, R. K., M. A. Kohler, and J. L. H. Paulhus, 1949, Applied hydrology, McGraw-Hill, New York, pp. 544-559.
24. Mitchell, W. D., 1950, Water-supply characteristics of Illinois streams, Illinois Dept. of Public Works and Bldgs., Division of Waterways, Springfield, 311 pp.

25. Potter, W. D., 1949, Simplification of the Gumbel method for computing probability curves, Soil Conservation Service TP-78, Washington, D. C., 22 pp.
26. Subcommittee of the Joint Division Committee on Floods, 1953, Review of flood frequency methods, Trans. Amer. Soc. Civil Engrs., v. 118, pp. 1220-1230.
27. Todd, D. K., 1953, Stream-flow frequency distributions in California, Trans. Amer. Geophys. Union, v. 34, pp. 897-905.

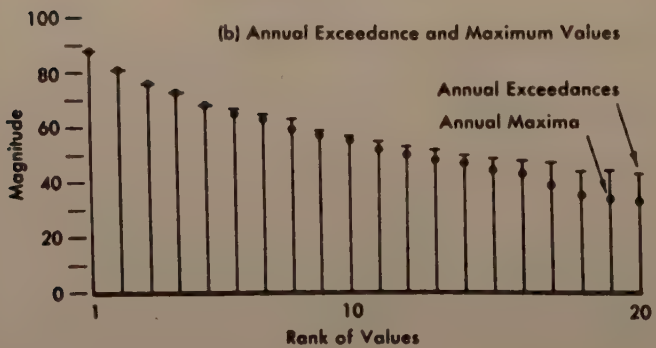
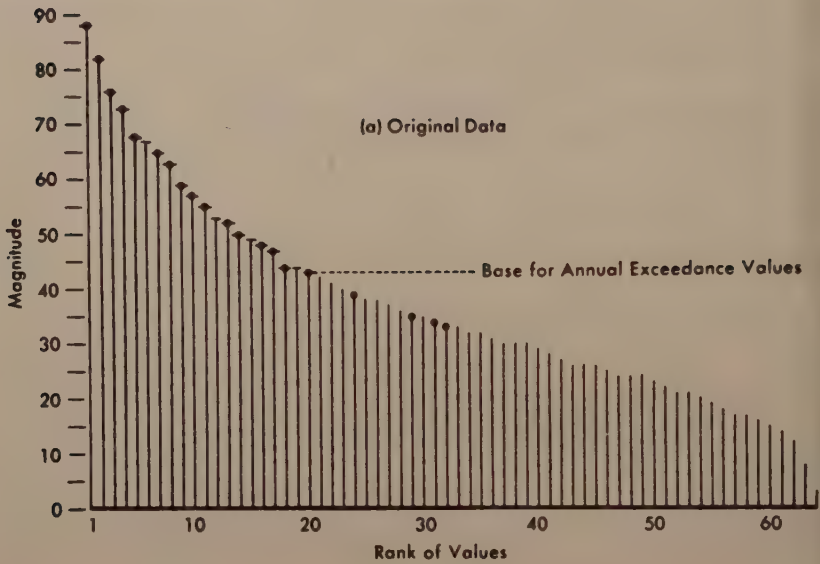


FIG.1 HYDROLOGIC DATA ARRANGED BY ORDER OF MAGNITUDE (AFTER 7)

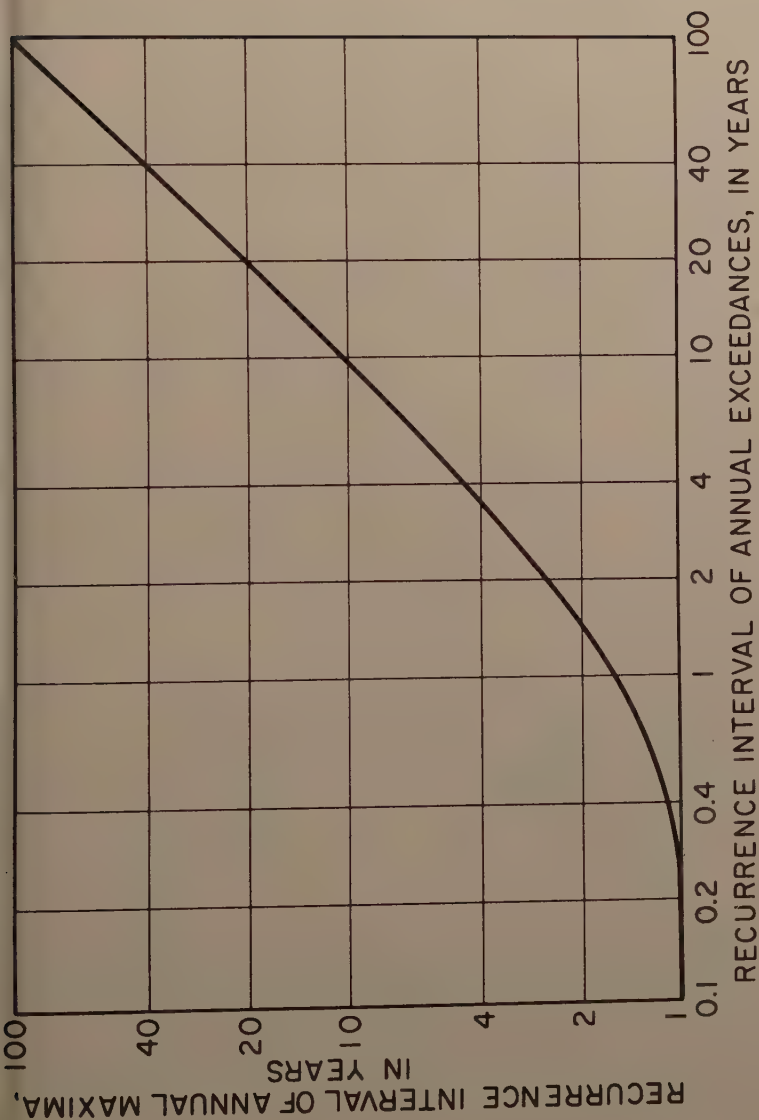


FIG. 2 RELATIONSHIP BETWEEN RECURRENCE INTERVALS
BY TWO METHODS. (AFTER 7)

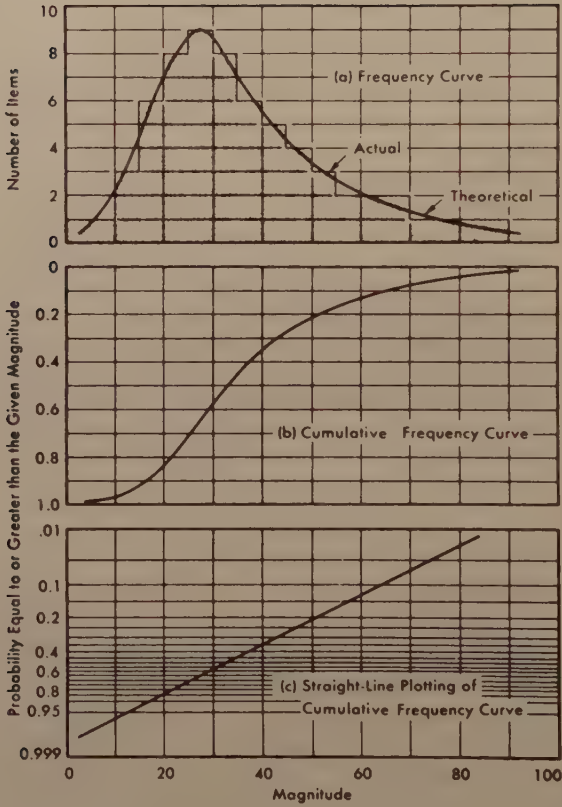


FIG. 3 GRAPHICAL REPRESENTATION OF FREQUENCY DISTRIBUTION OF HYPOTHETICAL FLOOD DATA (AFTER 7)

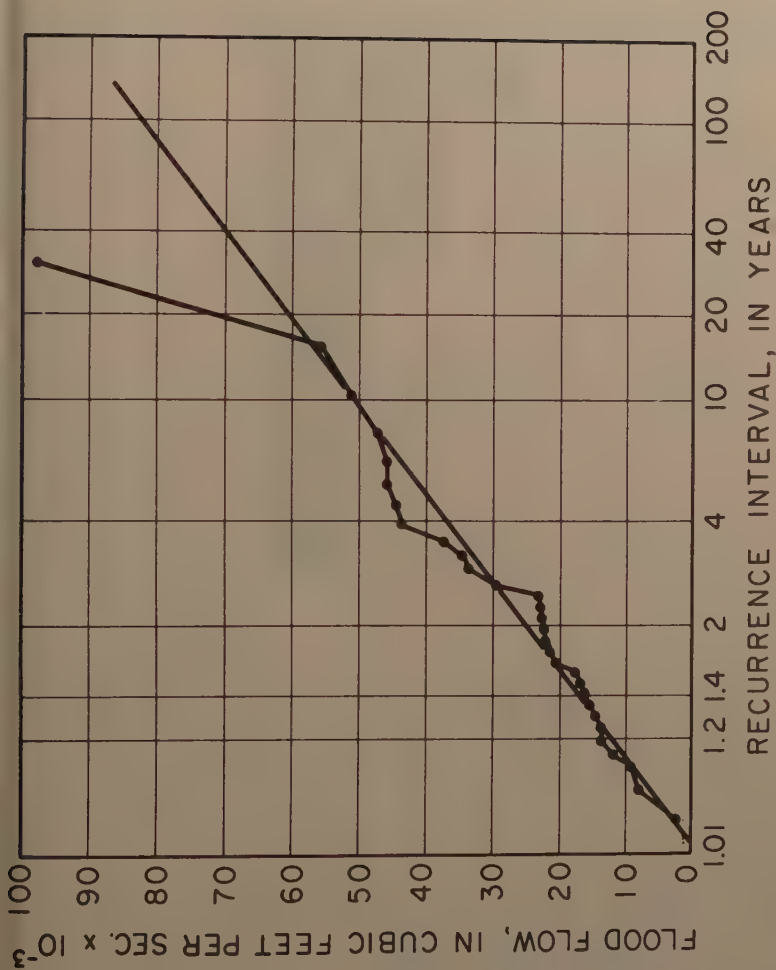


FIG. 4 FREQUENCY CURVE, BIG BLUE RIVER AT RANDOLPH, KANSAS
(AFTER 19)

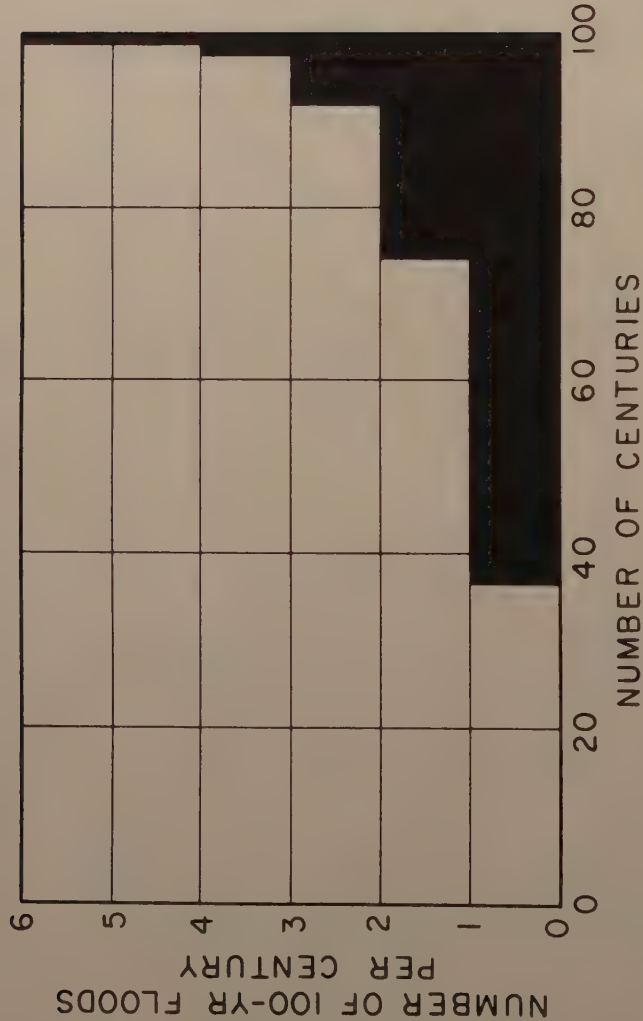


FIG. 5 PROBABLE DISTRIBUTION OF 100-YEAR FLOODS
IN 10,000 YEARS

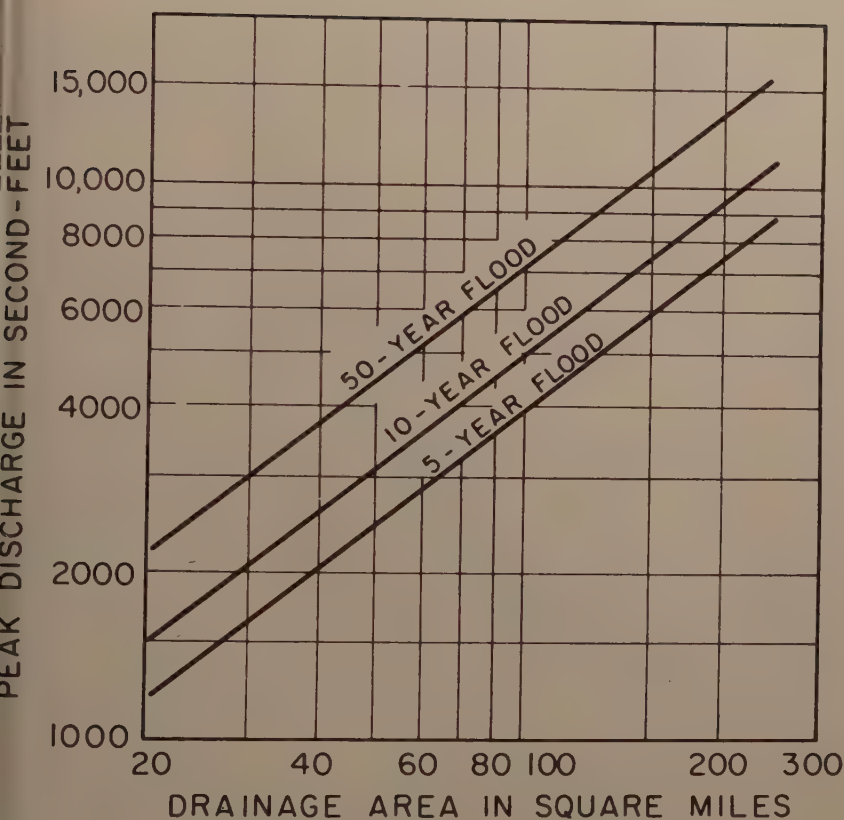


FIG. 6 FREQUENCY OF ANNUAL FLOODS IN THE ATLANTA, GEORGIA, METROPOLITAN AREA (AFTER 5)

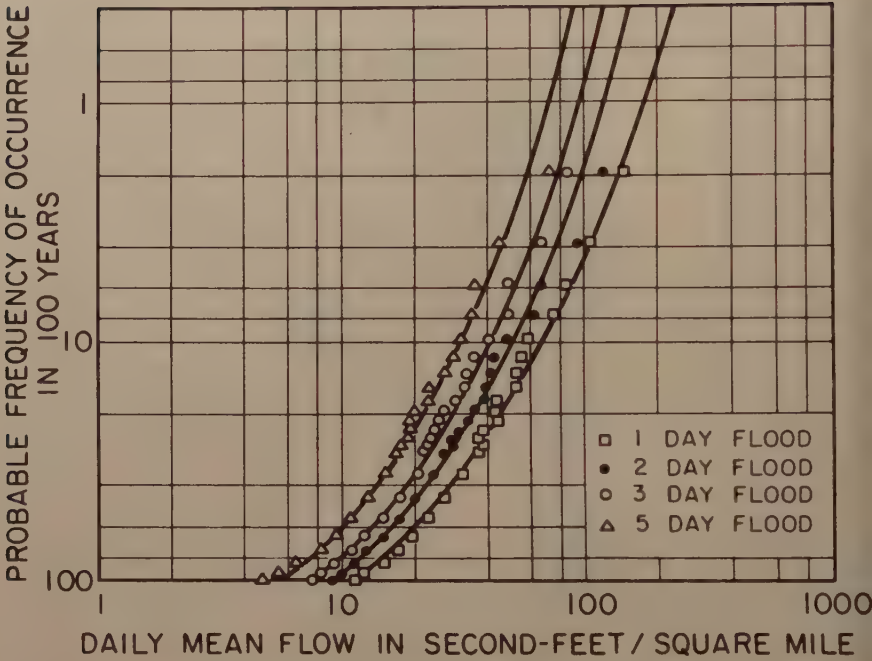


FIG. 7 FLOOD FREQUENCY CURVES FOR VARIOUS DURATIONS, SAN GABRIEL RIVER NEAR AZUSA, CALIFORNIA (AFTER 4)

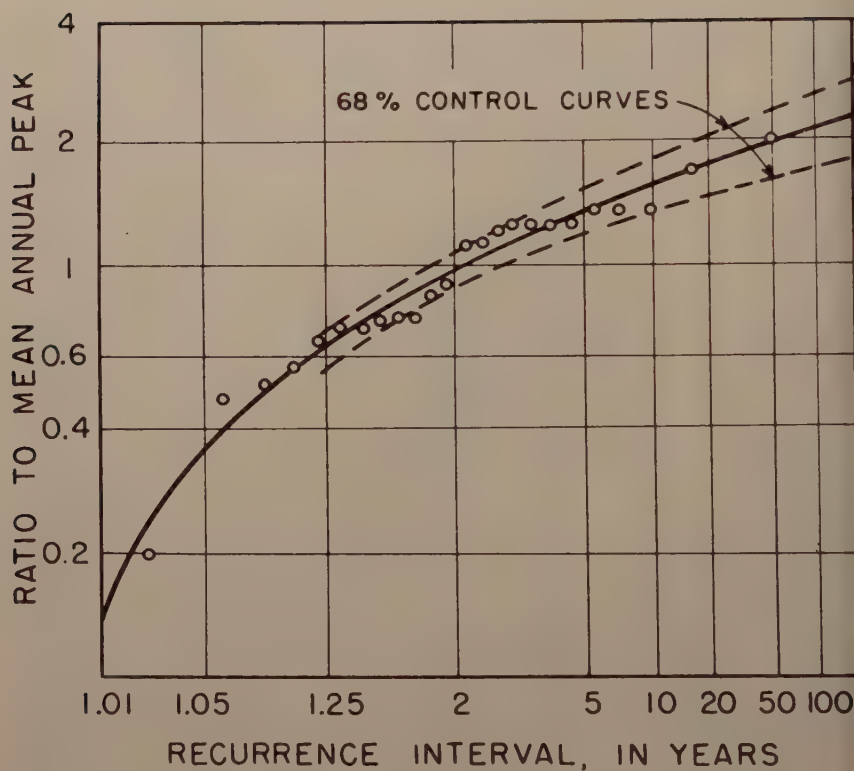


FIG. 9 FREQUENCY CURVE AND CONFIDENCE LIMITS, ASHLEY CREEK NEAR VERNAL, UTAH

Journal of the
HYDRAULICS DIVISION
Proceedings of the American Society of Civil Engineers

BUTTERFLY VALVE FLOW CHARACTERISTICS

M. B. McPherson,¹ A.M. ASCE, H. S. Strausser,² and
J. C. Williams, Jr.,³ Junior Members, ASCE
(Proc. Paper 1167)

ABSTRACT

Flow coefficients are given for free and submerged discharge as well as two cases with enclosed flow piping. The effects of type of installation, blade shape and closure angle for control-type valves (using water) are demonstrated. Correlation of analytical relations with performance provides a basis for predicting incipient cavitation.

INTRODUCTION

Butterfly valves installed in pipes or penstocks are normally used for one of two basic services: either as closure or "on-off" valves, or for flow rate control or "governing." Valuable information for fully-open service has been presented elsewhere.⁽¹⁾4 Nearly all of the present discussion is limited to the flow of water through control-type valves for near-closed to near-open positions.

The three major geometric variables affecting flow performance, in order of relative importance, are: (a) piping arrangement, (b) shape of blade, and (c) closing angle. For most applications flow characteristics are a function of geometry only. Available information on flow coefficients is limited and specialized. The first attempt at collecting and collating published data was made by Cohn,⁽²⁾ but major variables were not delineated.

This paper includes a demonstration of the effects of geometric variables and presents a basis for the analytical determination of flow coefficients. Also presented is a basis for the prediction of anticipatory minimum pressures related to cavitation inception.

Note: Discussion open until July 1, 1957. Paper 1167 is part of the copyrighted Journal of the Hydraulics Division of the American Society of Civil Engineers, Vol. 83, No. HY 1, February, 1957.

1. Associate Prof. of Civ. Eng., Lehigh Univ., Bethlehem, Pa.
2. Asst. Prof. of Civ. Eng., Univ. of Washington, Seattle, Wash.
3. Senior Project Engr., CDC Control Services, Inc., Hatboro, Pa.
4. Numbers in parentheses refer to references listed at the end of the paper.

Definition of Terms

Installations with equal internal diameters of valve body and upstream pipe have been investigated, with all variations in piping arrangement made beyond the valve. In figure 1, Station (1) is sufficiently upstream from the valve as to insure unaffected, parallel streamlines (uniform flow). Conditions at Station (3) are variable. Station (2) is generally within the valve body and represents the cross-section of the jets where uniform flow takes place. For the sake of correlation, the flow formula adopted by Cohn is used throughout:

$$Q = C_Q D^2 \sqrt{g} \sqrt{\Delta H} \quad (1)$$

- where Q is the discharge in cu. ft./sec.,
 C_Q is a coefficient of flow,
 D is the internal diameter of the valve body in feet,
 g is 32.2 ft./sec./sec.,
 ΔH is the net difference in total head between Station (1) and (3), in feet of the fluid flowing; i.e., the valve loss.

In order that the reader can immediately appreciate the effect of piping arrangement on the flow coefficient, the following flow coefficient curves are presented in Figure 2 for a specific valve. Station (3) for each of the curves respectively is:

- Downstream from a 4" x 6" diffuser, 9" long;
- in a pipe of same diameter as Station (1) and the valve,
- in the atmosphere beyond live jet (water discharging into air); and
- in still water beyond jet (water discharging into water).

Referring again to Figure 1, "left" applies to the downstream half of the blade and "right" to the half projecting upstream of the hub. For each value of the angle of inclination of the blade, α_0 (0° at wide open position), there is a corresponding specific value of x and y , left and right. The z and y dimensions may be affected by viscosity and might therefore vary with both α_0 and a Reynolds number.

This paper is restricted to a consideration of incompressible turbulent flow.

Basic Analysis - Free Discharge

Flow between Stations (1) and (2) is accompanied by an increase in velocity with distance, a highly efficient process. For all installations reported here, the head or energy loss between these two stations due to the flow acceleration is therefore neglected as being relatively minor.

In true free discharge the pressure at Station (2) is atmospheric. Since uniform flow occurs at this station (so long as z_L does not project beyond the valve body), the pressure distribution in the jets at this station is hydrostatic and at equal elevation the velocities of the two jets are equal.

If the areas of the two jets at Station (2) are known, it is then possible to estimate the jet velocity head (in this case, the head or energy lost from the

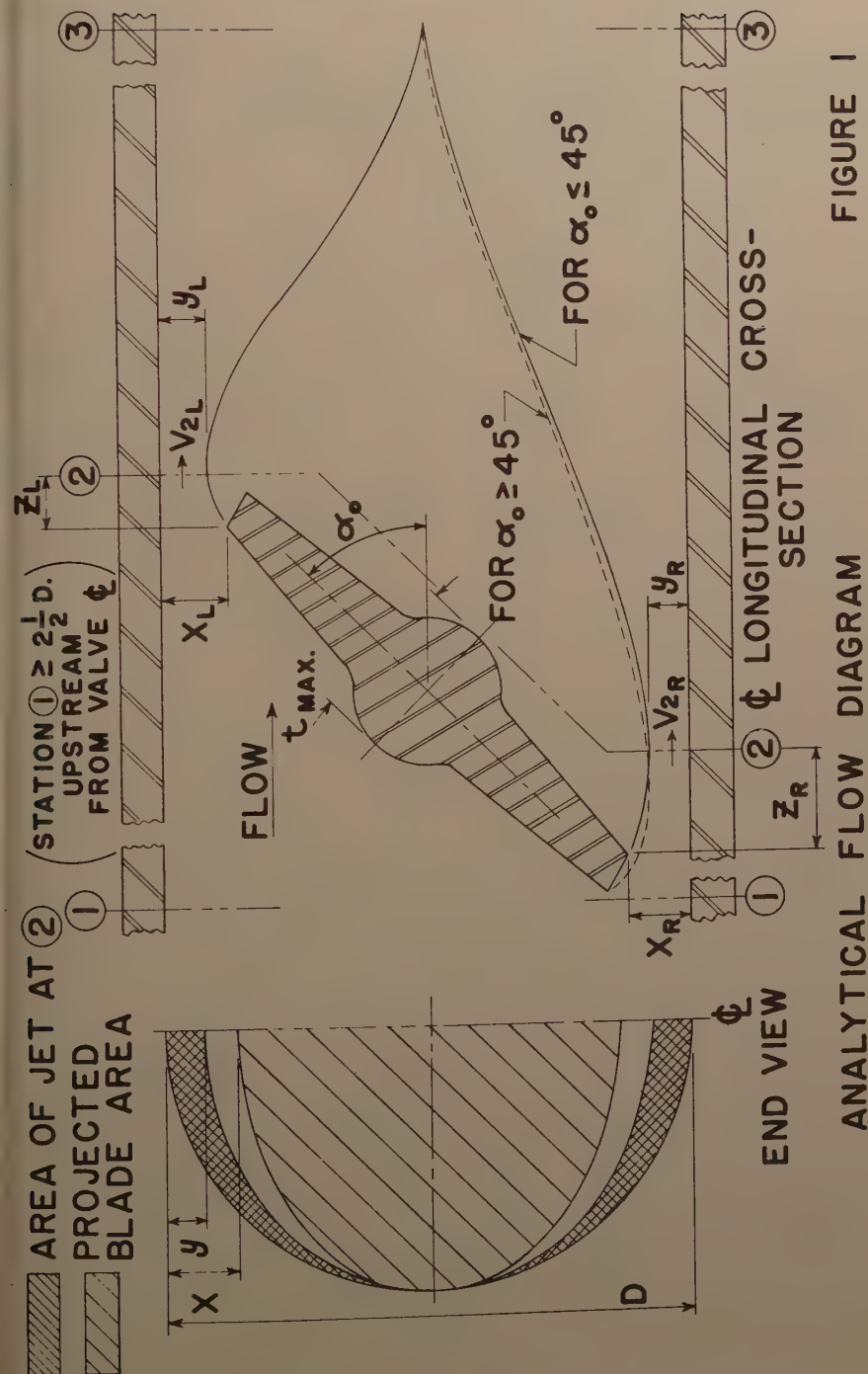


FIGURE 2

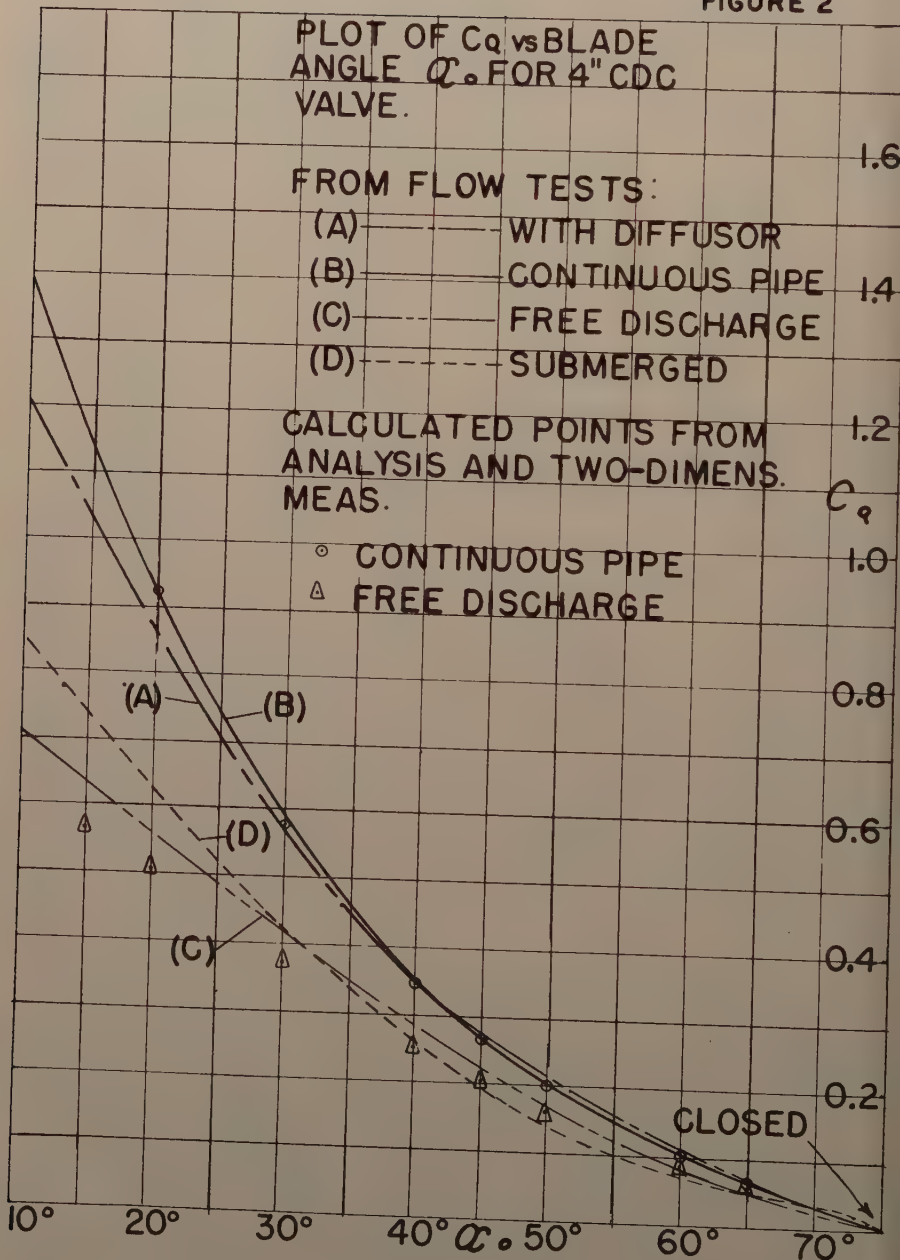
PLOT OF C_q vs BLADE
ANGLE α FOR 4" CDC
VALVE.

FROM FLOW TESTS:

- (A) ——— WITH DIFFUSOR
- (B) ——— CONTINUOUS PIPE
- (C) - - - - - FREE DISCHARGE
- (D) - - - - - SUBMERGED

CALCULATED POINTS FROM
ANALYSIS AND TWO-DIMENS.
MEAS.

- CONTINUOUS PIPE
- △ FREE DISCHARGE



system) for a given blade setting, without recourse to an actual flow measurement.

The jet area at Station (2) is bounded by a circle and an ellipse. The jet area on one side is therefore equal to $\pi Dy/4$. Since the jet area is a function of the variable y , measurements of the jet thickness in a two-dimensional flow model, representing a narrow section of the center part of the blade, should provide a basis to understand and predict prototype performance.

Two-Dimensional Flow Distribution Study and Prototype Verification - Free Discharge - 6-Inch CDC Valve

A two-dimensional plastic flow section (Figure 3) was constructed (cross-section 8" x 1") and measurements of y_L and y_R were made for the four blade shapes shown in Figure 4.

The length from the centerline of the blade to the end of the valve body is $5D/8$ for both the 4-inch and 6-inch CDC prototype valves (for consistency this same length was used for all four blade shapes in the two-dimensional free discharge tests).

Since the pressure at both left and right jets at Station (2) is zero, both jet velocities are equal. It follows then that

$$V_{2L} = q_L / Y_L \quad (2-a)$$

and
$$V_{2R} = q_R / Y_R \quad (2-b)$$

then
$$q_L / q_T = \frac{Y_L}{Y_L + Y_R} \quad (2-c)$$

where $q_L + q_R = q_T$, total flow in cu. ft./sec./unit width. For three-dimensional flow, the area of one jet is $\pi Dy/4$, rather than y as above, but the discharge ratio is the same -

$$Q_L / Q_T = \frac{Y_L}{Y_L + Y_R} \quad (2-cc)$$

where $Q_L + Q_R = Q_T$, total flow in cu. ft./sec.

Gaden(3) was probably the first to make an issue of the fact that the quantity of flow leaving each side of the blade is not equal.

To substantiate Gaden's contention, free discharge tests were run on the two-dimensional apparatus and measurements of y and q were made at various blade angles, using a valve body length equivalent to the prototype valve, the 6-inch CDC valve. Measurements of flow distribution were made also on the prototype valve. The results appear in Table I, and were of sufficient precision and promise to encourage further study.

In the prototype tests, a limiting minimum Reynolds number ($N_R = V_1 D / \nu$, where V_1 is the average approach pipe velocity, D is the upstream pipe and valve diameter and ν is the fluid kinematic viscosity in ft.²/sec.) was found

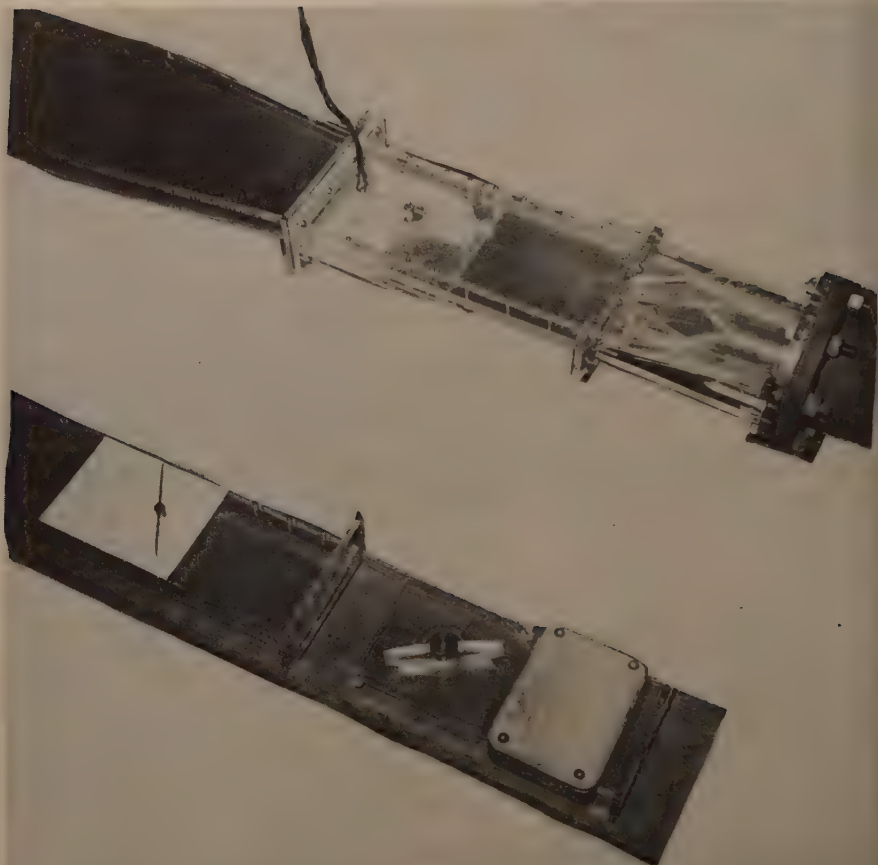
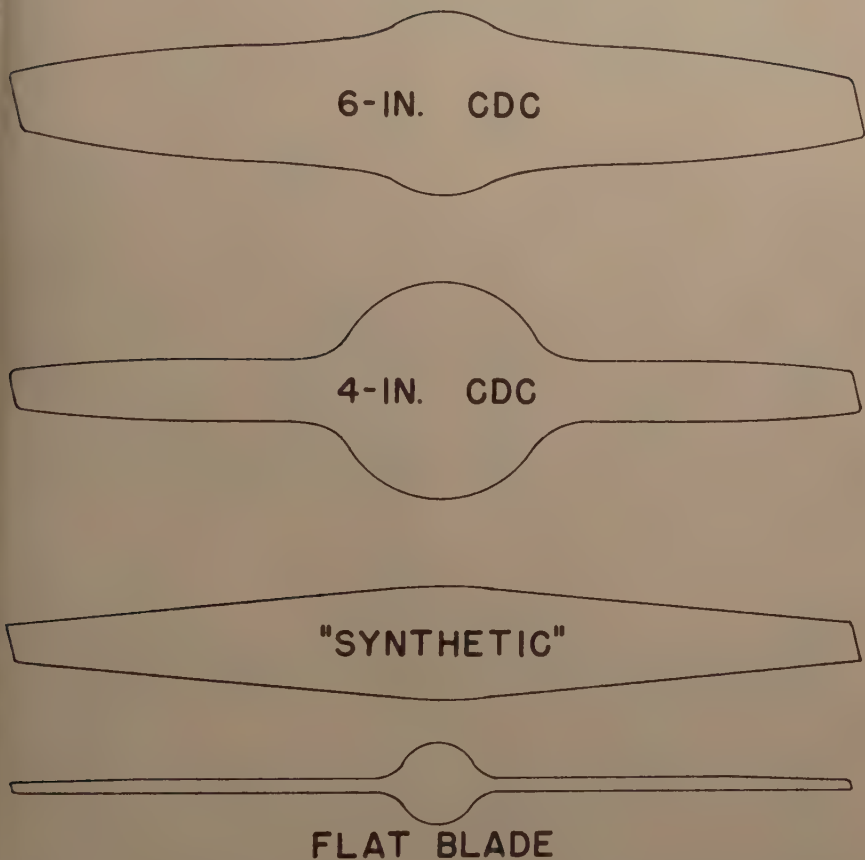


FIGURE 3

TWO DIMENSIONAL JET APPARATUS
SHOWN SET UP FOR THE 4" CDC VALVE FOLLOWED BY A DIFFUSOR

(6" Free Discharge Piece and Extension for
"Continuous Pipe" are shown at bottom of photo).



BLADE PROFILES
TWO-DIMENSIONAL STUDY
(REPRESENT PROFILES AT ϕ OF PROTOTYPE)

FIGURE 4

for a constant flow coefficient, C_Q , as depicted in Figure 5. The prototype flow ratios of Table I represent values of N_R in excess of these minimums. Referring again to Figure 5, the ratio Q_L/Q_R ceased to be constant once the N_R fell below the minimum for a constant C_Q . Figure 5 should be a guide for free-discharge conditions in general, but the effect of a different blade shape and/or valve body length would be unknown factors with another valve.

Free Discharge and Submerged Flow Characteristics

For free discharge, then, there is a definite minimum Reynolds number, N_R , for a constant flow coefficient. This is due in part to the fact that y , and particularly Z_L (Fig. 1), may be influenced by boundary-layer effects at lower Reynolds numbers. Z_L might thus be contained within, project beyond or coincide with the termination of the valve body at different N_R values. Also, the jet may be affected by distortion of the spray in the lateral expansion beyond the uniform flow at Station (2). Therefore, if the ratio of jet thickness is upset, both C_Q and Q_L/Q_T will be affected.

As stated previously, the head loss from Station (1) to (2) due to acceleration should be insignificant inasmuch as an increase in velocity obtains. With h being the piezometric head at a given station (pressure head plus elevation), the equation for free discharge into the atmosphere with $h_3 = 0$ becomes:

$$\frac{V_1^2}{2g} + h_1 = \frac{V_2^2}{2g} = \Delta H \quad (3)$$

With submerged flow (flow of water from valve discharging directly into a large body of water), the equation is assumed to be:

$$\frac{V_1^2}{2g} + h_1 - h_3 = \Delta H \quad (4)$$

where h_3 is the depth of still water above the valve centerline. Free discharge tests were run on the 6" CDC valve, and free discharge and submerged tests were run on the 4" CDC valve. The 4" valve test results, given in Table II and plotted in Fig. 2, show that there is a distinct difference between the free discharge and submerged flow values. This difference had been inferred in studying available data, listed in Table III and plotted in Fig. 6.

The Schmidt and Davis data (air flowing into air) are given by Cohn, in his Fig. 7, p. 883, but details are lacking. The Génissiat data⁽⁴⁾ are for a valve body which converges to 84% of the upstream pipe diameter, between the centerline and the end of the valve body, and are included for comparison only. The Dow data are given by Gaden⁽⁵⁾ and apparently are for the 78-inch valve of Fig. 8, p. 667 by Dow.⁽⁶⁾ (The original Génissiat data was given by Laurent).⁽⁷⁾

Note that the data for the 4-inch valve tested under submerged discharge conditions corresponds quite closely with the data of Schmidt and Davis, except in the near-closed positions. This discrepancy can be explained by the

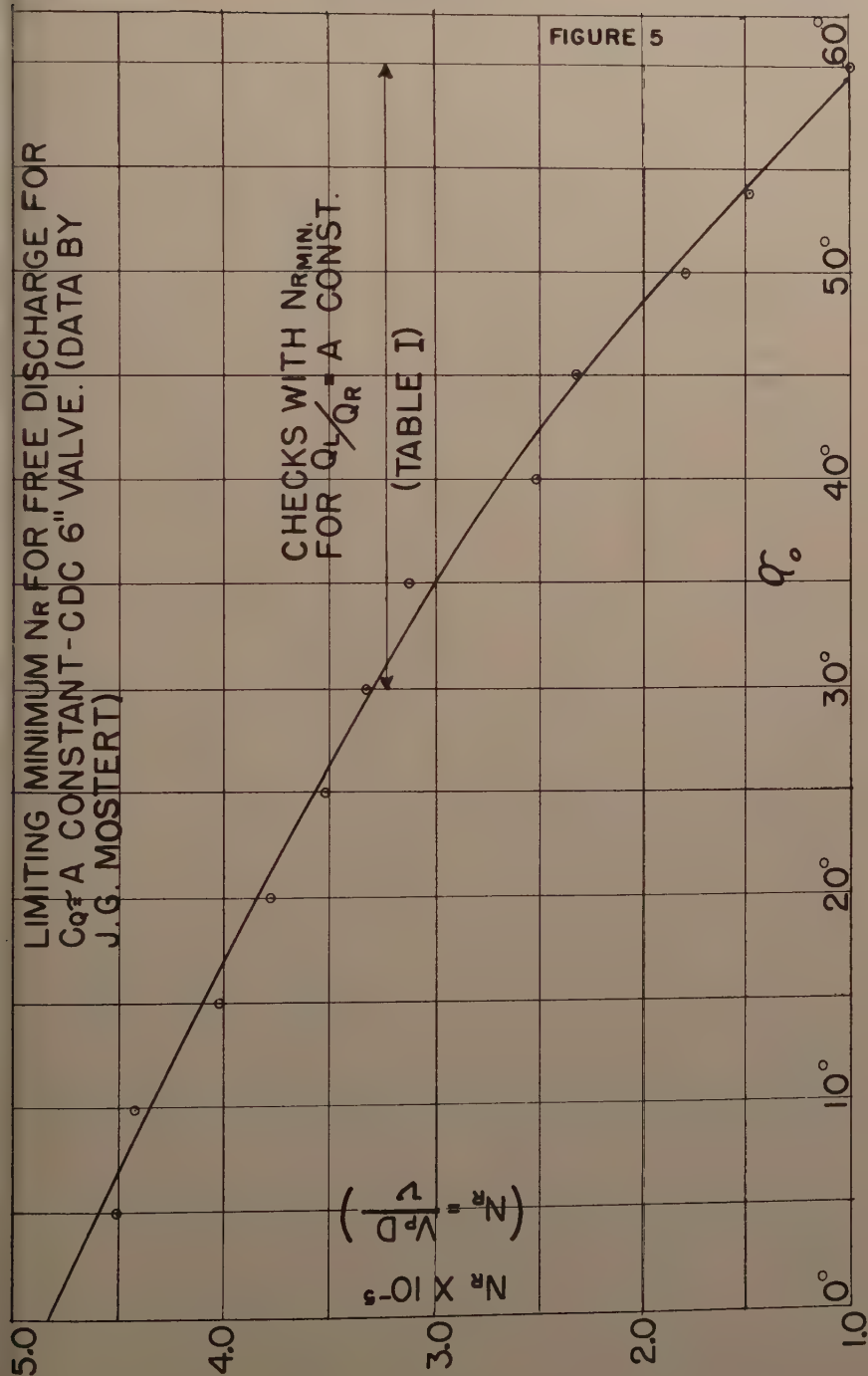


TABLE I

6-INCH CDC VALVE DATA - FREE DISCHARGE

| α° | Two-Dim. App. Measurements | | | Prototype Valve Data | |
|----------------|----------------------------|-------------------------|-------------------------|-----------------------------------|--|
| | $\frac{y_L}{y_L + y_R}$ | $\frac{q_L}{q_L + q_R}$ | Equiv. Pipe N_R | $\frac{Q_L}{Q_L + Q_R}$ (meas.) * | Pipe N_R for Const. C_Q (Fig. 5) |
| 0° | .498 | .500 | 5.6×10^5 | - | 4.8×10^5 |
| 5° | .504 | .504 | 6.1 | - | 4.6 |
| 10° | .560 | .569 | 5.6 | - | 4.3 |
| 15° | .568 | .561 | 5.0 | - | 4.1 |
| 20° | .570 | .568 | 3.9 | - | 3.8 |
| 25° | .555 | .562 | 3.6 | - | 3.6 |
| 30° | .545 | .553 | 3.1 | 0.560 | 3.3 |
| 35° | - | - | - | 0.550 | 3.0 |
| 40° | .556 | .555 | 0.7 | 0.540 | 2.7 |
| 45° | .540 | .548 | 0.6 | 0.535 | 2.3 |
| 50° | .537 | .534 | 0.8 | 0.532 | 1.9 |
| 55° | .513 | .517 | 0.9 | 0.528 | 1.3 |
| 60° | .520 | .504 | 0.7 | 0.525 | 1.0 |
| 65° | .534 | .521 | 0.4 | 0.523 | - |

*At sufficiently high N_R to obtain constant Q-ratio; required minimum N_R close that per constant C_Q of Fig. 5. These are averages of flow measurements on each side of the blade, i.e., Q_L vs Q_T and Q_R vs Q_T .

TABLE II1-INCH CDC VALVEEFFECT OF SUBMERGENCE

| <u>\angle</u> | <u>C_Q (For Jet Submerged)</u> | <u>C_Q (Discharge into Air)</u> |
|----------------------------|---|--|
| 10° | 0.85 | 0.71 |
| 15° | 0.743 | 0.635 |
| 20° | 0.63 | 0.565 |
| 25° | 0.52 | 0.49 |
| 30° | 0.425 | 0.42 |
| 35° | 0.34 | 0.355 |
| 40° | 0.265 | 0.285 |
| 45° | 0.195 | 0.223 |
| 50° | 0.140 | 0.166 |
| 55° | 0.100 | 0.120 |
| 60° | 0.07 | 0.083 |
| 65° | 0.05 | 0.053 |

TABLE III
FLOW COEFFICIENT C_Q

| α | Free Discharge | | Submerged | | Free Discharge | |
|-----------------|------------------|------------------|-----------|---------|-------------------------------------|------|
| | CDC 4" ϕ | CDC 6" ϕ | Schmidt | Davis | Génissiat (Converging) 200 mm | Down |
| 0° | - | - | 1.30 | - | 0.74 | 0.67 |
| 5° | - | 0.634 | - | - | - | - |
| 10° | 0.71 | 0.620 | 0.94 | 0.90 | 0.69 | 0.66 |
| 15° | 0.635 | 0.57 | - | - | 0.61 | 0.61 |
| 20° | 0.565 | 0.528 | 0.65 | 0.64 | 0.53 | 0.55 |
| 25° | 0.490 | 0.476 | - | - | - | 0.47 |
| 30° | 0.420 | 0.405 | 0.45 | 0.44 | 0.38 | 0.40 |
| 35° | 0.355 | 0.345 | - | - | - | 0.33 |
| 40° | 0.285 | 0.285 | 0.31 | 0.29 | 0.26 | 0.27 |
| 45° | 0.223 | 0.232 | - | - | - | - |
| 50° | 0.166 | 0.183 | 0.21 | 0.19 | 0.15 | - |
| 55° | 0.120 | 0.134 | - | - | - | - |
| 60° | 0.083 | 0.088 | 0.11 | 0.11 | 0.09 | - |
| 65° | 0.053 | - | - | - | - | - |
| 70° | - | - | 0.06 | 0.07 | - | - |
| 75° | x | - | - | - | - | - |
| 80° | x | x | 0.04 | 0.02 | - | - |
| 85° | x | x | x | x | x | - |
| 90° | x | x | x | x | x | - |
| Closure | 75° | 77.5° | 90°? | 90°? | 90° | U |
| Upstream ϕ | 6 | 4.7 | unknown | unknown | 0.83? | n |
| t_{\max}/D | 0.269 | 0.225 | unknown | unknown | 0.225 | k |
| Fluid | water | water | Air | Air | water | n |
| | | | | | | o |
| | | | | | | w |
| | | | | | | n |

FIGURE 6

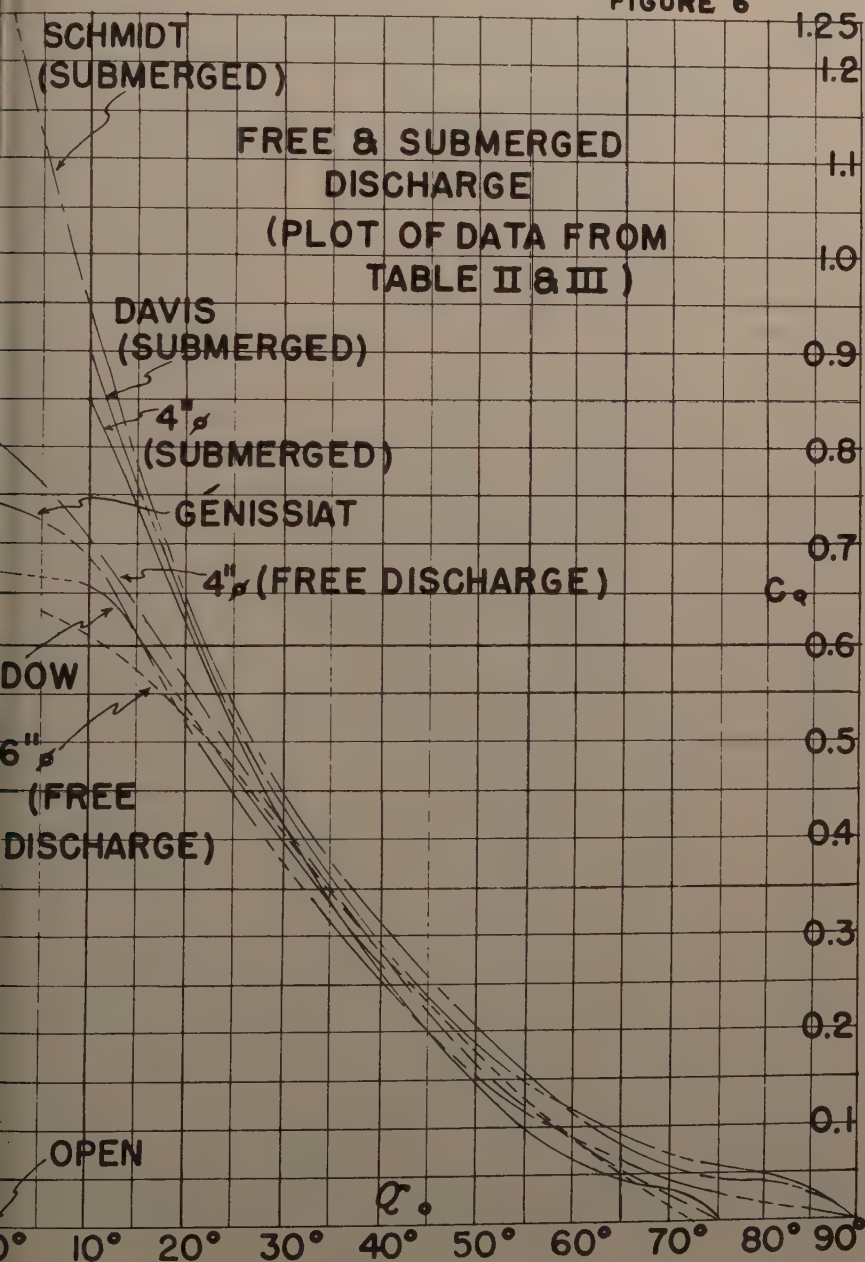
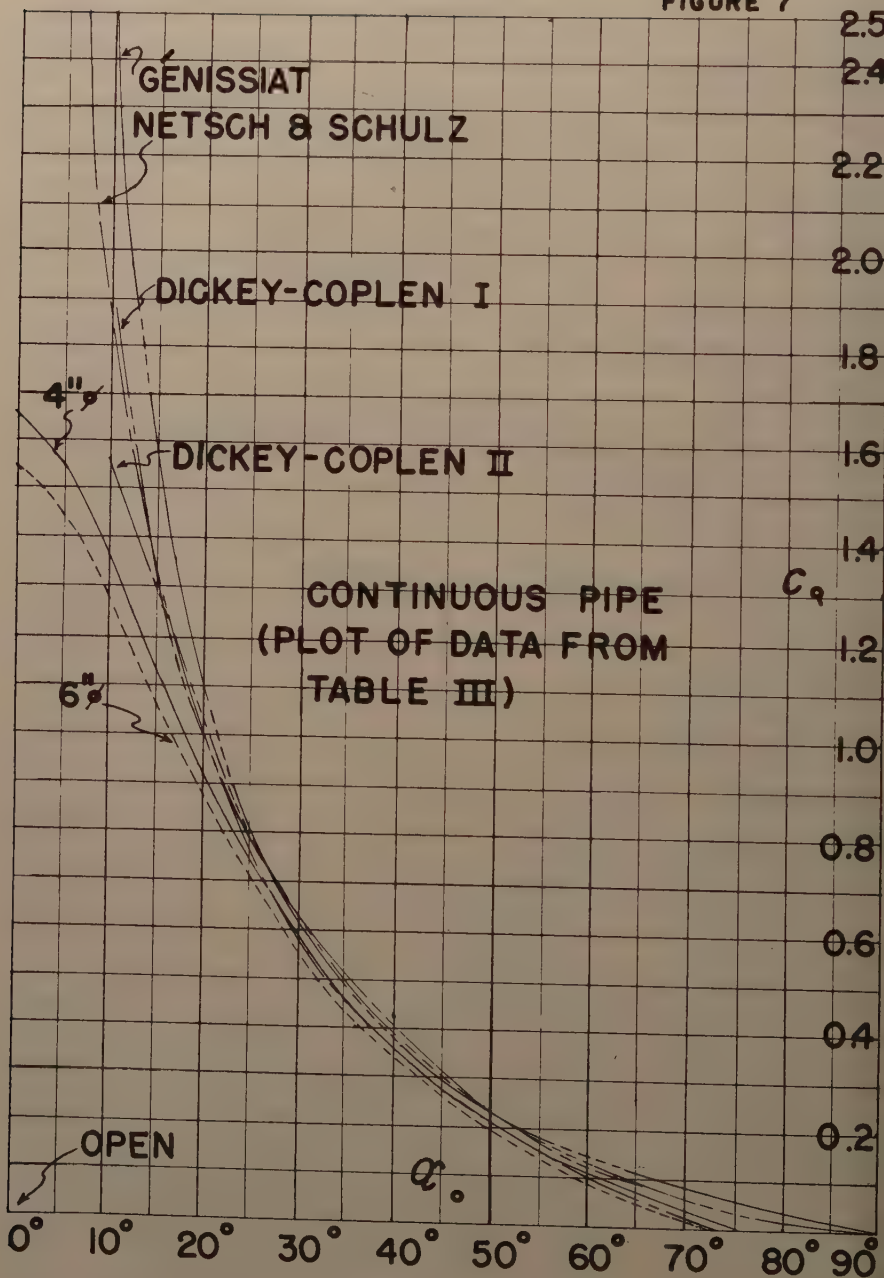


FIGURE 7



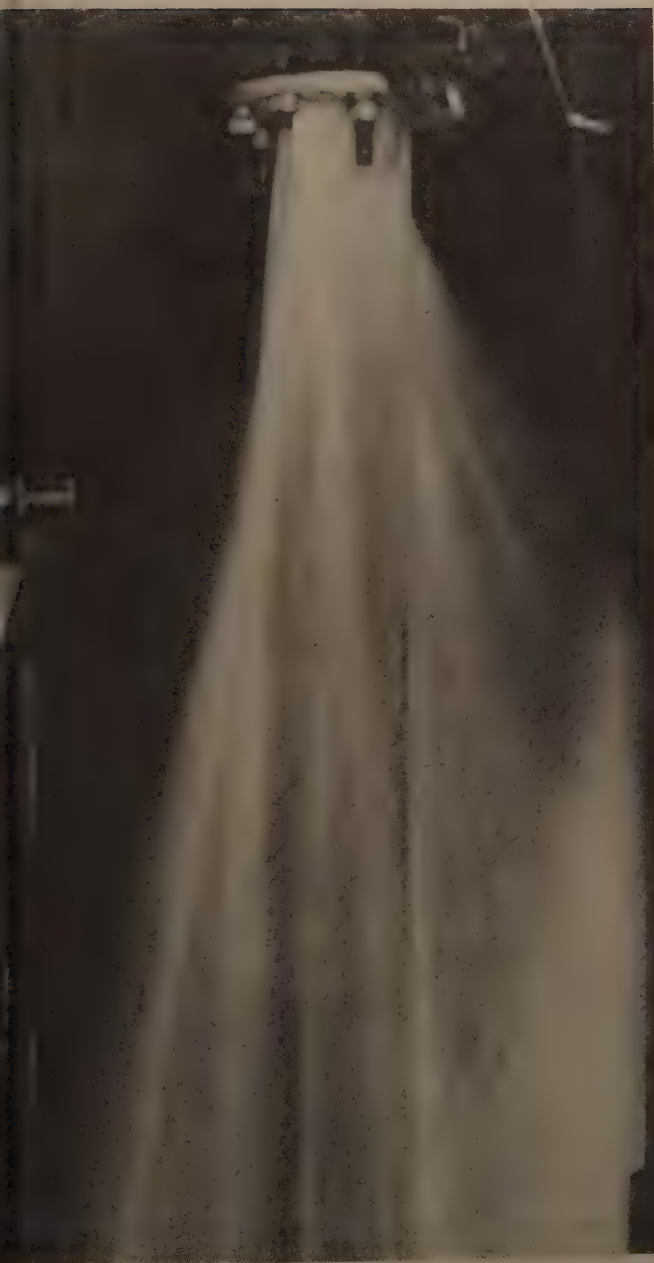


FIGURE 8

FREE DISCHARGE SPRAY PATTERN FOR SPECIAL 6" CDC WAFER VALVE
("Left", or Leading Edge is Down; Valve Shaft is Horizontal;
Special Tests of June 1952)

large difference in closure angle. Good correlation was also obtained between data from the 6" and 4" free discharge tests. These data, fortified by the other free discharge data, indicate a separate trend of their own.

The free-discharge and submerged characteristics appear to be related, but are distinctly different at the near-open positions. In submerged flow, the fluid fills or nearly fills the void between the two jets up to the blade, resulting in an expansion of the given fluid within the same fluid. In free discharge of a liquid, the void is normally filled with air. For this reason, it would be logical to assume that the flow characteristics might not be identical even though the installations are quite similar. This assumption is borne out to some extent by the fact that the free discharge analysis was substantiated more closely by prototype data than was the submerged case.

Continuous Pipe Flow Characteristics

By a continuous pipe is meant a constant diameter D between Stations (1) and (3). With the 6" CDC valve it was found that for this type of installation hydraulic grade (or piezometric head) lines unaffected by the valve could be obtained as close as $2D$ upstream and $5D$ downstream from the valve body. In the near-closed positions the distance requirements are less. In general, a distance of $2\frac{1}{2} D$ upstream can be recommended as safe. Lack of sufficient data prohibits any recommendation concerning the safe downstream distance.

The continuous pipe tests were conducted at a wide range of N_R , in many instances well below the minimums set forth in Fig. 5 for free discharge. The lowest pipe N_R reached was 8×10^4 (at $\alpha_0 = 45^\circ$ with the 4" valve, and $\alpha_0 = 65^\circ$ with the 6" valve). The flow coefficient for $\alpha_0 \geq 30^\circ$ was relatively constant and no obvious viscous effects were noted. This is entirely logical since the head loss in the expansion beyond the valve is practically independent of boundary friction and due primarily to the flow expansion from Station (2) to (3).

For this piping arrangement, since $V_1 = V_3$,

$$h_1 - h_3 = \Delta H \quad (5)$$

The data of Table IV, plotted in Fig. 7 are in close agreement for $\alpha_0 \geq 20^\circ$ even though the blade shapes and closure angles differ. Flow coefficients for the near-open positions are influenced by the relative blade thickness and the blade shape. According to Netsch and Schulz,(8) viscous effects are noted with $\alpha_0 = 0^\circ$ to 20° . Attainment of a high degree of test accuracy within this range is difficult because of the relatively large discharge rates and small head losses involved.

In all data presented in Table IV a deduction from the overall loss has been made for equivalent pipe friction to and from the valve body for purposes of correlation.

The Netsch & Schulz data(9) are all for an N_R of 3.5×10^5 .

The Dickey and Coplen data(10) for Disk "I" and Disk "II," with D about 13.5 inches, are for air velocities from 500 to 5000 ft./min. A great variety of downstream pressures were used. They state that C_Q is unaffected by size or velocity. Disk "I" was a thin, flat plate with short hubs only at the outer edges. Disk "II" was of uniform thickness with edges rounded to 6% of D .

TABLE IV

FLOW COEFFICIENT, C_Q

CONTINUOUS PIPE DATA

| | CDC 4" ϕ | CDC 6" ϕ | Netsch & Schulz 10 cm Blade "B" | Dickey- Coplen Disk I (Thin) | Dickey- Coplen Disk II | Genissiat (Converging) | Square Damper Dickey- Coplen |
|-------------------|------------------|------------------|--|---------------------------------------|------------------------------|---------------------------|---------------------------------------|
| 0° | 1.65 | - | 5.97 | - | - | - | - |
| 5° | - | - | - | - | - | - | 3.54 |
| 10° | 1.38 | 1.23-1.35 | 1.78 | 1.87 | 1.56 | 2.47 | 2.35 |
| 15° | - | - | - | - | - | 1.59 | - |
| 20° | 0.92 | 0.89-0.99 | 0.01 | 1.00 | 1.03 | 1.10 | 1.29 |
| 25° | - | - | - | - | - | - | - |
| 30° | 0.592 | 0.564 | 0.582 | 0.63 | 0.625 | 0.62 | 0.767 |
| 35° | - | - | 0.440 | - | - | - | - |
| 40° | 0.354 | 0.330 | 0.351 | 0.39 | 0.38 | 0.38 | 0.454 |
| 45° | 0.272 | 0.260 | 0.269 | - | - | - | - |
| 50° | 0.208 | 0.194 | 0.202 | 0.22 | 0.22 | 0.21 | 0.272 |
| 55° | - | - | 0.141 | - | - | - | - |
| 60° | 0.106 | 0.092 | 0.100 | 0.120 | 0.125 | 0.14 | 0.147 |
| 65° | 0.064 | 0.059 | 0.060 | - | - | - | - |
| 70° | - | - | 0.020 | 0.062 | 0.063 | - | 0.0685 |
| 75° | x | - | x | - | - | - | - |
| 80° | x | x | x | 0.028 | 0.037 | - | 0.0274 |
| 85° | x | x | x | - | - | - | x |
| 90° | x | x | x | x | x | x | x |
| Closure | 75° | 77.5° | 72° | 90° | 90° | 90° | 90° |
| Upstream ϕ | 2 | 2 | 2.5 | unknown | unknown | ~1 | unknown |
| Downstream ϕ | 5 | 5 | 3.5 | unknown | unknown | ~7 | unknown |
| t_{max}/D | 0.269 | 0.225 | 0.12 | 0.01 | 0.17 | 0.225 | 0.01 |
| Fluid | water | water | water | Air | Air | water | Air |

Their tests were run at 80°F. (The square damper had the same profile as Disk "I", and is included for comparison only).

The Génissiat data is for a D of 155 mm, converging to 84% of D from the centerline of the valve to the end of the valve body. These data are included for purposes of comparison.

Lack of consistency and/or necessary details precluded use of data for Gaden's Disk "A" or for data presented by Keller and Salzmann.(11)

The 4" CDC Valve Followed by a Specific Diffusor

In this series of tests the 4" CDC valve was preceded by 4" diameter pipe and followed immediately by a standard 9" long diffusor and a 6" diameter pipe. The basic data are listed in Table V and plotted in Fig. 2. The flow coefficients for this arrangement are nearly equal to those for a continuous pipe. It should be stressed, however, that this comparison should not be expected for any other combination of valve and diffusor.

As with the continuous pipe tests, no viscous effects were noted for N_R as low as 8×10^4 (at 45° and 65°). A deduction from the overall loss has been made for pipe friction, but no deductions were made for the wall friction losses through the valve body and the diffusor.

For this arrangement:

$$\frac{V_1^2}{2g} + h_1 - \frac{V_3^2}{2g} - h_3 = \Delta H \quad (6)$$

Sufficient piezometer stations were established to insure adequate determination of gradients:

| Valve | Installation | Number of Upstream Stations | Number of Downstream Stations |
|--------|-----------------|--------------------------------|----------------------------------|
| 6" CDC | Continuous Pipe | 5 | 8 |
| 4" CDC | Continuous Pipe | 4 | 4 |
| 4" CDC | Diffusor | 4 | 10 |

General Analysis for Enclosed Flow

As argued previously, the loss of head or energy between Stations (1) and (2) in addition to pipe friction should be relatively minor. In contrast, there is an abrupt decrease in velocity with distance between Stations (2) and (3). Separation occurs within the fluid for enclosed flow conditions (such as with a continuous pipe or a diffusor, or submerged).

The high intensity of shear in the vicinity of the separation surface and the eddy rollers formed between the live jets are manifested in a non-recoverable head or energy loss. The initial point of expansion is at Station (2), for both jets, and is not far from the initial point of separation at the edge of the blade tip. In general, it has been observed that the piezometric head within the zone of separation (here, between the live jets) is constant, and equal to the piezometric head at the point of

TABLE V4-INCH CDC VALVE FOLLOWED BY A DIFFUSOR

| <u>K_c</u> | <u>C_D</u> | |
|-------------------------|-------------------------|---|
| 0° | 1.2 | Notes: |
| 0° | 0.85 | 4" ϕ CDC valve followed immediately |
| 0° | 0.56 | by a 9", 4" x 6" diffuser (internal angle, |
| 0° | 0.35 | 12.5°). Uniform hydraulic gradient for data |
| 5° | 0.27 | obtained extends to about 8 valve diameters |
| 0° | 0.21 | downstream as opposed to only about 5 valve |
| 0° | 0.11 | diameters for continuous piping; two valve |
| 5° | 0.07 | diameters were used for the upstream station. |

separation.(12) Within the live jets at Station (2) the pressure distribution should be hydrostatic (constant piezometric head), since uniform flow occurs at these sections. It is assumed that the piezometric head is the same in the live jets at the separation surface at Station (2) and within the adjacent zone of separation. With this assumption, it would be within the same contracting surface of separation. With this assumption, it would be reasonable to conclude that there is some path between the left jet and the right jet at Station (2) over which the pressure distribution is hydrostatic. To illustrate, if the longitudinal section of Fig. 1 is placed in a horizontal plane (for liquid flow the pressure within the left jet at Station (2) is thus equal to the pressure along some connecting path, through the zone of separation to and within the right jet at Station (2); in this instance the pressure within the two jets would be constant and equal.

As was the situation for free discharge, it then follows that V_{2L} equals V_{2R} . Determination of the velocity distribution at the point of separation would not be practicable. The relative magnitude of the velocity at Station (2) however, can be expressed in terms of the uniform flow width, y . Inasmuch as the surface of separation originating from a fixed point (here the blade tip) is usually fixed in space for all but low values of N_R , y should be constant for a given blade setting.

The continuous pipe and special diffuser installations were duplicated with the two-dimensional test device and values of y were measured. In these tests, the magnitude of y was not noticeably changed by varying the discharge. Differentiation of the live jets was facilitated by injecting dye or air bubbles downstream from the blade.

The flow expansion between Stations (2) and (3) is extremely abrupt and the effect of boundary-layer development, or the boundary shear stress involved is comparatively negligible. Once the jet thickness is known, it is possible to appraise the energy loss due to the expansion alone, by means of the principle of conservation of momentum. It is assumed throughout that the valve loss is very nearly equal to the loss due to flow expansion, with the loss along the boundary between Stations (1) and (3) and within the fluid between Stations (1) and (2) being relatively minor.

Comparison of Actual and Analytical Flow Coefficients

The jet area has been shown to be a function of y (see Fig. 1). Also, $V_L \cong V_R$ for all piping arrangements, so long as any boundary alignment change occurs downstream from the distance Z .

$$\text{Then } Q_L/Q_R = Y_L/Y_R,$$

$$\text{or } Q_T = V_2 \times (\text{the area of the two jets}).$$

$$\text{Or, } Q_T = (V_2) (\pi D y_a / 2)$$

$$\text{and } A_v/A_j = D/2y_a,$$

where y_a is the average of y_L and y_R ,

A_j is equal to Q/V_2 ,

and A_v is the area of the valve body.

Note that A_v is identical with the area at Station (1) for all cases studied.

It is now possible to write an equation for the conservation of momentum between Stations (2) and (3), with the basic relationship established for the flow areas.

For free discharge, since $\Delta H = V_2^2/2g = V_1^2/2g + h_1$, it may be shown that

$$C_Q = \frac{\pi/(2\sqrt{2})}{A_V/A_J} \quad (7-a)$$

For a continuous pipe, theoretically $\Delta H = (V_2 - V_3)^2/2g$ (the Borda-Carnot loss), from which

$$C_Q = \frac{\pi/(2\sqrt{2})}{\frac{A_V}{A_J} - 1} \quad (7-b)$$

For the particular 2 = 3 ratio diffuser tested, assuming that $\Delta H = (V_2 - V_3)^2/2g$,

$$C_Q = \frac{\pi/(2\sqrt{2})}{\frac{A_V}{A_J} - \frac{4}{9}} \quad (7-c)$$

Both the free discharge and the continuous pipe data (particularly the latter) provided good agreement with these equations for C_Q using values of y_a obtained from the two-dimensional apparatus. The diffuser data was consistent, and when arbitrarily corrected as follows, provided equally good agreement:

$$C_Q = \frac{\pi/(2\sqrt{2})}{\frac{A_V}{1.2A_J} - \frac{4}{9}} \quad (7-cc)$$

By coincidence, the area ratio A_V/A_J is equal to $D/2y_a$ for both the two-dimensional and three-dimensional cases. Although the two-dimensional values for A_V/A_J using $D/2y_a$ were fairly close to those computed from measured values of C_Q and Eq. (7-a), (7-b), and (7-cc), quite close correlation for all installations was obtained by adjusting the two-dimensional values as follows:

$$A_V/A_J = 1.2(D/2y_a)^{0.85} \quad (8)$$

Eq. (8) applied equally well to both the 4-in. and 6-in. CDC valves. In using $D/2y_a$ as the area ratio, it had been assumed that the flow was strictly rectilinear at Station (2). Warpage of flow filaments was evident in the 4-in. CDC valve free discharge tests, particularly on the "left" side. The result in this instance was a much wider spray pattern in the vicinity of the "left" and "right" side than in the larger periphery between. A picture illustrating both the warpage and the uneven spray is presented in Figure 8. In this arrangement, a special test not otherwise discussed in this paper, the "left" side of the blade is below the horizontal shaft.

The 4-inch CDC valve area ratios are given in Table VI and those for the 6-inch CDC valve in Table VII. There is good agreement between all columns, showing the validity of the analytical equations. Note that the area ratios are little influenced by downstream conditions. There is not much difference between the 4-inch and 6-inch CDC valves, since the effects of blade shape and closure angle on C_Q are obvious only at the near-closed or near-open positions.

To illustrate the possible use of the two-dimensional apparatus in predicting performance, some values of C_Q for continuous piping and free discharge for the 4-inch CDC valve were computed from apparatus data using Eq. (7-a), (7-b), and (8), and are plotted in Figure 2.

Reference data is given for continuous pipe arrangements in Table VIII. The two-dimensional "Synthetic Blade" was very similar in shape to the blade used by Netsch and Schulz. A special flat blade was fabricated for the two-dimensional studies comparable to the Dickey-Coplen Disk "I." (See Fig. 4).

In passing, it may be noted in Fig. 1 that two separation surfaces are shown for the "right" jet. For a blade with a relatively wide tip, the point of separation will be at one or the other edge, depending upon the relative blade angle. The sudden, slight shift of C_Q trends for some valves is due to this transfer of the separation point.

Prediction of Incipient Cavitation

With V_1 , h_1 , h_3 , and α_0 given for an installation, values of V_2 and hence h_2 can be calculated once the magnitude of A_v/A_j is known. By using C_Q values from flow tests in equations such as (7-a) and (7-b), it is believed that a reasonable approximation of A_v/A_j should be obtained from which h_2 can be computed. An anticipated h_2 for specific conditions is outlined in the sample calculations of Table IX.

Fully Open Position

In the fully open position ($\alpha_0 = 0^\circ$) the point of separation has been found by Mueller⁽¹³⁾ to depend upon the blade shape and the Reynolds number involved. The variation in C_Q for the 6" CDC valve, Table IV for 10° and 20° might have been the result of a shifting point of separation. As stated previously, Netsch and Schulz⁽⁸⁾ noted viscous effects for continuous piping with $\alpha_0 = 0^\circ$ to 20° .

TABLE VI

COMPARISON OF AREA RATIOS FOR 4" CDC VALVE

as computed by using analytical equations for C_Q , and as
obtained from two-dimensional flow test measurements.

| | From Flow Tests | | | | Two-Dim. Measurements | | |
|-----|------------------------|--------------------------------|---------------------------|-----------------------|--|---------------|----------|
| | A_v/A_j | | | | $A_v/A_j = 1.2 \left(\frac{D}{2y_a} \right)^{0.85}$; Eq. (8) | | |
| | Eq.(7-a)* Submerged | Eq.(7-a). Free Discharge | Eq.(7b). Cont. Pipe | Eq.(7-cc) Diffusor | Free Discharge | Cont. Pipe | Diffusor |
| 0° | - | - | - | - | - | - | 1.74 |
| 5° | - | - | - | - | - | - | - |
| 10° | 1.31 | 1.56 | 1.80 | - | - | - | 1.84 |
| 15° | 1.50 | 1.75 | - | - | 1.96 | 1.91 | 2.02 |
| 20° | 1.77 | 1.97 | 2.21 | 2.10 | 2.18 | 2.18 | 2.24 |
| 25° | 2.14 | 2.26 | 2.50 | - | 2.51 | 2.50 | 2.58 |
| 30° | 2.62 | 2.64 | 2.89 | 2.94 | 2.94 | 2.92 | 3.02 |
| 35° | 3.27 | 3.12 | 3.42 | - | 3.53 | 3.50 | 3.65 |
| 40° | 4.19 | 3.89 | 4.18 | 4.39 | 4.30 | 4.24 | 4.45 |
| 45° | 5.70 | 4.98 | 5.15 | 5.48 | 5.37 | 5.28 | 5.58 |
| 50° | 7.94 | 6.68 | 6.50 | 6.90 | 6.72 | 6.55 | 6.50 |
| 55° | 11.1 | 9.25 | 8.41 | - | 8.72 | 8.40 | 8.60 |
| 60° | 15.9 | 13.4 | 11.58 | 12.65 | 12.20 | 11.70 | 12.1 |
| 65° | 22.2 | 20.9 | 17.35 | 20.25 | 19.4 | 18.2 | 21.2 |
| 70° | 31.8 | - | - | - | - | - | - |

* Assuming Eq. (7-a) for Free Discharge can be applied to Submerged Flow.

TABLE VIICOMPARISON OF AREA RATIOS FOR 6" CDC VALVEas obtained by using analytical equations for C_Q , and

as obtained from

two-dimensional flow test measurements

| <u>α</u> | <u>From Flow Tests</u> | | <u>Two-Dim. Measurements</u> | |
|----------------------------|--------------------------------|----------------------------|--|---------------|
| | A_v/A_j | | $A_v/A_j = 1.2 \left(\frac{D}{2y_a} \right)^{0.85}$; Eq. (8) | |
| | Eq. (7-a) Free Discharge | Eq. (7-b) Cont. Pipe | Free Discharge | Cont. Pipe |
| 10° | 1.80 | - | 1.65 | - |
| 15° | 1.95 | - | 1.90 | 1.97 |
| 20° | 2.11 | - | 2.15 | 2.22 |
| 25° | 2.34 | - | 2.51 | 2.58 |
| 30° | 2.74 | 2.97 | 2.90 | 2.98 |
| 35° | 3.23 | 3.53 | 3.40 | 3.57 |
| 40° | 4.79 | 5.28 | 5.05 | 5.30 |
| 50° | 6.07 | 6.73 | 6.35 | 6.60 |
| 55° | 8.30 | 8.94 | 8.40 | 8.45 |
| 60° | 12.55 | 13.1 | 12.0 | 11.60 |
| 65° | - | 19.9 | 21.5 | 18.2 |

TABLE VIII

COMPARISON OF AREA RATIOS FOR VARIOUS VALVES

as obtained by using analytical equations for C_Q , and as
obtained from two-dimensional flow test measurements

All for Continuous Pipe

| | <u>From Flow Data</u> | | | <u>Two-Dim. Measurements</u> | |
|----------|------------------------------------|--------------------------------------|--------------------------------------|--|------------------------------------|
| | A_v/A_j , from Eq. (7-b) | | | $A_v/A_j = 1.2 \left(\frac{D}{2y_a} \right)^{0.85}$; Eq. (8) | |
| α | <u>Netsch & Schulz</u> | <u>Dickey- Coplen Disk I</u> | <u>Square Damper D. - C.</u> | <u>Synthetic Blade (N. & S.)</u> | <u>Flat Blade (Disk I)</u> |
| 5° | - | - | 1.4 | - | - |
| 10° | - | 1.60 | 1.61 | - | 1.58 |
| 15° | - | - | - | 1.90 | 1.84 |
| 20° | 2.10 | 2.11 | 2.10 | 2.16 | 2.14 |
| 25° | - | - | - | 2.47 | 2.47 |
| 30° | 2.91 | 2.77 | 2.85 | 2.87 | 2.90 |
| 35° | 3.53 | - | - | 3.35 | 3.47 |
| 40° | 4.17 | 3.85 | 4.12 | 4.03 | 4.10 |
| 45° | 5.14 | - | - | 4.97 | 5.00 |
| 50° | 6.50 | 6.05 | 6.20 | 6.20 | 6.20 |
| 55° | 8.90 | - | - | 8.20 | 8.00 |
| 60° | 12.10 | 10.3 | 10.65 | 11.8 | 10.5 |
| 65° | 19.55 | - | - | 21.5 | 14.9 |
| 70° | - | 19.0 | 21.65 | - | - |

TABLE IXSAMPLE CALCULATIONS - ANTICIPATED h_2

The 4-inch CDC valve installed in horizontal "continuous pipe" with $h_3 = 10$ ft., $Q = 2.00$ cfs and $\alpha_0 = 35^\circ$, compute h_2 .

From Fig. 2 $C_Q = 0.46$

From Eq. (1) $\Delta H = Q^2 / (C_Q^2 D^4 g)$
 $\Delta H = (2.00)^2 / (0.46)^2 (0.333)^4 (32.2)$
 $\Delta H = 47.7$ ft.

Therefore $h_1 = \Delta H + h_3 = 57.7$ ft.

Using Eq. (7-b), $A_v/A_j = \frac{\pi}{2\sqrt{2} C_Q} + 1 = 3.42$

With $A_v = A_1 = A_3 = \frac{\pi}{36}$ sq. ft.

Then $A_j = \frac{\pi}{36} / 3.42 = 0.0255$ sq. ft.

$$V_j = 2.00 / 0.0255 = 78.4 \text{ ft./sec.}$$

$$V_j^2 / 2g = 95.4 \text{ ft.}$$

$$V_1 = \frac{2.00}{\pi/36} = 23.0 \text{ ft./sec.}$$

$$V_1^2 / 2g = 8.2 \text{ ft.}$$

Since $V_1^2 / 2g + h_1 = V_2^2 / 2g + h_2$,

$$h_2 = 8.2 + 57.7 - 95.4 = -29.5 \text{ ft.}$$

For 60°F water service, vaporization is probable and cavitation effect likely.

Note that h_1 and h_2 are related directly to h_3 (although h_2 is limit vaporization of the liquid) as shown in the tabulation below:

| h_3 ft. | h_1 ft. | h_2 ft. |
|-----------|-----------|-----------|
| 10 | 57.7 | -29.5 |
| 20 | 67.7 | -19.5 |
| 30 | 77.7 | -9.5 |
| 40 | 87.7 | +0.5 |

SUMMARY

The effect of piping arrangement on the flow characteristics of a specific valve has been demonstrated. Evidence has been submitted to prove that free, submerged and continuous piping discharge arrangements have separate and distinct flow characteristics. For the valves discussed in this paper, the flow characteristics for a given type of installation were not appreciably influenced by either the shape of the blade (except at the near-open positions) or by the closing angle (except at the near-closed positions).

Analytical relationships have been presented. Measurements from a two-dimensional model have been combined with those for prototype valves to demonstrate the basic validity of these relationships. As a by-product of this study, it may be noted that relatively good anticipatory values of flow coefficients for other types of installations could be obtained by means of inexpensive two-dimensional tests using water, air, smoke, a polarized or diffracted fluid, etc.

Probably the most important use of the relationships offered will be in calculating anticipated conditions for incipient cavitation.

It is felt that the accuracy attained in the studies reported is adequate for normal application of the results.

ACKNOWLEDGMENTS

This program was conducted by the hydraulic division of Fritz Engineering Laboratory at Lehigh University under the direction of the senior author, and under the sponsorship of CDC Control Services, Inc., Hatboro, Penna., C. D. Reese, President.

The discharge distribution tests for the 6-inch CDC valve were conducted by J. G. Mostert. P. J. Colleville made most of the measurements with the two-dimensional device. The high caliber of service rendered by these two former graduate students contributed significantly to the success of this program; they participated in nearly all tests.

Administration of the program was supervised by W. J. Eney, Director of Fritz Engineering Laboratory.

- - - - -

(A limited number of extra copies of translations (without figures) of the Heller and the Armanet papers are available at Fritz Laboratory.)

REFERENCES

- J. W. James, "Investigation of Losses in Butterfly Valves" (using low-velocity air flow), a thesis, Mechanical Engineering Department, University of Toronto, Canada, April 15, 1951.
- Sylvia D. Cohn, "Performance Analysis of Butterfly Valves," *Instruments* - Vol. 24, p. 880-884, August, 1951.
- D. Gaden, "A Contribution to The Study of Butterfly Valves," Water Power, Part 1 - p. 456-474, Dec. 1951 and Part 2 - p. 16-22, January 1952.

4. L. Armanet, "Vannes-papillon des turbines" (Génissiat hydropower development), La Houille Blanche p. 199-219, Grenoble, France, 1950.
5. D. Gaden, "Contribution à l'étude des vannes-papillons," Schweizerische Bauzeitung, p. 262-268, 275-277, 291-295, May 21 & 28 and June 4, 1950.
6. "Penstock Valves," National Electric Light Association Proceedings Publication 289-72, Vol. 86, p. 662-682, 1929.
7. Jean-Paul Laurent, "Essais sur Modèles Réduits des vannes - Papillon Alsthom-Charmilles de L'Usine de Génissiat," Revue Générale de L'Hydraulique, Paris, December 1947.
8. Netsch and Schulz, "Versuche an profilierten Drosselklappen," Maschinenbau und Wärmewirtschaft, Vol. 4, No. 9, p. 141-147, Sept. 1950.
9. Netsch & Schulz, "Tests on Streamlined Butterfly Valves," Engineering Digest Vol. 11, No. 8, p. 280-282, August 1950.
10. Dickey & Coplen, "A Study of Damper Characteristics," ASME Transactions, 1942.
11. Keller and Salzmann, "Aerodynamic Model Tests on Butterfly Valve," Escher Wyss News, Vol. IX, No. 1, January - March 1936.
12. Hunter Rouse, Engineering Hydraulics, John Wiley & Sons, New York, 1950.
13. H. Mueller, "Drosselklappen für hohe Geschwindigkeiten zum Einbau in Grundablässen" Forschung auf dem Gebiete des Ingenieurwesens, (V) Vol. 4, p. 249-253, Berlin, 1933.

Journal of the HYDRAULICS DIVISION

Proceedings of the American Society of Civil Engineers

CONTENTS

DISCUSSION (Proc. Paper 1177)

| | Page |
|--|---------|
| Sal Currents at Inlets in the United States, by Joseph M. Caldwell. Proc. Paper 716. Prior discussion: 881. Discussion closed.) by Joseph M. Caldwell (closure) | 1177-3 |
| Attending Stream-flow Data, by W. B. Langbein and C. H. Hardison. Proc. Paper 826. Prior discussion: 955. Discussion closed.) by W. B. Langbein and C. H. Hardison (closure). | 1177-5 |
| egrating the Equation of Gradually Varied Flow, by Ven Te Chow. Proc. Paper 838. Prior discussion: 955, 1010. Discussion closed.) by Ven Te Chow (closure) | 1177-9 |
| ee Outlet and Self-Priming Action of Culverts, by Wen-Hsiung Li d Calvin C. Patterson. (Proc. Paper 1009. Prior discussion: 1131. Discussion closed.) by J. E. Flack | 1177-23 |
| by John L. French | 1177-26 |
| portional Weirs for Sedimentation Tanks, by J. C. Stevens. Proc. Paper 1015. Prior discussion: none. Discussion closed.) by Guido di Ricco | 1177-41 |
| e Application of Sediment-Transport Mechanics to Stable-Channel sign, by Emmett M. Laursen. (Proc. Paper 1034. Prior discus- sion: none. Discussion closed.) by Sam Shulits | 1177-49 |

Discussion of
"TIDAL CURRENTS AT INLETS IN THE UNITED STATES"

by Joseph M. Caldwell
(Proc. Paper 176)

JOSEPH M. CALDWELL,¹ M. ASCE.—Mr. Baines has presented a rather interesting analysis of one facet of tidal current action at inlets. It was, of course, the writer's intention in the paper to present a very simple hydraulic classification of tidal inlet based on a minimum of data. In this sense, Mr. Baines' analysis goes beyond the simplified concepts presented by the writer.

Mr. Baines prefers to treat the writer's class 2 and class 3 inlets as examples of a general type of inlet. The class 3 inlet (the inlet with an inadequate entrance) is not influenced by the length of the contiguous bay or estuary. On the other hand, the class 2 inlet (short inlet with adequate entrance) is so definitely related to the length of the contiguous bay or estuary that, in the writer's thought, the distinction between the class 2 and class 3 inlets should be preserved. Methods of treating two or all of the classes 1, 2, and 3 of inlets by a single mathematical concept (Einstein,⁽¹⁾ Dronkers)⁽²⁾ invariably leads to complications; the writer has attempted to assist the user who is not in a position to utilize the more complicated methods in approaching a problem dealing with tidal inlets.

REFERENCES

- 1. Einstein, H. A., "Computations of Tides and Tidal Currents—United States Practice," Proc. ASCE, Vol. 81, Separate No. 715, June 1955.
- 2. Dronkers, J. J. and J. C. Schonfeld, "Tidal Computations in Shallow Water," Proc. ASCE, Vol. 81, Separate No. 714, June 1955.

¹Chief, Research Div., Beach Erosion Board, Corps of Engrs., U. S. Dept. of the Army, Washington, D. C.

Discussion of
"EXTENDING STREAMFLOW DATA"

by W. B. Langbein and C. H. Hardison
(Proc. Paper 826)

W. B. LANGBEIN** and C. H. HARDISON,** A.M., ASCE.—The authors deeply appreciate the very profitable and constructive discussion and criticism of their paper. We are particularly indebted, not only to Mr. R. D. Goodrich's discussion, but also to many of his earlier works for numerous suggestions and findings of value.

Messrs. Merriam and Schuleen introduce a number of items that unfortunately could not be presented with the ample consideration they properly deserve within limits of a discussion. They tempt us with all-too-brief presentations of new methodologies and ideas they have developed. We were particularly interested in their use of punched cards to develop interstation relations.

The authors are in substantial agreement with Mr. W. M. Snyder and acknowledge his efforts to clear up several important details.

Mr. Snyder mentions that "the use of the geometric mean to obtain a unique value of relation between two variables has been mentioned by other authors." We credited this device to Goodrich whose description of it was apparently contemporaneous with that by Gumbel.

The equations and discussion by Snyder on the variance of a forecast are repeated in an earlier paper¹ where it was shown how the correlations between the flow of adjoining streams can be applied to the design of networks of base and secondary stream-gaging stations.

Snyder recommends that we use the term "standard deviation of the residuals" in lieu of the more usual "standard error of estimate." Our usage is confirmed by several texts, but to be strictly correct for small samples the standard deviation of the residuals should be adjusted for the degrees of freedom lost in drawing the curve of relation. Thus on figure 1, assuming 6 degrees of freedom consumed by the nature of the graph shown, the standard error of estimate should be $0.086 \sqrt{\frac{60}{60-6}}$ or $0.0906 \log_{10}$ units. The standard error of a graph, s_g , is usually computed by the following equation:

$$s_g = \frac{s}{\sqrt{n}} \sqrt{1 + \left(\frac{x - \bar{x}}{\sigma}\right)^2} \quad (1)$$

where s is the standard error of estimate computed as above, $x - \bar{x}$ is the deviation from the mean of the x values, σ is the standard deviation of the x values, and n is the number of data used to define the relation. Eq. 1 premises random data, whereas the data we have to deal with are time series.

Hydr. Engrs., U. S. Geological Survey, Washington, D. C.
Langbein, W. B., Stream-gaging networks, Publication No. 38 de la
Association Internationale d'Hydrologie, 1954.

This means our data have some properties that differ from the kinds of data usually treated in statistical literature. One of the more important of these differences is that our data are related to each other in sequence; that is, one day's flow is somewhat related to that of the preceding and following day. The same is true of months, seasons, and years. For example, as observed by Johnson, deviations from a correlation tend to persist for periods of several months. Our record, therefore, consists of data more or less interdependent; or, in different terms, our record represents fewer independent events than would be indicated by the number of items in the list. The actual number of independent events, using monthly data, depends on the tendency toward serial correlation among the monthly data. Further research is needed on this point, but at this time we would judge that an estimate of the proper value of n in Eq. 1 could be taken as twice the number of changes in sign of the net deviations arranged chronologically (assuming plus and minus signs to be equal in number), but in no case to exceed the number of months. This rule applied to the Murder Creek example would yield 40 independent data instead of 60. In the case of Rock Creek in Utah, the indicated number of independent data is 36 out of a 72-month list.

In usual practice, the index of correlation is computed from the ratio of the standard error of estimate (adjusted for degrees of freedom lost in defining the relation) to the standard deviation of the monthly discharges. However, because of the tendency for similar months to cluster, it is believed that more realistic values of the correlation index can be computed by taking the ratio of the adjusted standard error of estimate to the standard deviation of the monthly discharges about their respective monthly means. To be consistent, this standard deviation, obtained by pooling variances, should be adjusted for the 12 degrees of freedom lost in defining the monthly means.

In the Murder Creek example, the coefficient of correlation of 0.93 shown in figure 1 is computed from a standard deviation of the residuals (error of estimate) of 0.086 and a standard deviation of 0.231. The standard error adjusted for 6 lost degrees of freedom is 0.0906 as computed previously. The standard deviation of the monthly discharges, about the means of the respective calendar months has been computed to be 0.18. The standard deviation adjusted for the 12 degrees of freedom lost in using the means of the calendar months becomes $0.18\sqrt{\frac{60}{60-12}}$ or 0.201.

The index of correlation computed from these adjusted values is:

$$\sqrt{1 - \left(\frac{0.0906}{0.201}\right)^2} = 0.885$$

In this example the change in the index of correlation is not great, but in streams where the seasonal variations are more marked, as in the case of western snow-fed streams, it is of greater significance. In one case, for example, Rock Creek vs. South Fork Ogden River in Utah (70 miles distant) the following were observed:

Standard error of estimate = 0.12 log₁₀ units

Standard deviation of monthly discharges about the general mean = .41

$$r = \sqrt{1 - \left(\frac{.12}{.41}\right)^2} = 0.95$$

However, it was also observed that standard deviation of the several months about the means of the respective calendar months is not much larger than the standard error of estimate. Computing the index of correlation relative to the standard deviations (adjusted for 12 lost degrees of freedom) about the mean of the respective calendar months gives a non-significant value and a curve of relationship apparently offers no special advantage in this case.

For a correlation between monthly flow of Rock Creek and that of Yellowstone Creek, 18 miles apart, the respective factors are:

| | |
|--|---------------------------------|
| Standard error of estimate (adjusted) | = 0.050 log ₁₀ units |
| Standard deviation of monthly data about general mean | = .41 |
| Standard deviation of monthly data about means of respective months (adjusted) | = .12 |
| Index of correlation relative to general mean | = .99 |
| Index of correlation relative to means of calendar months | = .91 |

Consequently, the flow of Rock Creek correlates satisfactorily with that of Yellowstone Creek but not with the flow of South Fork of Ogden River.

Use of rainfall data: It is the practice to include rainfall data in extending stream-flow data wherever such use is beneficial. The authors suggested, as Mr. Johnson was kind enough to demonstrate, that adjustment of the correlation between the flows of two streams on the basis of the relative rainfall on the two drainage basins, might afford a superior arrangement.

In extending a record in time there is always the question whether the relationship may shift due to such factors as a shift in rainfall distribution. Including rainfall in the correlation or correlating with streams on either side normal to the prevailing storm tracks as suggested by Johnson can minimize the effects of shifts from this cause. The greater number of independent data that are used, the more stable the correlation.

Discussion of
"INTEGRATING THE EQUATION OF GRADUALLY VARIED FLOW"

by Ven Te Chow
(Proc. Paper 838)

VEN TE CHOW,¹ A.M. ASCE.—The writer wishes to express his deep appreciation for the constructive comments presented by the discussers.

The major advantage of the direct method is to perform the computation of a flow profile through only a single operation or step. This will save a great deal of effort in developing a family of flow characteristic curves such as those demonstrated by Bakhmeteff⁽¹³⁾2 for canal design. The writer recognizes at the same time the advantages of the step method when applied to problems in which the integration method becomes evidently disadvantageous or fails. He therefore believes that a hydraulic engineer should learn the technique of both methods and know how to use the right method in a given problem to its best advantage. Mr. Silvester describes a step method with the aid of graphs, which should help the solution of a problem by the step method.

For most open channels encountered in hydraulic engineering, the hydraulic exponents vary rather slowly in the design range of flow. Moreover, as the equation for the length of flow profile is a function of the differences between two varied flow functions of the same hydraulic exponent, the error introduced in the result due to variation in hydraulic exponent is compensative. However, when the range of flow becomes large, some of the basic assumptions for gradually varied flow will not be satisfactory. For example, the Manning coefficient of roughness changes a great deal in practically any channel when the variation in depth extends to a considerable range. In fact, the value of n for average clean sewer pipes and drain tiles, both clay and concrete, has been shown to increase by as much as 28 percent from depths equal to 1.00 to 0.25 times the diameter ($D-1$). For high accuracy, any method assuming a constant value of n is questionable.

When the water approaches the top of a gradually closed conduit, the hydraulic exponents may change rapidly. The situation becomes further complicated due to the creation of a conjugate normal depth which will be described later. In such problems, the numerical integration method developed by Messrs. Keifer and Chu has the great advantage, because in this method the effect due to the variation of hydraulic exponents is included in the variation of the flow function.

One of the disadvantages of the Bakhmeteff method is the introduction of an additional item σ for critical slope. This item is often confused with the normal critical slope S_c . The connotation of this item is rather difficult, particularly for beginners, to conceive. Theoretically, the Bakhmeteff equation should be identical with the author's equation. The presence of the third

1. Research Associate Prof. of Hydr. Eng., Graduate College, Univ. of Illinois, Urbana, Ill.

2. Numerals in parentheses refer to corresponding items in the List of References in the paper and in this discussion.

term in the author's equation, however, will not introduce complicated computation, but rather simple and systematic procedure as shown in the given example. On the other hand, the use of the item σ requires additional determination of its value even with the aid of the Kirpich graphs.

During a visit to Europe in the summer of 1956, the writer had an opportunity to see the original work by G. Mouret (D-2). It was a manuscript in mimeographed form as shown to the writer by Professor G. de Marchi, Director of Istituto di Idraulica e Costruzioni Idrauliche, Politecnico di Milano, in Milan, Italy. It is believed that Mouret's "Hydraulique Générale" as mentioned by Professor Hom-ma was based on this work and published later in 1927 in Paris. The problem of the point of inflection is discussed on pages 447-458 of the manuscript. This discussion covers also another point of inflection which occurs theoretically on the curve for $y < y_c < y_n$ (Fig. D-1). This is the point which has been brought out independently for discussion in American literature by Gunder (D-3) in 1943. In Belgium, however, Professor L. J. Tison of the University of Ghent has told the writer that the point of inflection on a theoretical backwater curve was probably first described analytically by Merten (D-4) in 1906, and that the possibility of a point of inflection on the curve was mentioned without theoretical treatment by Boudin (D-5)¹ at even an earlier date in 1861. The condition for an inflection point as given by Professor Hom-ma is obtained by placing $d^2x/du^2 = 0$. Using the example in the paper, where $N = 3.65$, $M = 3.43$ and $y_n/y_c = 3.36/2.16 = 1.555$, the writer found another point of inflection having $u = 940$ or $y = 940y_n$. Apparently, this point is also beyond practical consideration. However, this point is on the curve for $y > y_n > y_c$, whereas the point obtained by Professor Hom-ma is actually for $y < y_c < y_n$.

Owing to the peculiar hydraulic characteristics of a circular conduit or any conduit with a gradually closing top, a point of inflection may be shown to be possible at the depth of maximum discharge. Figure D-2A shows the variation of the normal discharge in a conduit with a gradually closing top. It is known that as the depth of flow increases the discharge will increase to the full discharge at a depth less than the full depth y_0 . For a circular conduit, this depth $y'_0 = 0.82y_0$ where y_0 is the diameter of the conduit. Thereafter, it will reach a maximum discharge at a depth y_n^* . For a circular conduit, $y_n^* = 0.938y_0$. After reaching the maximum value, the discharge will decrease to the full discharge when the flow touches the top of the conduit. Within the region of $y = y'_0$ and $y = y_0$, there are two possible normal depths for a given discharge, namely, the lower normal depth y_n and the upper or conjugate normal depth y_n' . At maximum discharge, the two depths become one depth y_n^* . It can be demonstrated analytically that four types of flow profiles are possible for a given slope. Figures D-2B, D-2C, and D-2D show these profiles for mild and steep slopes. It should be noted that the critical depth in Fig. D-2D is greater than the normal depths y_n' and y_n , but its corresponding lower normal depth is less than y_n' and y_n . Consequently, the corresponding critical slope should be less than the normal slope, and the channel slope is considered as mild.

The writer appreciates the demonstration by Mr. Harrison for extending the method to horizontal channels. For adverse channels, the slope of the

1. The complete title of this reference was supplied by Professor G. A. Heyndrickx of Institut Supérieur Agronomique, Département de Hydraulique Agricole, Ghent, Belgium.

channel bottom may be taken as negative. Thus, the general differential equation of gradually varied flow becomes

$$\frac{dy}{dx} = \frac{S_o + S}{1 + \frac{d}{dy} \left(\frac{V^2}{2g} \right)} \quad (D-1)$$

The corresponding equation for the flow profile is

$$x = \frac{y_n}{S_o} \left[u - \int_0^u \frac{du}{1+u^N} - (y_c/y_n)^M \int_0^u \frac{u^{N-M}}{1+u^N} du \right] + \text{a constant} \quad (D-2)$$

in which the varied flow function can be developed as

$$F(u, N)_{-S_o} = \int_0^u \frac{du}{1+u^N} = \int_0^u \frac{du}{1-u^{2N}} + \int_0^u \frac{u^N}{1-u^{2N}} du \quad (D-3)$$

The first integral is equal to $F(u, 2N)$ and the second integral can be easily shown to be $(N+1)^{-1} F(u^{N+1}, \frac{2N}{N+1})$. Therefore,

$$F(u, N)_{-S_o} = F(u, 2N) + \frac{1}{N+1} F(u^{N+1}, \frac{2N}{N+1}) \quad (D-4)$$

In other words, the varied flow function for adverse slopes can be computed directly from the varied flow functions for positive slopes. For the simplicity of computation, a table of the varied flow function for adverse slopes has been prepared as shown in Table D-1.

The length of water surface curve between two sections 1 and 2 is

$$L = - \frac{y_n}{S_o} \left\{ (u_1 - u_2) - \left[F(u_1, N)_{-S_o} - F(u_2, N)_{-S_o} \right] \right. \\ \left. - (y_c/y_n)^M (J/N) \left[F(v_1, J)_{-S_o} - F(v_2, J)_{-S_o} \right] \right\} \quad (D-5)$$

Example Assume a channel of adverse slope equal to 0.0016 with the same cross section as the example in the paper. A vertical drop controls the water surface at critical depth at the downstream end of the channel. Determine how far upstream the depth will be 10 ft.

Solution 1. From the example $y_c = 2.16$ ft. and $y_n = 3.36$ ft.

2. From 2.16 ft. to 10 ft., the average depth is 6.08 ft., and the average hydraulic exponents are $N = 3.83$ and $M = 3.57$. Thus, $J = 3.04$.

3. The value of $(y_c/y_n)^M (J/N) = 0.164$

4. Computation of the distance is as follows:

| y | u | v | $F(u, N)_{-S_0}$ | $F(v, J)_{-S_0}$ |
|--------|--------|-------|------------------|------------------|
| 2.16 | 0.643 | 0.573 | 0.621 | 0.549 |
| 10.00 | 2.976 | 3.950 | 1.106 | 1.171 |
| Diff.: | -2.333 | | -0.485 | -0.622 |

$$L = -2,100 \left[-2.333 - (-0.485) - (0.164)(-0.622) \right] = 3,670 \text{ ft.}$$

Regarding the Coriolis correction factor as mentioned by Professor Kolupaila, the factor α can be easily added to the equation of the length of flow profile as follows:

$$L = \frac{y_n}{S_0} \left\{ (u_1 - u_2) - [F(u_1, N) - F(u_2, N)] + \alpha (y_c / y_n)^M (J/N) [F(v_1, J) - F(v_2, J)] \right\} \quad (D-6)$$

LIST OF REFERENCES

- D-1. "Discussion on Determination of Kutter's n for Sewers Partly Filled," Thomas R. Camp, Trans. ASCE, Vol. 109, 1944, pp. 240-243.
- D-2. "Hydrauliques, Cours de Mécanique Appliquée, Ecole Nationale des Ponts et Chaussées," G. Mouret, Paris, 1922-1923, pp. 447-458.
- D-3. "Profile Curves for Open-Channel Flow," Dwight F. Gunder, Trans. ASCE, Vol. 108, 1943, pp. 481-488.
- D-4. "Recherches sur la Forme des Axes Hydrauliques dans un Lit Prismatique," A. Merten, Series 3, Vol. V, Annales de l'Association des Ingénieurs Sortis des Ecoles Spéciales de Gand, 1906.
- D-5. "De l'Axe Hydraulique des Cours d'Eau Contenus dans un Lit Prismatique et des Dispositifs Réalisant, en Pratique, ses Formes Diverses," M. Boudin, Annales des Travaux Publics de Belgique, Vol. XX, 1861-1862, pp. 397-555.



FIG.D-1 POINTS OF INFLECTION ON FLOW PROFILES

Table D-1 The Varied Flow Function Table for Adverse Slopes

| $\frac{N}{u}$ | 2.0 | 2.2 | 2.4 | 2.6 | 2.8 | 3.0 | 3.2 | 3.4 | 3.6 | 3.8 |
|---------------|-------|-------|-------|-------|-------|-------|-------|-------|-------|-------|
| 0.00 | 0.000 | 0.000 | 0.000 | 0.000 | 0.000 | 0.000 | 0.000 | 0.000 | 0.000 | 0.000 |
| 0.02 | 0.020 | 0.020 | 0.020 | 0.020 | 0.020 | 0.020 | 0.020 | 0.020 | 0.020 | 0.020 |
| 0.04 | 0.040 | 0.040 | 0.040 | 0.040 | 0.040 | 0.040 | 0.040 | 0.040 | 0.040 | 0.040 |
| 0.06 | 0.060 | 0.060 | 0.060 | 0.060 | 0.060 | 0.060 | 0.060 | 0.060 | 0.060 | 0.060 |
| 0.08 | 0.080 | 0.080 | 0.080 | 0.080 | 0.080 | 0.080 | 0.080 | 0.080 | 0.080 | 0.080 |
| 0.10 | 0.099 | 0.100 | 0.100 | 0.100 | 0.100 | 0.100 | 0.100 | 0.100 | 0.100 | 0.100 |
| 0.12 | 0.119 | 0.119 | 0.120 | 0.120 | 0.120 | 0.120 | 0.120 | 0.120 | 0.120 | 0.120 |
| 0.14 | 0.139 | 0.139 | 0.140 | 0.140 | 0.140 | 0.140 | 0.140 | 0.140 | 0.140 | 0.140 |
| 0.16 | 0.158 | 0.159 | 0.159 | 0.160 | 0.160 | 0.160 | 0.160 | 0.160 | 0.160 | 0.160 |
| 0.18 | 0.178 | 0.179 | 0.179 | 0.180 | 0.180 | 0.180 | 0.180 | 0.180 | 0.180 | 0.180 |
| 0.20 | 0.197 | 0.198 | 0.199 | 0.199 | 0.200 | 0.200 | 0.200 | 0.200 | 0.200 | 0.200 |
| 0.22 | 0.216 | 0.217 | 0.218 | 0.219 | 0.219 | 0.220 | 0.220 | 0.220 | 0.220 | 0.220 |
| 0.24 | 0.234 | 0.236 | 0.237 | 0.238 | 0.239 | 0.240 | 0.240 | 0.240 | 0.240 | 0.240 |
| 0.26 | 0.253 | 0.255 | 0.256 | 0.257 | 0.258 | 0.259 | 0.259 | 0.260 | 0.260 | 0.260 |
| 0.28 | 0.272 | 0.274 | 0.275 | 0.276 | 0.277 | 0.278 | 0.278 | 0.279 | 0.280 | 0.280 |
| 0.30 | 0.291 | 0.293 | 0.294 | 0.295 | 0.296 | 0.297 | 0.298 | 0.298 | 0.299 | 0.299 |
| 0.32 | 0.308 | 0.311 | 0.313 | 0.314 | 0.316 | 0.317 | 0.318 | 0.318 | 0.319 | 0.319 |
| 0.34 | 0.326 | 0.329 | 0.331 | 0.333 | 0.335 | 0.337 | 0.338 | 0.338 | 0.339 | 0.339 |
| 0.36 | 0.344 | 0.347 | 0.350 | 0.352 | 0.354 | 0.356 | 0.357 | 0.357 | 0.358 | 0.358 |
| 0.38 | 0.362 | 0.355 | 0.368 | 0.371 | 0.373 | 0.374 | 0.375 | 0.376 | 0.377 | 0.377 |
| 0.40 | 0.380 | 0.384 | 0.387 | 0.390 | 0.392 | 0.393 | 0.394 | 0.395 | 0.396 | 0.396 |
| 0.42 | 0.397 | 0.401 | 0.405 | 0.407 | 0.409 | 0.411 | 0.412 | 0.413 | 0.414 | 0.414 |
| 0.44 | 0.414 | 0.419 | 0.423 | 0.426 | 0.429 | 0.430 | 0.432 | 0.433 | 0.434 | 0.435 |
| 0.46 | 0.431 | 0.437 | 0.440 | 0.444 | 0.447 | 0.449 | 0.451 | 0.452 | 0.453 | 0.454 |
| 0.48 | 0.447 | 0.453 | 0.458 | 0.461 | 0.464 | 0.467 | 0.469 | 0.471 | 0.472 | 0.473 |
| 0.50 | 0.463 | 0.470 | 0.475 | 0.479 | 0.482 | 0.485 | 0.487 | 0.489 | 0.491 | 0.492 |
| 0.52 | 0.479 | 0.485 | 0.491 | 0.494 | 0.499 | 0.502 | 0.505 | 0.507 | 0.509 | 0.511 |
| 0.54 | 0.494 | 0.501 | 0.507 | 0.512 | 0.516 | 0.520 | 0.522 | 0.525 | 0.527 | 0.529 |
| 0.56 | 0.509 | 0.517 | 0.523 | 0.528 | 0.533 | 0.537 | 0.540 | 0.543 | 0.545 | 0.547 |
| 0.58 | 0.524 | 0.533 | 0.539 | 0.545 | 0.550 | 0.554 | 0.558 | 0.561 | 0.563 | 0.567 |
| 0.60 | 0.540 | 0.548 | 0.555 | 0.561 | 0.566 | 0.571 | 0.575 | 0.578 | 0.581 | 0.583 |
| 0.61 | 0.547 | 0.556 | 0.563 | 0.569 | 0.575 | 0.579 | 0.583 | 0.587 | 0.589 | 0.592 |
| 0.62 | 0.554 | 0.563 | 0.571 | 0.578 | 0.583 | 0.578 | 0.591 | 0.595 | 0.598 | 0.600 |
| 0.63 | 0.562 | 0.571 | 0.579 | 0.585 | 0.590 | 0.595 | 0.599 | 0.603 | 0.607 | 0.609 |
| 0.64 | 0.569 | 0.579 | 0.586 | 0.592 | 0.598 | 0.602 | 0.607 | 0.611 | 0.615 | 0.618 |
| 0.65 | 0.576 | 0.585 | 0.592 | 0.599 | 0.606 | 0.610 | 0.615 | 0.619 | 0.623 | 0.626 |
| 0.66 | 0.583 | 0.593 | 0.600 | 0.607 | 0.613 | 0.618 | 0.622 | 0.626 | 0.630 | 0.634 |
| 0.67 | 0.590 | 0.599 | 0.607 | 0.614 | 0.621 | 0.626 | 0.631 | 0.635 | 0.639 | 0.643 |
| 0.68 | 0.597 | 0.607 | 0.615 | 0.622 | 0.628 | 0.634 | 0.639 | 0.643 | 0.647 | 0.651 |
| 0.69 | 0.603 | 0.613 | 0.621 | 0.629 | 0.635 | 0.641 | 0.646 | 0.651 | 0.655 | 0.659 |

Table D-1 The Varied Flow Function Table for Adverse Slopes

| $\frac{N}{u}$ | 2.0 | 2.2 | 2.4 | 2.6 | 2.8 | 3.0 | 3.2 | 3.4 | 3.6 | 3.8 |
|---------------|-------|-------|-------|-------|-------|-------|-------|-------|-------|-------|
| 0.70 | 0.610 | 0.620 | 0.629 | 0.637 | 0.644 | 0.649 | 0.654 | 0.659 | 0.663 | 0.667 |
| 0.71 | 0.617 | 0.627 | 0.636 | 0.644 | 0.651 | 0.657 | 0.661 | 0.666 | 0.671 | 0.674 |
| 0.72 | 0.624 | 0.634 | 0.643 | 0.651 | 0.658 | 0.664 | 0.669 | 0.674 | 0.679 | 0.682 |
| 0.73 | 0.630 | 0.641 | 0.650 | 0.659 | 0.665 | 0.672 | 0.677 | 0.682 | 0.687 | 0.691 |
| 0.74 | 0.637 | 0.648 | 0.657 | 0.665 | 0.672 | 0.679 | 0.684 | 0.689 | 0.694 | 0.698 |
| 0.75 | 0.643 | 0.655 | 0.664 | 0.671 | 0.679 | 0.686 | 0.691 | 0.696 | 0.701 | 0.705 |
| 0.76 | 0.649 | 0.661 | 0.670 | 0.679 | 0.687 | 0.693 | 0.699 | 0.704 | 0.709 | 0.713 |
| 0.77 | 0.656 | 0.667 | 0.677 | 0.685 | 0.693 | 0.700 | 0.705 | 0.711 | 0.715 | 0.719 |
| 0.78 | 0.662 | 0.673 | 0.683 | 0.692 | 0.700 | 0.707 | 0.713 | 0.718 | 0.723 | 0.727 |
| 0.79 | 0.668 | 0.680 | 0.689 | 0.698 | 0.705 | 0.713 | 0.719 | 0.724 | 0.729 | 0.733 |
| 0.80 | 0.674 | 0.685 | 0.695 | 0.703 | 0.712 | 0.720 | 0.726 | 0.732 | 0.737 | 0.741 |
| 0.81 | 0.680 | 0.691 | 0.701 | 0.710 | 0.719 | 0.727 | 0.733 | 0.739 | 0.744 | 0.749 |
| 0.82 | 0.686 | 0.698 | 0.707 | 0.717 | 0.725 | 0.733 | 0.740 | 0.745 | 0.751 | 0.755 |
| 0.83 | 0.692 | 0.703 | 0.713 | 0.722 | 0.731 | 0.740 | 0.746 | 0.752 | 0.757 | 0.762 |
| 0.84 | 0.698 | 0.709 | 0.719 | 0.729 | 0.737 | 0.746 | 0.752 | 0.758 | 0.764 | 0.769 |
| 0.85 | 0.704 | 0.715 | 0.725 | 0.735 | 0.744 | 0.752 | 0.759 | 0.765 | 0.770 | 0.775 |
| 0.86 | 0.710 | 0.721 | 0.731 | 0.741 | 0.750 | 0.758 | 0.765 | 0.771 | 0.777 | 0.782 |
| 0.87 | 0.715 | 0.727 | 0.738 | 0.747 | 0.756 | 0.764 | 0.771 | 0.777 | 0.783 | 0.788 |
| 0.88 | 0.721 | 0.733 | 0.743 | 0.753 | 0.762 | 0.770 | 0.777 | 0.783 | 0.789 | 0.794 |
| 0.89 | 0.727 | 0.739 | 0.749 | 0.758 | 0.767 | 0.776 | 0.783 | 0.789 | 0.795 | 0.800 |
| 0.90 | 0.732 | 0.744 | 0.754 | 0.764 | 0.773 | 0.781 | 0.789 | 0.795 | 0.801 | 0.807 |
| 0.91 | 0.738 | 0.750 | 0.760 | 0.770 | 0.779 | 0.787 | 0.795 | 0.801 | 0.807 | 0.812 |
| 0.92 | 0.743 | 0.754 | 0.766 | 0.776 | 0.785 | 0.793 | 0.800 | 0.807 | 0.813 | 0.818 |
| 0.93 | 0.749 | 0.761 | 0.772 | 0.782 | 0.791 | 0.799 | 0.807 | 0.812 | 0.818 | 0.823 |
| 0.94 | 0.754 | 0.767 | 0.777 | 0.787 | 0.795 | 0.804 | 0.813 | 0.818 | 0.824 | 0.829 |
| 0.950 | 0.759 | 0.772 | 0.783 | 0.793 | 0.801 | 0.809 | 0.819 | 0.823 | 0.829 | 0.835 |
| 0.960 | 0.764 | 0.777 | 0.788 | 0.798 | 0.807 | 0.815 | 0.824 | 0.829 | 0.835 | 0.841 |
| 0.970 | 0.770 | 0.782 | 0.793 | 0.803 | 0.812 | 0.820 | 0.826 | 0.834 | 0.840 | 0.846 |
| 0.975 | 0.772 | 0.785 | 0.796 | 0.805 | 0.814 | 0.822 | 0.828 | 0.836 | 0.843 | 0.848 |
| 0.980 | 0.775 | 0.787 | 0.798 | 0.808 | 0.818 | 0.825 | 0.830 | 0.839 | 0.845 | 0.851 |
| 0.985 | 0.777 | 0.790 | 0.801 | 0.811 | 0.820 | 0.827 | 0.833 | 0.841 | 0.847 | 0.853 |
| 0.990 | 0.780 | 0.793 | 0.804 | 0.814 | 0.822 | 0.830 | 0.837 | 0.844 | 0.850 | 0.856 |
| 0.995 | 0.782 | 0.795 | 0.806 | 0.816 | 0.824 | 0.832 | 0.840 | 0.847 | 0.853 | 0.859 |
| 1.000 | 0.785 | 0.797 | 0.808 | 0.818 | 0.826 | 0.834 | 0.842 | 0.849 | 0.856 | 0.862 |

Table D-2 The Varied Flow Function Table for Adverse Slopes

| $\frac{N}{u}$ | 2.0 | 2.2 | 2.4 | 2.6 | 2.8 | 3.0 | 3.2 | 3.4 | 3.6 | 3.8 |
|---------------|-------|-------|-------|-------|-------|-------|-------|-------|-------|-------|
| 1.000 | 0.785 | 0.797 | 0.808 | 0.818 | 0.826 | 0.834 | 0.842 | 0.849 | 0.856 | 0.862 |
| 1.005 | 0.788 | 0.799 | 0.810 | 0.820 | 0.829 | 0.837 | 0.845 | 0.852 | 0.858 | 0.864 |
| 1.010 | 0.790 | 0.801 | 0.812 | 0.822 | 0.831 | 0.840 | 0.847 | 0.855 | 0.861 | 0.867 |
| 1.015 | 0.793 | 0.804 | 0.815 | 0.824 | 0.833 | 0.843 | 0.850 | 0.858 | 0.864 | 0.870 |
| 1.020 | 0.795 | 0.807 | 0.818 | 0.828 | 0.837 | 0.845 | 0.853 | 0.860 | 0.866 | 0.872 |
| 1.03 | 0.800 | 0.811 | 0.822 | 0.832 | 0.841 | 0.850 | 0.857 | 0.864 | 0.871 | 0.877 |
| 1.04 | 0.805 | 0.816 | 0.829 | 0.837 | 0.846 | 0.855 | 0.862 | 0.870 | 0.877 | 0.883 |
| 1.05 | 0.810 | 0.821 | 0.831 | 0.841 | 0.851 | 0.859 | 0.867 | 0.874 | 0.881 | 0.887 |
| 1.06 | 0.815 | 0.826 | 0.837 | 0.846 | 0.855 | 0.864 | 0.871 | 0.879 | 0.885 | 0.891 |
| 1.07 | 0.819 | 0.831 | 0.841 | 0.851 | 0.860 | 0.869 | 0.876 | 0.883 | 0.889 | 0.896 |
| 1.08 | 0.824 | 0.836 | 0.846 | 0.856 | 0.865 | 0.873 | 0.880 | 0.887 | 0.893 | 0.900 |
| 1.09 | 0.828 | 0.840 | 0.851 | 0.860 | 0.870 | 0.877 | 0.885 | 0.892 | 0.898 | 0.904 |
| 1.10 | 0.833 | 0.845 | 0.855 | 0.865 | 0.874 | 0.881 | 0.890 | 0.897 | 0.903 | 0.908 |
| 1.11 | 0.837 | 0.849 | 0.860 | 0.870 | 0.878 | 0.886 | 0.894 | 0.900 | 0.907 | 0.912 |
| 1.12 | 0.842 | 0.854 | 0.864 | 0.873 | 0.882 | 0.891 | 0.897 | 0.904 | 0.910 | 0.916 |
| 1.13 | 0.846 | 0.858 | 0.868 | 0.878 | 0.886 | 0.895 | 0.902 | 0.908 | 0.914 | 0.919 |
| 1.14 | 0.851 | 0.861 | 0.872 | 0.881 | 0.890 | 0.899 | 0.905 | 0.912 | 0.918 | 0.923 |
| 1.15 | 0.855 | 0.866 | 0.876 | 0.886 | 0.895 | 0.903 | 0.910 | 0.916 | 0.922 | 0.928 |
| 1.16 | 0.859 | 0.870 | 0.880 | 0.890 | 0.899 | 0.907 | 0.914 | 0.920 | 0.926 | 0.931 |
| 1.17 | 0.864 | 0.874 | 0.884 | 0.893 | 0.902 | 0.911 | 0.917 | 0.923 | 0.930 | 0.934 |
| 1.18 | 0.868 | 0.878 | 0.888 | 0.897 | 0.906 | 0.915 | 0.921 | 0.927 | 0.933 | 0.939 |
| 1.19 | 0.872 | 0.882 | 0.892 | 0.901 | 0.910 | 0.918 | 0.925 | 0.931 | 0.937 | 0.942 |
| 1.20 | 0.876 | 0.886 | 0.896 | 0.904 | 0.913 | 0.921 | 0.928 | 0.934 | 0.940 | 0.945 |
| 1.22 | 0.880 | 0.891 | 0.900 | 0.909 | 0.917 | 0.929 | 0.932 | 0.938 | 0.944 | 0.949 |
| 1.24 | 0.888 | 0.898 | 0.908 | 0.917 | 0.925 | 0.935 | 0.940 | 0.945 | 0.950 | 0.955 |
| 1.26 | 0.900 | 0.910 | 0.919 | 0.927 | 0.935 | 0.942 | 0.948 | 0.954 | 0.960 | 0.964 |
| 1.28 | 0.908 | 0.917 | 0.926 | 0.934 | 0.945 | 0.948 | 0.954 | 0.960 | 0.965 | 0.970 |
| 1.30 | 0.915 | 0.925 | 0.933 | 0.941 | 0.948 | 0.955 | 0.961 | 0.966 | 0.981 | 0.975 |
| 1.32 | 0.922 | 0.931 | 0.940 | 0.948 | 0.955 | 0.961 | 0.967 | 0.972 | 0.976 | 0.980 |
| 1.34 | 0.930 | 0.939 | 0.948 | 0.955 | 0.962 | 0.967 | 0.973 | 0.978 | 0.982 | 0.986 |
| 1.36 | 0.937 | 0.946 | 0.954 | 0.961 | 0.968 | 0.973 | 0.979 | 0.983 | 0.987 | 0.991 |
| 1.38 | 0.944 | 0.952 | 0.960 | 0.967 | 0.974 | 0.979 | 0.985 | 0.989 | 0.993 | 0.996 |
| 1.40 | 0.951 | 0.959 | 0.966 | 0.973 | 0.979 | 0.984 | 0.989 | 0.993 | 0.997 | 1.000 |
| 1.42 | 0.957 | 0.965 | 0.972 | 0.979 | 0.984 | 0.989 | 0.995 | 0.998 | 1.001 | 1.004 |
| 1.44 | 0.964 | 0.972 | 0.979 | 0.984 | 0.990 | 0.995 | 1.000 | 1.003 | 1.006 | 1.009 |

Table D-2 The Varied Flow Function Table for Adverse Slopes

| $\frac{N}{u}$ | 2.0 | 2.2 | 2.4 | 2.6 | 2.8 | 3.0 | 3.2 | 3.4 | 3.6 | 3.8 |
|---------------|-------|-------|-------|-------|-------|-------|-------|-------|-------|-------|
| 1.46 | 0.970 | 0.977 | 0.983 | 0.989 | 0.995 | 1.000 | 1.004 | 1.007 | 1.010 | 1.012 |
| 1.48 | 0.977 | 0.983 | 0.989 | 0.994 | 0.999 | 1.005 | 1.008 | 1.011 | 1.014 | 1.016 |
| 1.50 | 0.983 | 0.990 | 0.996 | 1.001 | 1.005 | 1.009 | 1.012 | 1.015 | 1.017 | 1.019 |
| 1.55 | 0.997 | 1.002 | 1.007 | 1.012 | 1.016 | 1.020 | 1.022 | 1.024 | 1.026 | 1.028 |
| 1.60 | 1.012 | 1.017 | 1.020 | 1.024 | 1.027 | 1.030 | 1.032 | 1.034 | 1.035 | 1.035 |
| 1.65 | 1.026 | 1.029 | 1.032 | 1.035 | 1.037 | 1.039 | 1.041 | 1.041 | 1.042 | 1.042 |
| 1.70 | 1.039 | 1.042 | 1.044 | 1.045 | 1.047 | 1.048 | 1.049 | 1.049 | 1.049 | 1.048 |
| 1.75 | 1.052 | 1.053 | 1.054 | 1.055 | 1.056 | 1.057 | 1.056 | 1.056 | 1.055 | 1.053 |
| 1.80 | 1.064 | 1.064 | 1.064 | 1.064 | 1.065 | 1.065 | 1.064 | 1.062 | 1.060 | 1.058 |
| 1.85 | 1.075 | 1.074 | 1.074 | 1.073 | 1.072 | 1.071 | 1.069 | 1.067 | 1.066 | 1.063 |
| 1.90 | 1.086 | 1.085 | 1.084 | 1.082 | 1.081 | 1.079 | 1.077 | 1.074 | 1.071 | 1.066 |
| 1.95 | 1.097 | 1.095 | 1.092 | 1.090 | 1.087 | 1.085 | 1.081 | 1.079 | 1.075 | 1.071 |
| 2.00 | 1.107 | 1.103 | 1.100 | 1.096 | 1.093 | 1.090 | 1.085 | 1.082 | 1.078 | 1.075 |
| 2.10 | 1.126 | 1.120 | 1.115 | 1.110 | 1.104 | 1.100 | 1.094 | 1.089 | 1.085 | 1.080 |
| 2.20 | 1.144 | 1.136 | 1.129 | 1.122 | 1.115 | 1.109 | 1.102 | 1.096 | 1.090 | 1.085 |
| 2.3 | 1.161 | 1.150 | 1.141 | 1.133 | 1.124 | 1.117 | 1.110 | 1.103 | 1.097 | 1.090 |
| 2.4 | 1.176 | 1.163 | 1.152 | 1.142 | 1.133 | 1.124 | 1.116 | 1.109 | 1.101 | 1.094 |
| 2.5 | 1.190 | 1.175 | 1.162 | 1.150 | 1.140 | 1.131 | 1.121 | 1.113 | 1.105 | 1.098 |
| 2.6 | 1.204 | 1.187 | 1.172 | 1.159 | 1.147 | 1.137 | 1.126 | 1.117 | 1.106 | 1.000 |
| 2.7 | 1.216 | 1.196 | 1.180 | 1.166 | 1.153 | 1.142 | 1.130 | 1.120 | 1.110 | 1.102 |
| 2.8 | 1.228 | 1.208 | 1.189 | 1.173 | 1.158 | 1.146 | 1.132 | 1.122 | 1.112 | 1.103 |
| 2.9 | 1.239 | 1.216 | 1.196 | 1.178 | 1.162 | 1.150 | 1.137 | 1.125 | 1.115 | 1.106 |
| 3.0 | 1.249 | 1.224 | 1.203 | 1.184 | 1.168 | 1.154 | 1.140 | 1.128 | 1.117 | 1.107 |
| 3.5 | 1.292 | 1.260 | 1.232 | 1.206 | 1.185 | 1.167 | 1.151 | 1.138 | 1.125 | 1.113 |
| 4.0 | 1.326 | 1.286 | 1.251 | 1.223 | 1.198 | 1.176 | 1.158 | 1.142 | 1.129 | 1.117 |
| 4.5 | 1.352 | 1.308 | 1.270 | 1.235 | 1.205 | 1.183 | 1.162 | 1.146 | 1.131 | 1.119 |
| 5.0 | 1.374 | 1.325 | 1.283 | 1.245 | 1.212 | 1.188 | 1.166 | 1.149 | 1.134 | 1.121 |
| 6.0 | 1.406 | 1.342 | 1.292 | 1.252 | 1.221 | 1.195 | 1.171 | 1.152 | 1.136 | 1.122 |
| 7.0 | 1.430 | 1.360 | 1.303 | 1.260 | 1.225 | 1.199 | 1.174 | 1.153 | 1.136 | 1.122 |
| 8.0 | 1.447 | 1.373 | 1.313 | 1.266 | 1.229 | 1.201 | 1.175 | 1.154 | 1.137 | 1.122 |
| 9.0 | 1.461 | 1.384 | 1.319 | 1.269 | 1.123 | 1.203 | 1.176 | 1.156 | 1.137 | 1.122 |
| 10.0 | 1.471 | 1.394 | 1.324 | 1.272 | 1.233 | 1.203 | 1.176 | 1.156 | 1.137 | 1.122 |

Table D-2 The Varied Flow Function Table for Adverse Slopes

| $\frac{N}{u}$ | 4.0 | 4.2 | 4.5 | 5.0 | 5.5 |
|---------------|-------|-------|-------|-------|-------|
| 0.00 | 0.000 | 0.000 | 0.000 | 0.000 | 0.000 |
| 0.02 | 0.020 | 0.020 | 0.020 | 0.020 | 0.020 |
| 0.04 | 0.040 | 0.040 | 0.040 | 0.040 | 0.040 |
| 0.06 | 0.060 | 0.060 | 0.060 | 0.060 | 0.060 |
| 0.08 | 0.080 | 0.080 | 0.080 | 0.080 | 0.080 |
| 0.10 | 0.100 | 0.100 | 0.100 | 0.100 | 0.100 |
| 0.12 | 0.120 | 0.120 | 0.120 | 0.120 | 0.120 |
| 0.14 | 0.140 | 0.140 | 0.140 | 0.140 | 0.140 |
| 0.16 | 0.160 | 0.160 | 0.160 | 0.160 | 0.160 |
| 0.18 | 0.180 | 0.180 | 0.180 | 0.180 | 0.180 |
| 0.20 | 0.200 | 0.200 | 0.200 | 0.200 | 0.200 |
| 0.22 | 0.220 | 0.220 | 0.220 | 0.220 | 0.220 |
| 0.24 | 0.240 | 0.240 | 0.240 | 0.240 | 0.240 |
| 0.26 | 0.260 | 0.260 | 0.260 | 0.260 | 0.260 |
| 0.28 | 0.280 | 0.280 | 0.280 | 0.280 | 0.280 |
| 0.30 | 0.300 | 0.300 | 0.300 | 0.300 | 0.300 |
| 0.32 | 0.320 | 0.320 | 0.320 | 0.320 | 0.320 |
| 0.34 | 0.339 | 0.340 | 0.340 | 0.340 | 0.340 |
| 0.36 | 0.359 | 0.360 | 0.360 | 0.360 | 0.360 |
| 0.38 | 0.378 | 0.379 | 0.380 | 0.380 | 0.380 |
| 0.40 | 0.397 | 0.398 | 0.398 | 0.400 | 0.400 |
| 0.42 | 0.417 | 0.418 | 0.418 | 0.419 | 0.420 |
| 0.44 | 0.436 | 0.437 | 0.437 | 0.439 | 0.440 |
| 0.46 | 0.455 | 0.456 | 0.457 | 0.458 | 0.459 |
| 0.48 | 0.474 | 0.475 | 0.476 | 0.478 | 0.479 |
| 0.50 | 0.493 | 0.494 | 0.495 | 0.497 | 0.498 |
| 0.52 | 0.512 | 0.513 | 0.515 | 0.517 | 0.518 |
| 0.54 | 0.531 | 0.532 | 0.533 | 0.536 | 0.537 |
| 0.56 | 0.549 | 0.550 | 0.552 | 0.555 | 0.558 |
| 0.58 | 0.567 | 0.569 | 0.570 | 0.574 | 0.576 |
| 0.60 | 0.585 | 0.587 | 0.589 | 0.593 | 0.595 |
| 0.61 | 0.594 | 0.596 | 0.598 | 0.602 | 0.604 |
| 0.62 | 0.603 | 0.605 | 0.607 | 0.611 | 0.613 |
| 0.63 | 0.612 | 0.615 | 0.616 | 0.620 | 0.622 |
| 0.64 | 0.620 | 0.623 | 0.625 | 0.629 | 0.631 |
| 0.65 | 0.629 | 0.632 | 0.634 | 0.638 | 0.640 |
| 0.66 | 0.637 | 0.640 | 0.643 | 0.647 | 0.650 |
| 0.67 | 0.646 | 0.649 | 0.652 | 0.656 | 0.659 |
| 0.68 | 0.654 | 0.657 | 0.660 | 0.665 | 0.668 |
| 0.69 | 0.662 | 0.665 | 0.668 | 0.674 | 0.677 |

Table D-2 The Varied Flow Function Table for Adverse Slopes

| $\frac{N}{u}$ | 4.0 | 4.2 | 4.5 | 5.0 | 5.5 |
|---------------|-------|-------|-------|-------|-------|
| 0.70 | 0.670 | 0.673 | 0.677 | 0.682 | 0.686 |
| 0.71 | 0.678 | 0.681 | 0.685 | 0.690 | 0.694 |
| 0.72 | 0.686 | 0.689 | 0.694 | 0.699 | 0.703 |
| 0.73 | 0.694 | 0.698 | 0.702 | 0.707 | 0.712 |
| 0.74 | 0.702 | 0.705 | 0.710 | 0.716 | 0.720 |
| 0.75 | 0.709 | 0.712 | 0.717 | 0.724 | 0.728 |
| 0.76 | 0.717 | 0.720 | 0.725 | 0.731 | 0.736 |
| 0.77 | 0.724 | 0.727 | 0.733 | 0.739 | 0.744 |
| 0.78 | 0.731 | 0.735 | 0.740 | 0.747 | 0.752 |
| 0.79 | 0.738 | 0.742 | 0.748 | 0.754 | 0.760 |
| 0.80 | 0.746 | 0.750 | 0.755 | 0.762 | 0.768 |
| 0.81 | 0.753 | 0.757 | 0.762 | 0.770 | 0.776 |
| 0.82 | 0.760 | 0.764 | 0.769 | 0.777 | 0.783 |
| 0.83 | 0.766 | 0.771 | 0.776 | 0.784 | 0.790 |
| 0.84 | 0.773 | 0.778 | 0.783 | 0.791 | 0.798 |
| 0.85 | 0.780 | 0.784 | 0.790 | 0.798 | 0.805 |
| 0.86 | 0.786 | 0.791 | 0.797 | 0.804 | 0.812 |
| 0.87 | 0.793 | 0.797 | 0.803 | 0.811 | 0.819 |
| 0.88 | 0.799 | 0.803 | 0.810 | 0.818 | 0.826 |
| 0.89 | 0.805 | 0.810 | 0.816 | 0.825 | 0.832 |
| 0.90 | 0.811 | 0.816 | 0.822 | 0.831 | 0.839 |
| 0.91 | 0.817 | 0.821 | 0.822 | 0.837 | 0.845 |
| 0.92 | 0.823 | 0.828 | 0.834 | 0.844 | 0.851 |
| 0.93 | 0.829 | 0.833 | 0.840 | 0.850 | 0.857 |
| 0.94 | 0.835 | 0.840 | 0.846 | 0.856 | 0.864 |
| 0.950 | 0.840 | 0.845 | 0.852 | 0.861 | 0.869 |
| 0.960 | 0.846 | 0.861 | 0.857 | 0.867 | 0.875 |
| 0.970 | 0.851 | 0.866 | 0.863 | 0.872 | 0.881 |
| 0.975 | 0.854 | 0.859 | 0.866 | 0.875 | 0.883 |
| 0.980 | 0.857 | 0.861 | 0.868 | 0.878 | 0.886 |
| 0.985 | 0.859 | 0.863 | 0.870 | 0.880 | 0.889 |
| 0.990 | 0.861 | 0.867 | 0.873 | 0.883 | 0.891 |
| 0.995 | 0.864 | 0.869 | 0.876 | 0.885 | 0.894 |
| 1.000 | 0.867 | 0.873 | 0.879 | 0.887 | 0.897 |

Table D-2 The Varied Flow Function Table for Adverse Slopes

| $\begin{matrix} N \\ u \end{matrix}$ | 4.0 | 4.2 | 4.5 | 5.0 | 5.5 |
|--------------------------------------|-------|-------|-------|-------|-------|
| 1.000 | 0.867 | 0.873 | 0.879 | 0.887 | 0.897 |
| 1.005 | 0.870 | 0.874 | 0.881 | 0.890 | 0.899 |
| 1.010 | 0.873 | 0.878 | 0.884 | 0.893 | 0.902 |
| 1.015 | 0.875 | 0.880 | 0.886 | 0.896 | 0.904 |
| 1.020 | 0.877 | 0.883 | 0.889 | 0.898 | 0.907 |
| 1.03 | 0.882 | 0.887 | 0.893 | 0.902 | 0.911 |
| 1.04 | 0.888 | 0.893 | 0.898 | 0.907 | 0.916 |
| 1.05 | 0.892 | 0.897 | 0.903 | 0.911 | 0.920 |
| 1.06 | 0.896 | 0.901 | 0.907 | 0.915 | 0.924 |
| 1.07 | 0.901 | 0.906 | 0.911 | 0.919 | 0.928 |
| 1.08 | 0.905 | 0.910 | 0.916 | 0.923 | 0.932 |
| 1.09 | 0.909 | 0.914 | 0.920 | 0.927 | 0.936 |
| 1.10 | 0.913 | 0.918 | 0.923 | 0.931 | 0.940 |
| 1.11 | 0.917 | 0.921 | 0.927 | 0.935 | 0.944 |
| 1.12 | 0.921 | 0.926 | 0.931 | 0.939 | 0.948 |
| 1.13 | 0.925 | 0.929 | 0.935 | 0.943 | 0.951 |
| 1.14 | 0.928 | 0.933 | 0.938 | 0.947 | 0.954 |
| 1.15 | 0.932 | 0.936 | 0.942 | 0.950 | 0.957 |
| 1.16 | 0.936 | 0.941 | 0.945 | 0.953 | 0.960 |
| 1.17 | 0.939 | 0.944 | 0.948 | 0.957 | 0.963 |
| 1.18 | 0.943 | 0.947 | 0.951 | 0.960 | 0.965 |
| 1.19 | 0.947 | 0.950 | 0.954 | 0.963 | 0.968 |
| 1.20 | 0.950 | 0.953 | 0.958 | 0.966 | 0.970 |
| 1.22 | 0.956 | 0.957 | 0.964 | 0.972 | 0.976 |
| 1.24 | 0.962 | 0.962 | 0.970 | 0.977 | 0.981 |
| 1.26 | 0.968 | 0.971 | 0.975 | 0.982 | 0.986 |
| 1.28 | 0.974 | 0.977 | 0.981 | 0.987 | 0.990 |
| 1.30 | 0.979 | 0.978 | 0.985 | 0.991 | 0.994 |
| 1.32 | 0.985 | 0.986 | 0.990 | 0.995 | 0.997 |
| 1.34 | 0.990 | 0.992 | 0.995 | 0.999 | 1.001 |
| 1.36 | 0.994 | 0.996 | 0.999 | 1.002 | 1.005 |
| 1.38 | 0.998 | 1.000 | 1.003 | 1.006 | 1.008 |
| 1.40 | 1.001 | 1.004 | 1.006 | 1.009 | 1.011 |
| 1.42 | 1.005 | 1.008 | 1.010 | 1.012 | 1.014 |
| 1.44 | 1.009 | 1.013 | 1.014 | 1.016 | 1.016 |

Table D-2 The Varied Flow Function Table for Adverse Slopes

| $\frac{N}{u}$ | 4.0 | 4.2 | 4.5 | 5.0 | 5.5 |
|---------------|-------|-------|-------|-------|-------|
| 1.46 | 1.014 | 1.016 | 1.017 | 1.019 | 1.018 |
| 1.48 | 1.016 | 1.019 | 1.020 | 1.020 | 1.020 |
| 1.50 | 1.020 | 1.021 | 1.022 | 1.022 | 1.022 |
| 1.55 | 1.029 | 1.029 | 1.029 | 1.028 | 1.028 |
| 1.60 | 1.035 | 1.035 | 1.034 | 1.032 | 1.030 |
| 1.65 | 1.041 | 1.040 | 1.039 | 1.036 | 1.034 |
| 1.70 | 1.047 | 1.046 | 1.043 | 1.039 | 1.037 |
| 1.75 | 1.052 | 1.051 | 1.047 | 1.042 | 1.039 |
| 1.80 | 1.057 | 1.055 | 1.051 | 1.045 | 1.041 |
| 1.85 | 1.061 | 1.059 | 1.054 | 1.047 | 1.043 |
| 1.90 | 1.065 | 1.060 | 1.057 | 1.049 | 1.045 |
| 1.95 | 1.068 | 1.064 | 1.059 | 1.051 | 1.046 |
| 2.00 | 1.071 | 1.068 | 1.062 | 1.053 | 1.047 |
| 2.10 | 1.076 | 1.071 | 1.065 | 1.056 | 1.049 |
| 2.20 | 1.080 | 1.073 | 1.068 | 1.058 | 1.050 |
| 2.3 | 1.084 | 1.079 | 1.071 | 1.060 | 1.051 |
| 2.4 | 1.084 | 1.081 | 1.073 | 1.061 | 1.052 |
| 2.5 | 1.090 | 1.083 | 1.075 | 1.062 | 1.053 |
| 2.6 | 1.092 | 1.085 | 1.076 | 1.063 | 1.054 |
| 2.7 | 1.094 | 1.087 | 1.077 | 1.063 | 1.054 |
| 2.8 | 1.096 | 1.088 | 1.078 | 1.064 | 1.054 |
| 2.9 | 1.098 | 1.089 | 1.079 | 1.065 | 1.055 |
| 3.0 | 1.099 | 1.090 | 1.080 | 1.065 | 1.055 |
| 3.5 | 1.103 | 1.093 | 1.082 | 1.066 | 1.055 |
| 4.0 | 1.106 | 1.097 | 1.084 | 1.067 | 1.056 |
| 4.5 | 1.108 | 1.098 | 1.085 | 1.067 | 1.056 |
| 5.0 | 1.110 | 1.099 | 1.085 | 1.068 | 1.056 |
| 6.0 | 1.111 | 1.100 | 1.085 | 1.068 | 1.056 |
| 7.0 | 1.111 | 1.100 | 1.086 | 1.068 | 1.056 |
| 8.0 | 1.111 | 1.100 | 1.086 | 1.068 | 1.056 |
| 9.0 | 1.111 | 1.100 | 1.086 | 1.068 | 1.056 |
| 10.0 | 1.111 | 1.100 | 1.086 | 1.068 | 1.056 |

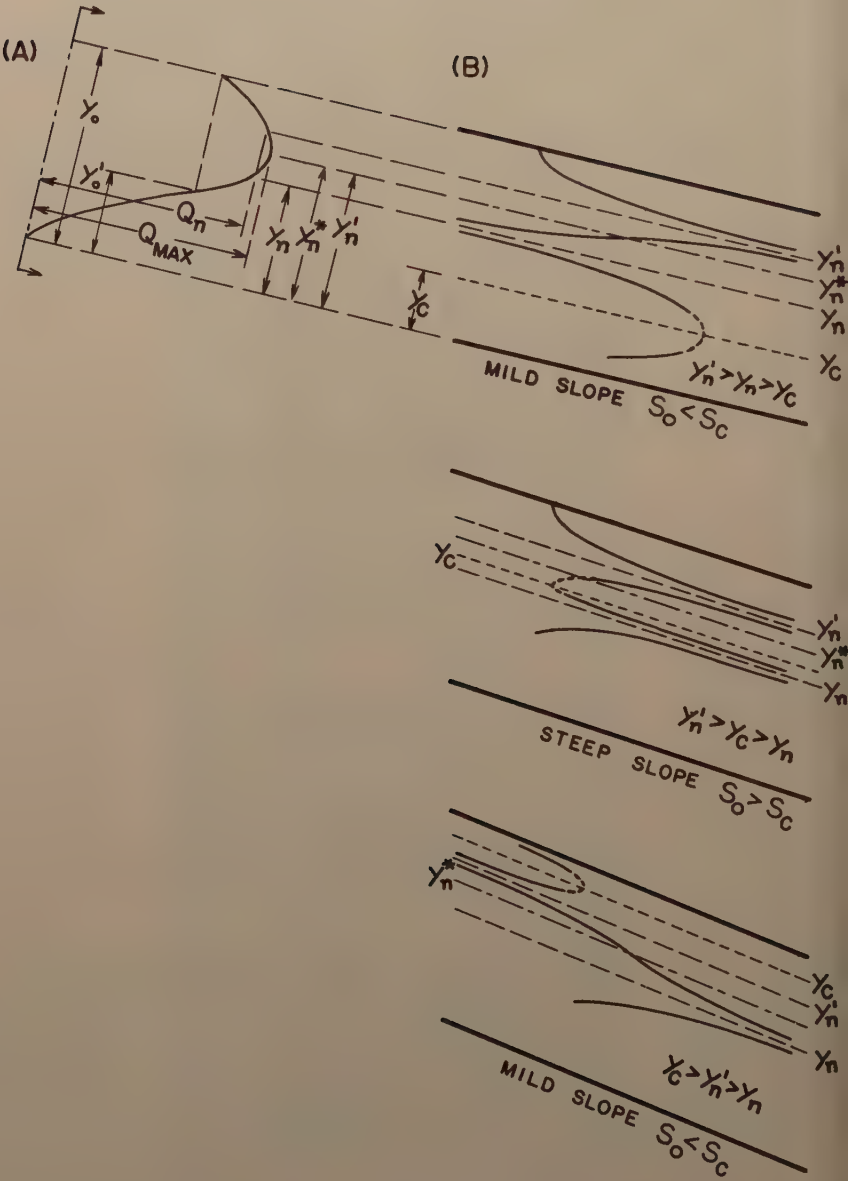


FIG.D-2 FLOW PROFILES OF A CLOSED CONDUIT

Discussion of
"FREE OUTLET AND SELF-PRIMING ACTION OF CULVERTS"

by Wen-Hsiung Li and Calvin C. Patterson
(Proc. Paper 1009)

J. E. FLACK,* J.M. ASCE.—The authors' presentation deals with some aspects of culvert flow that are not ordinarily considered when designing these structures.(1) Experiments with which the writer is familiar, conducted at the Iowa Institute of Hydraulic Research by graduate students in the Department of Mechanics and Hydraulics, are hereafter described because of the similarity and extension to the results as presented in the paper under discussion.

Piezometric Grade Line

The Iowa experiments determined the location of the intersection of the hydraulic grade line with the plane of the culvert outlet, for free flow, for a 4 inch round conduit by Rueda(2) and for a 3 inch square box culvert model by the writer.(3) The evaluation of the factor m , i.e., the ratio, expressed as a decimal, of the height of the intersection of the hydraulic grade line with the plane of the outlet to the total height of the pipe or culvert, was determined by extending the hydraulic grade line to the plane of the outlet. The hydraulic grade line in the culvert barrel was determined by piezometer connections at points along the length of the culvert. All measurements were made with the culvert horizontal and flowing full.

The variation of m with the Froude number of the flow was determined for both the round conduit and the box culvert, and the results are shown on Figure 1. Also shown are two values for m as determined by the staff of the Institute using the relaxation method for a two-dimensional, frictionless, conduit outlet. The authors' curves are also reproduced for comparison purposes.

For the round pipe, the authors' curve is lower than that of Rueda at Froude numbers greater than 1.0. For the box culvert, the departure of the authors' curve from the plotted values as obtained in the Iowa experiments is significant above Froude numbers of 1.5, with the Iowa results consistently lower.

Since the experiments were similar the discrepancy in results can, perhaps, be attributed to the different methods of evaluating m , although some of the authors' plotted values are quite close to those as obtained in the Iowa experiments. Further experimentation is suggested to determine values of m for higher values of the Froude number of the flow before the authors' curves are used to "furnish proper values of m for design."

* Instr., Dept. of Civ. Eng., Univ. of Colorado, Boulder, Colo.

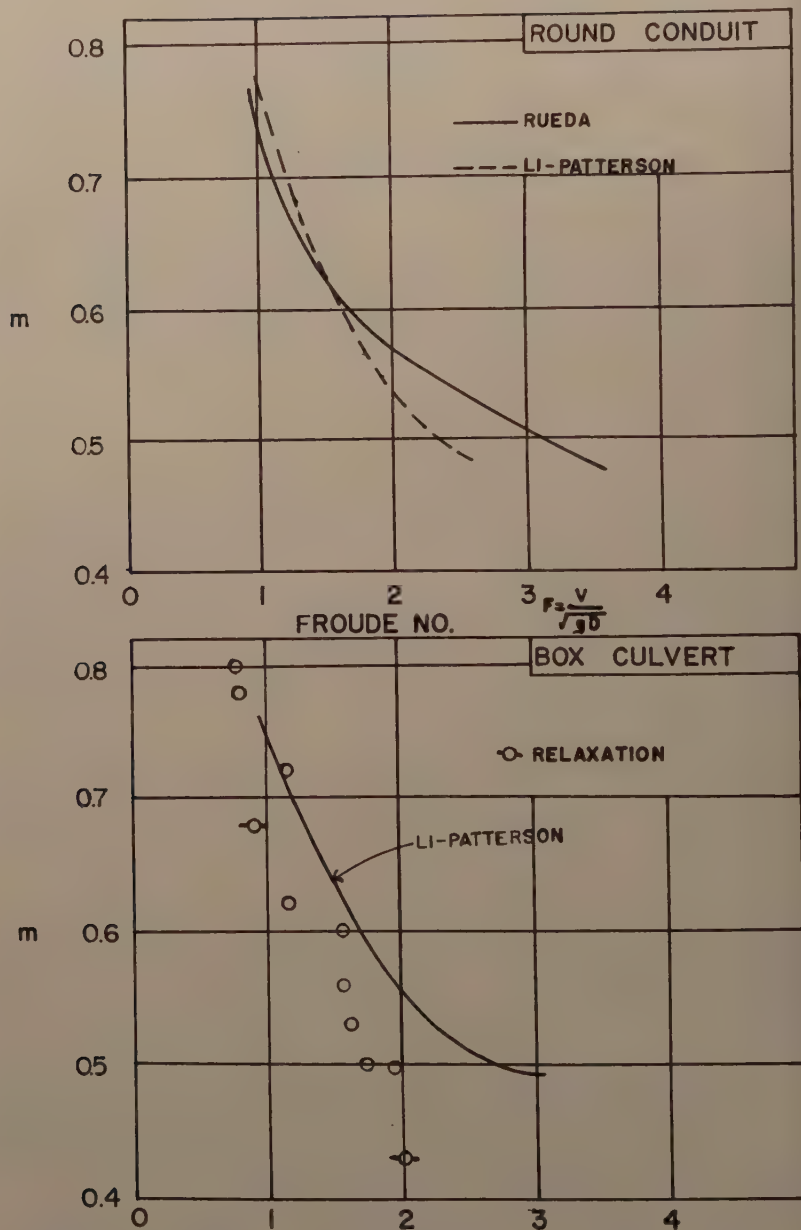


FIG.1 HYDRAULIC GRADE LINE AT THE OUTLET OF A HORIZONTAL CONDUIT



Fig. 2 Vortex Over a Well-Rounded Inlet.
(Culvert Flowing Full)

Priming

Self-priming of culverts was also noted in the Iowa experiments. A significant phenomena, apparently not encountered by the authors, was the formation of vortices over the culvert inlet. These had the effect of counteracting the priming action by feeding air to the zone of separation. In most cases, the Iowa models differed from those of the authors only in that the slope of the top of the wing-walls was continued above the culvert much like a highway embankment. Figure 2 is a photograph of a vortex over a well founded inlet of a culvert flowing full.

A model of a standard culvert inlet, with square entrance and flaring wingwalls, was modified and the results can be summarized as follows:

1. The standard inlet will perform more efficiently with the addition of a smooth well-rounded entrance. It is more important to round the top than the sides.
2. A well-rounded inlet, with rounding on the top and sides, and a headwall as high as the design head and approximately twice as wide as the culvert will give the most efficient performance, and vortex action will be eliminated.

Another aspect noted was the scale effect in evaluating prototype performance for culverts. In the Iowa tests a 6 inch model box culvert, as tested by Maksoud,⁽⁴⁾ gave appreciably better performance than a 3 inch model of similar design. It might be expected that results of similar significance can be expected with larger models and prototype structures.

REFERENCES

1. California Culvert Practice, 2nd Edition, Division of Highways, Department of Public Works, Sacramento, California, Chart B.
2. Rueda-Briceno, Daniel, "Pressure Conditions at the outlet of a Pipe," unpublished M.S. thesis, State University of Iowa, February, 1954.
3. Flack, J. E., "Improved Culvert Inlet Design," unpublished M.S. thesis, State University of Iowa, August, 1954.
4. Maksoud, H., "Effect of Inlet Design on Square Culvert Flow," unpublished M.S. Thesis, State University of Iowa, February, 1954.

JOHN L. FRENCH,* A.M. ASCE.—The authors are to be congratulated on their contributions to culvert hydraulics. These contributions are two-fold: first, they have devised an ingenious experimental method for determining the effective pressure at the culvert outlet and secondly, they have contributed significantly to a better understanding of the various complex phenomena by which the regime of flow in a culvert may change from part full to full conduit flow.

During the past two years the Bureau of Public Roads has sponsored an investigation of pipe culvert flow in the hydraulic laboratory of the National Bureau of Standards. While the project is not yet completed, some of the experimental data now available are pertinent to the problems investigated by the authors.

* Hydr. Engr., National Bureau of Standards, U. S. Dept. of Commerce, Washington, D. C.

In a sufficiently long culvert, flowing full, three distinct zones of flow along the culvert may be observed. The first may be termed the zone of flow establishment in which boundary layer development plays an important role, with consequent variation of the velocity profile with distance from the inlet. As the flow proceeds downstream the developing boundary layer grows progressively thicker and eventually reaches the center of the pipe. At this point the velocity profile becomes stable with no further variation of shape with distance from the inlet. This constancy of the velocity profile is a characteristic of the second zone of flow, sometimes termed the zone of established flow.

At the outlet, assuming a non-submerged condition with either free fall or in apron support, non-hydrostatic pressure distribution prevails. Owing to the necessary redistribution of pressures required by the change from hydrostatic pressure distribution in the zone of established flow to the non-hydrostatic pressure distribution at the outlet, a terminal length exists near the outlet in which accelerative effects become important with consequent distortion of the axisymmetrical velocity profile of the zone of established flow to a non-symmetrical velocity distribution at the outlet. It is the phenomenon occurring in the terminal length with regard to redistribution of pressures and velocities which makes necessary the determination of an effective pressure at the outlet for use with the one-dimensional method of analysis of full conduit flow in culverts. The authors have investigated this problem in an ingenious and simple experimental manner for a conduit 20 diameters in length.

The authors' basic equation for defining m , is

$$H_1 + SL = \alpha_1 \frac{V^2}{2g} + mD + \Delta_1, \quad (15)$$

which follows directly from the authors' equation (1) on the assumption that the approach velocity is negligible. In equation (15) the energy correction factor α_1 applies to the outlet section. Under these circumstances the authors correctly define mD as the mean piezometric head at the outlet section; i.e.

$$mD = \frac{1}{Q} \int_Q \left(\frac{p_1}{\rho g} + z \right) dQ, \quad (16)$$

where p_1 is the pressure at the outlet section a vertical distance z above the invert. At the same time the authors state the "... effective value of mD for long culverts can also be obtained by projecting the hydraulic grade line to the outlet section." There would appear to be a conflict of ideas here.

Let βD be the elevation above the invert at the outlet section of the extended straight line hydraulic gradient of the zone of established flow. It then follows that

$$h - \beta D = f \frac{\ell_t}{D} \frac{V^2}{2g}, \quad (17)$$

where ℓ_t is the length of the terminal segment and h is the piezometric head at the upstream end of the terminal length, the datum being taken as the invert of the outlet section.

For the segment of the culvert including only the zone of flow establishment and the zone of established flow it is clear that

$$H_1 + SL - h = h_e + \alpha'_1 \frac{V^2}{2g} + f \frac{(L - \ell_t)}{D} \frac{V^2}{2g}, \quad (18)$$

where α'_1 is the kinetic energy factor for the zone of established flow and h_e is the so-called entrance loss. Eliminating h through equation (17),

$$H_1 + SL = \alpha'_1 \frac{V^2}{2g} + \beta D + (h_e + f \frac{L}{D} \frac{V^2}{2g}). \quad (19)$$

Subtracting equation (15),

$$mD = \beta D - \frac{V^2}{2g} (\alpha_1 - \alpha'_1) - \left[\Delta_1 - (h_e + f \frac{L}{D} \frac{V^2}{2g}) \right], \quad (20)$$

and it is clear that m and β are not identical. The distinction between the two is that mD is the mean piezometric head at the outlet, as defined by equation (16) which follows from equation (15), while βD is an effective piezometric head defined by

$$\beta D = \frac{1}{Q} \int_Q \left(\frac{p_1}{\rho g} + z \right) dQ + \frac{V^2}{2g} (\alpha_1 - \alpha'_1) + \left[\Delta_1 - (h_e + f \frac{L}{D} \frac{V^2}{2g}) \right], \quad (21)$$

which follows from equations (16) and (20) through the definition of the effective piezometric head at the outlet section as being the elevation above the invert of the point at which the extended straight line piezometric gradient of the zone of established flow pierces the outlet plane.

Consideration of equation (21) will show that the experimental problem of determining βD , as well as mD , of course, stems entirely from the deviation of the pressure distribution from hydrostatic at the outlet. That is, if hydrostatic pressure distribution prevails throughout the terminal length, vertical accelerations in the terminal length will be absent and it follows that curvature of the stream lines in the terminal length can not occur. Hence the axisymmetrical velocity distribution of the zone of established flow will continue undistorted through the terminal length, and referring to equation (21)

$$\frac{1}{Q} \int_Q \frac{z}{D} dQ = \frac{1}{2},$$

$$\alpha_1 - \alpha'_1 = 0,$$

and

$$\Delta_1 - (h_e + f \frac{L}{D} \frac{V^2}{2g}) = 0,$$

from which

$$\beta = \frac{1}{2} + \frac{1}{Q} \int_Q \frac{p_1}{\rho g D} dQ. \quad (22)$$

If it is further assumed that $\frac{1}{Q} \int_Q \frac{p_1}{\rho g D} dQ$ is zero, $\beta = 1/2$, the value commonly used in the conventional one-dimensional pipe flow theory for a non-submerged outlet.

If it is assumed that the outlet is submerged by a tail water depth T and that hydrostatic pressure distribution occurs at the outlet, it follows from equation (22) that $\beta = T/D$ the value commonly assumed for a submerged outlet.

With reference to the experimental method used by the authors let equation (19) as it refers to a particular type of outlet condition be

$$H_1 + SL = \alpha'_1 \frac{V^2}{2g} + \beta_1 D + (h_e + f \frac{L}{D} \frac{V^2}{2g})_1 \quad (23)$$

and with a second type of outlet condition

$$H_2 + SL = \alpha'_2 \frac{V^2}{2g} + \beta_2 D + (h_e + f \frac{L}{D} \frac{V^2}{2g})_2.$$

Subtracting equation (23) and rearranging

$$\beta_1 D = \beta_2 D - (H_2 - H_1) + \frac{V^2}{2g} (\alpha'_2 - \alpha'_1) + (h_{e2} - h_{e1}).$$

If the culvert is sufficiently long to have a zone of established flow, $\alpha'_2 = \alpha'_1$ and

$$\beta_1 D = \beta_2 D - (H_2 - H_1) + (h_{e2} - h_{e1}). \quad (24)$$

If it is now assumed that the subscript 2 refers to a submerged outlet in which the tail water elevation above the invert is T , equation (24) becomes on the assumptions that (a) $\beta_2 D = T$ and (b) $h_{e2} = h_{e1}$,

$$\beta_1 D = T - (H_2 - H_1),$$

the relation used by the authors to compute mD for the various outlet conditions.

Since both of these assumptions were made by the authors in the derivation of equation (4) as well as the assumption that the velocity distribution at the outlet face is identical for the submerged and nonsubmerged cases, it would

appear that the authors novel experimental method would determine β with perhaps greater accuracy than m .

The authors have used a conduit length of 20 diameters in determining the effective pressure at the outlet face. In view of the work of Morris⁷ it would appear questionable if the fully developed turbulent velocity profile characteristic of the zone of established flow actually existed at the upstream end of the terminal length. Some influence of velocity distribution at the upstream end of the terminal length on β or m would be expected. Whether the magnitude of this effect would be such as to have practical significance is not clear.

In this connection it may be observed that in the above discussion of β it was assumed that the culvert barrel was sufficiently long so that a zone of established flow existed. It is obvious that for culverts so short as not to possess a zone of established flow that the concept of the effective pressure head at the outlet as being the elevation above the invert at which the extended straight line piezometric gradient of the zone of established flow pierces the plane of the outlet is without direct physical significance. For such short culverts equation (19) employs a resistance coefficient f , which is no longer directly applicable to any segment of the culvert barrel, and it employs a kinetic energy factor α'_1 and an entrance head loss h_e , neither of which are now invariant with culvert length. Under these circumstances the utility of equation (19) with reference to short barrels is open to question, as is also, of course, the physical significance of equation (17) which defines β in terms of the resistance coefficient of the zone of established flow.

The authors describe three types of filling or priming phenomena characterizing the change from part full sluice type flow to full conduit flow. In tests made by the writer with a smooth lucite model culvert 5.5 inches in diameter and 63.9 diameters long, two additional types of filling phenomena were observed. These consisted of:

A. Filling through direct backwater effect. The authors under their type 1 priming phenomena for mild slopes describe the filling of a model culvert by means of a hydraulic jump. The presence of a jump in the authors' tests with sub-critical slopes would imply supercritical flow in the upstream portion of the barrel, with the presence of a typical vena contracta near the inlet. This type of flow may for convenience be termed contracted flow at the inlet. In the writer's tests for mild slopes this filling process by means of a hydraulic jump was also observed but as the slope was progressively decreased a point was reached where contracted flow at the inlet and hence a hydraulic jump did not occur and the filling mechanism consisted simply of a backwater effect in which the water surface near the inlet approached the barrel crown as $Q/D^{5/2}$ was increased.

It was observed experimentally that the filling mechanism consisted of the non-contracted flow backwater effect described above at zero slope. At a slope of 0.25% contracted flow occurred with filling by means of a hydraulic jump. The criterion which determines if filling by this method will occur is apparently the depth of water, due to backwater effect, at the section where the vena contracta would ordinarily form, when the inlet becomes submerged. If this depth due to backwater is greater than the conjugate or alternate depth

7. Preliminary Flow Tests on a Model Culvert, by Henry M. Morris, Project Report No. 7, St. Anthony Falls Hydraulic Laboratory, Univ. of Minn.

corresponding to the rate of discharge and the vena contracta depth, a jump cannot form because of momentum considerations, hence contracted flow cannot occur, and the filling mechanism consists simply of the backwater curve approaching the culvert crown at the inlet as the rate of discharge is sufficiently increased. However, if the depth referred to is less than the conjugate depth then a jump occurs, with contracted flow at the inlet, for sufficiently long culverts on sub-critical slopes, and filling occurs when the rate of discharge is increased sufficiently to cause the water surface immediately downstream of the jump to approach the culvert crown.

B. Combined free surface and full conduit flow. As the barrel slope is increased through critical slope, sub-critical flow can no longer exist in the downstream portion of the barrel, and hence filling by means of a hydraulic jump can no longer occur. For slopes in the range 0.6% to 1.25% the filling mechanism, for the 63.9 diameter long conduit used by the writer, was observed to consist of the following: The flow was supercritical throughout the culvert barrel, and because of boundary roughness the maximum depth of flow occurs at or slightly upstream from the outlet. Also owing to the supercritical flow, the water surface is subject to standing shock waves generated by the channel contraction at the inlet. As the flow is increased a point is reached where initial contact of the water surface with the culvert crown occurs one or two diameters upstream from the outlet. The contact point advances a short distance upstream and becomes stationary with the portion of the culvert barrel downstream of the contact point flowing full. This type of flow was characterized by entrained air being passed through the full conduit flow and the presence of an intermittent vortex in the upstream pool feeding air into the culvert barrel and thence to the air pocket extending from the inlet to the contact point marking the upstream end of the segment of the barrel flowing full. The pressure in the air pocket was appreciably sub-atmospheric. Flow conditions thus consisted of the portion of the barrel immediately above the outlet operating in full conduit flow and an upstream portion of the barrel operating in free surface flow, with the air space above the free surface under a non-steady, sub-atmospheric pressure with air being withdrawn at the downstream end of the 50 or 60 diameter long air pocket by air entrainment through the full conduit portion of the barrel and an intermittent supply of air coming to the air pocket from vortex action in the upstream pool.

After initial filling at the outlet, as the rate of discharge was increased the contact point of the free water surface with the culvert crown moved progressively upstream until it reached a distance of 15 or 20 diameters from the outlet. Any further increase in the rate of discharge then caused the culvert to fill throughout its entire length.

The filling mechanism in this case is connected with the internal forces controlling the relative magnitude of the rate of discharge Q_1 in the free surface segment of the barrel, and the rate of discharge Q_2 of the full conduit flow segment. If for a given location of the contact point of the free surface with the culvert crown (marking the upstream end of the full conduit flow segment), $Q_1 > Q_2$ the contact point will move upstream; if $Q_1 = Q_2$ an equilibrium condition will have been established and the contact point will be stationary, and if $Q_2 > Q_1$ the contact point will move downstream. The discharge Q_2 of the full conduit segment will of course be a function of the net pressures acting to force water through the full conduit flow segment. That

is, the effective pressure on the upstream end of the full conduit section and hence Q_2 will be determined by the air pressure over the free surface segment and by momentum considerations relating to the depth and velocity of the free surface flow immediately upstream from the full conduit flow segment. In like manner the rate of discharge Q_1 of the free surface flow will be determined, for a given inlet, by the depth of submergence of the inlet and the air pressure over the free surface flow.

With regard to the effect of the sub-atmospheric pressure over the free surface, consider the typical case with this type of filling mechanism in which a short segment of the barrel immediately upstream from the outlet is flowing full and the rest of the barrel is flowing with a free surface. Assume first that the air pressure over the free surface flow is atmospheric and that the flow is in equilibrium. That is, $Q_1 = Q_2$ and the contact point of the free surface with the barrel crown is stationary. If it is now assumed that a sub-atmospheric pressure develops over the free surface, it is obvious that Q_1 will increase and Q_2 will decrease. That is a non-steady flow condition will have developed in which $Q_1 > Q_2$ and consequently the contact point will move upstream either to a new equilibrium point, the internal forces permitting, or regime change to full conduit flow over the whole length of the barrel will occur. It is apparent that a decrease in pressure over the free surface will have the effect of causing the contact point to move upstream and hence would be expected to promote change to full conduit flow at lower inlet submergences.

That the air pressure over the free surface appreciably affects the filling mechanism was demonstrated experimentally by installing a small air vent over the free water surface. With the vent open for the passage of air from the atmosphere to the air pocket, filling occurred for a slope of 1.25% at an inlet submergence, 0.65D higher than when the vent was closed. Measurement of these sub-atmospheric pressures over the free surface indicate that they are not of inconsequential magnitude; the pressure head, referred to atmospheric, varying from -0.18D for a slope of 0.6% to -0.57D for a 1.25% slope. These measurements were made immediately after initial contact of the water surface with the barrel crown had occurred near the outlet, and represent an equilibrium condition in which the contact point was stationary (or more precisely, oscillating about a stationary point) approximately four to six diameters upstream from the outlet. They do not represent the pressures just prior to regime change to full conduit flow. That such pressures would show a further decrease is indicated by a preliminary set of data for the 0.6% slope in which the pressure head decreased from -0.18D for initial contact of the water surface with the crown to -0.25D just prior to regime change to full conduit flow throughout the culvert.

These sub-atmospheric pressures over the free surface flow are, as has been noted, the result of pumping air out of the air pocket through air entrainment at the upstream end of the full conduit flow section and an inflow of air through vortex action at the inlet.

It is to be noted in the above description that three conditions are necessary for this particular type of filling mechanism to occur. First the barrel length, slope and roughness must be such that initial contact of the water surface with the crown occurs at or slightly upstream from the outlet section. Second, the rate of discharge required to cause initial filling at the outlet section must be such that the internal forces corresponding to this rate of discharge may reach an equilibrium point where $Q_1 = Q_2$ for a contact point

less than L distant from the outlet. And third, as the discharge is increased a point must be reached where $Q_1 > Q_2$ throughout the culvert, with consequent regime change to full conduit flow.

For the 63.9 diameter long, smooth lucite culvert used in the writer's tests, regime change to full conduit flow by the phenomenon described in B above failed to occur as the slope was increased above 1.25% through inability of the flow to satisfy the second of the three requirements for type B filling. That is, regime change to full conduit flow throughout the entire barrel occurred immediately after initial filling of the conduit at the outlet section, in the same manner as described by the authors under "Self-priming with a divergent flow." In the tests made by the writer the initial section of filling was invariably within 2 to 4 diameters of the outlet.

In the writer's tests piezometer openings were placed on the culvert crown at points 0.7D, 7.6D, 24.2D and 43.2D from the inlet. These piezometer openings made it possible to measure the air pressure within the conduit during part full flow, as well as during the filling operation described under B above. Preliminary analysis of the data indicates that the air pressure, for a square edge inlet, may be represented to an approximation by a relation of the form

$$\frac{p_a}{\rho g D} = -\theta \left(\frac{Q}{D^{5/2}} \right)^6,$$

where θ is for the single 63.9 diameter long smooth culvert used, a function only of the distance from the inlet, and p_a is the air pressure over the free surface, referred to atmospheric as a datum.

The experimentally determined values of θ , at distances of 0.7D and 7.6D from the face of the inlet were 3.8×10^{-7} and 0.96×10^{-7} respectively, indicating first that a large adverse air pressure gradient exists near the inlet and secondly that the sub-atmospheric pressure head near the inlet is substantial for the higher rates of flow; amounting to $-0.25D$ at the first piezometer opening for $Q/D^{5/2} = 9.5$, a value of $Q/D^{5/2}$ still within the range of the outlet control filling mechanism described in the authors' type 2 filling.

In the writer's tests with a longer and greater diameter barrel than used by the authors the precise filling mechanism described by the authors under "(3) Self-priming due to standing surface waves," in which priming occurred near the inlet due to a wave crest approaching the barrel crown, was not observed. In this connection it may be noted that in the writer's tests the water surface for a distance of 6 or 8 diameters downstream from the inlet, except for a segment immediately downstream from the inlet of approximate length 1.5D, could not be observed visually because of a sheet of water flowing around the pipe boundary.

Since the rate of discharge required to cause the water surface to approach the outlet crown increases as the slope is increased, it is apparent, as was observed experimentally, that the inlet section must be subjected to increasingly large sub-atmospheric pressures as the slope increases with type 2 filling. As observed in the writer's tests with a longer barrel than the authors', this rapid increase in sub-atmospheric pressure in the inlet section as $Q/D^{5/2}$ approaches and increases above 9.5 appears to be an important part of the internal mechanism operating within the culvert to cause,

as the slope is increased above 1.8%, a change in the filling mechanism from outlet control in which filling occurs through the water surface approaching the culvert crown to a complex inlet filling mechanism involving both pneumatic and hydraulic phenomena.

For the 63.9D long smooth culvert used in the writer's tests, initial filling at the inlet occurred at slopes of 2% and greater. Owing to the supercritical flow, the water surface was subjected to shock waves caused by the channel contraction at the inlet, as observed by the authors. These shock waves exhibited the usual pattern of such waves, with the water surface transverse to the barrel axis deviating appreciably from a horizontal line. The waves were of appreciable magnitude near the inlet and decreased in amplitude as the outlet was approached. The barrel segment in the region from the inlet to a section approximately 8 diameters downstream was observed as previously stated to be under sub-atmospheric air pressures of relatively large magnitude just prior to regime change from part full to full conduit flow. Violent entrainment of air was observed near the inlet as reported by the authors. At a section 8 diameters downstream from the inlet the water was observed to contain many air bubbles. This relatively large volume of entrained air observed at this section was for the most part discharged from the water before a section approximately 12 to 15 diameters downstream from the inlet was reached.

Inasmuch as an air-carrying vortex is in general not present at the high pool levels required to cause regime change on the slopes now considered, the presence of entrained air in the inlet region indicates a flow of air above the water surface in the upstream direction. There would thus appear to be a relatively large local circulation of air in the barrel segment extending from the inlet to a section 12 to 15 diameters downstream. That is, air is entrained by the water near the inlet and carried 12 to 15 diameters downstream where it enters the air space above the free surface and then flows upstream to the inlet region where it is re-entrained.

As the rate of discharge is increased a point is eventually reached where the sluice type flow abruptly changes to full conduit flow. For all slopes tested of 2% to 9.39%, the initial change to full conduit flow occurred 6 or 8 diameters downstream from the inlet. Invariably after the initiation of full conduit flow at this section the region of full conduit flow spread abruptly upstream and downstream filling the entire conduit. Also invariably, the onset of full conduit flow was characterized by the abrupt appearance of foamy water throughout the conduit cross section. As indicated previously in no case was the filling mechanism for the 63.9 long barrel used by the writer observed to be the result of simple wave action as described by the authors for their shorter barrels under "Self-priming due to standing surface waves" with filling being caused by the gradual approach, as $Q/D^{5/2}$ was increased, of a wave crest to the culvert crown.

That the relatively large adverse air pressure gradient in the 5 to 10 diameter length segment immediately downstream from the inlet exerts a marked influence on the filling mechanism for this type of flow was demonstrated by allowing air to flow into the region from the atmosphere through the piezometer openings on the top of the culvert. This effect was first demonstrated by Straub, Anderson and Bowers,⁸ who showed that for a square

8. Effect of Inlet Capacity of Culverts on Steep Slopes by L. G. Straub,

(footnote contd. pg. 3)

edge inlet to a smooth lucite circular barrel of 105 diameters in length on a 4% slope, full conduit flow resulted at $Q/D^{5/2} = 9.35$ for normal operation, while it did not when the culvert was "ventilated," presumably by allowing air to flow into the sub-atmospheric pressure region above the free surface through piezometer openings in the crown of the barrel.

This demonstrated effect of the adverse air pressure gradient near the inlet, in lowering the pool level at which filling occurs, would be qualitatively expected from considerations of the effect of such a gradient on the downstream flow. In this connection it is obvious from energy considerations that for a given rate of flow, the effect of the adverse pressure gradient over the free surface will be to decrease the specific energy of the flow, and hence increase the depth of flow at points in the culvert barrel downstream of the inlet as compared with the depths that would have prevailed at the same rate of flow, had the adverse pressure gradient not been present. The increase in depth, for a given discharge, caused by the adverse pressure gradient at a given downstream point would be expected, of course, to cause regime change to full conduit flow at a lower value of $Q/D^{5/2}$ (and H/D) than would be the case had the gradient not been present.

As observed in the writer's tests, the precise mechanism by which filling occurs near the inlet, involving as it does an adverse air pressure gradient of appreciable magnitude, a relative large local air circulation in the barrel for some 12 to 15 diameters downstream, and an air entrainment process which involves the energy losses associated with the entrainment and transport of air from a region of low pressure to a region of higher pressure, well deserves further experimental study.

Filling of this type might be expected to be relatively insensitive to length except for barrel lengths which placed the outlet within the 12 to 15 diameter long segment of conduit being subject to the observed severe local circulation of air above the free water surface. Reduction of barrel length sufficiently to place the outlet in this region would be expected to lower the adverse pressure gradient and hence require increased rates of flow to cause filling.

The above comments on the filling mechanisms are the results of the writer's observations on a barrel length substantially longer and with an appreciably greater barrel diameter than any used by the authors.

Owing in part to the inferred importance of air entrainment phenomena on some of the filling mechanisms and in part to previous experimental work which demonstrated the substantial effect of approach flow turbulence level on the filling mechanism of rounded and pipe socket inlets at lengths of 14 to 41 diameters, additional tests were made with the square edge inlet with a 63.9 diameter long barrel in which the approach flow turbulence level was varied by means of screens and grids. The width of the approach channel was not varied, being 13.1 diameters in all cases and the grid and screens were installed 6 diameters above the inlet and 10.4 diameters downstream of the gravel baffle used in all the tests.

These data are shown in figure 13. The points plotted are the averages of as many as 5 consecutive runs under the same conditions. It will be noted in figure 13 that two series of tests were made with screens. In the first

A. G. Anderson and C. E. Bowers, Project Report No. 37, St. Anthony Falls Hydraulic Laboratory, University of Minnesota. Appendix V, Table II, runs 460 and 461.

series of tests one double screen was used. This consisted of a 1-inch by 4-inch wooden frame on each side of which commercial insect screen was tacked. This screen assembly thus consisted of two screens placed 4 inches apart. In the second series of screen tests two double screen assemblies were used resulting in 4 screens placed 4 inches apart. The insect screens used were made up of wires of 0.011-inch diameter spaced 14 wires to the inch in one direction and 16 to the inch in the other direction. It will be observed that there is no significant difference in results between the two series of screen tests, from which it is inferred that the screens used reduced the approach flow turbulence level sufficiently so that any further reduction in level would not significantly affect the filling mechanism.

The grid used consisted of vertical 2-inch wooden slats placed 1 inch apart. The fact that the data for the grid lie between those for the screens and the gravel baffle would indicate as noted previously by Rouse⁹ that the flow from a crushed stone baffle of high solidity ratio may of itself introduce a high level of turbulence. In the case of the writer's channel, the turbulence level owing to the gravel baffle was apparently sufficiently high so that the effect of the grid, of the size used was to reduce rather than increase the turbulence level at the inlet.

It will be noted from figure 13 that the filling mechanism over the range of slopes above 0.6% is sensitive to approach flow turbulence level and that a substantial effect exists.

Of significance also is the fact that type B filling described above was not observed in the tests with screens, and it would appear that approach flow turbulence level affects regime change from sluice type flow to full conduit flow in at least two ways. First, it may exert its effect of producing full conduit flow at a lower H/D simply by accentuating the intensity of a filling mechanism, for example, the air entrainment process at the greater slopes, or it can exert its effect by completely altering the type of filling mechanism occurring at a given slope, as was the case for type B filling with screens in the approach channel.

The data described above on the five distinct filling phenomena observed in tests with a 63.9 diameter long culvert are believed directly pertinent to the authors' results for shorter conduits only in regard to the general applicability of equation (14).

The authors' initial relation with reference to the development of equation (14) is equation (5) which is stated to follow from dimensional considerations. This is true, of course, only if it is assumed that at filling

$$f(L, D, g, Q, n, S) = 0. \quad (25)$$

In view of the demonstrated effect of approach channel turbulence, the important part played in the filling mechanism by vortex action and air entrainment in type B filling, and the existence for the higher slopes of a filling phenomenon involving a substantial air pressure gradient accompanied by violent air entrainment and strong local circulation of air in the inlet region, as observed in the writer's tests with the longer barrel and larger barrel diameter, the assumption of general applicability of equation (25), as a

9. An Investigation of Flow Through Screens, by W. D. Baines and E. G. Peterson, Transactions of the American Society of Mechanical Engineers, July 1951, discussion by Hunter Rouse.

preliminary to the derivation of equation (14) would appear to be an assumption of importance which deserves experimental exploration.

The authors reduce by one, the number of dimensionless groups of variables in equation (5) or (7) by use of the gradually varied flow equation and arrive at equation (14). This procedure involves the further assumption that since the variables L/D , $n^2/D^{1/3}$ and S may be combined to the groupings

$\frac{S}{D}$ and $\frac{SD^{1/3}}{n^2}$ to represent backwater effects upon the filling mechanism

that a similar combination of L/D , $D^{1/3}/n^2$ and S to represent (referring again to the writer's observations on the filling phenomena in longer and larger barrels than used by the authors) the two fluid phenomena of air-carrying vortices and the complex air entrainment process of types B, 2, and 3 filling is also valid. That is, there appear to be three basic physical phenomena controlling the five distinct filling mechanisms over the range of slopes tested by the writer. These involve (a) strictly backwater effects, (b) vortex action over the inlet supplying air to the culvert barrel, and (c) a violent air entrainment process near the inlet accompanied by a substantial adverse air pressure gradient over the free surface, and an energy dissipation process involving the transport of air from a region of low pressure to a region of high pressure.

The authors in deriving equation (14) from equation (5), on the basis of tests with barrels appreciably shorter and smaller in diameter than the writer's, base their development of equation (14) on phenomenon (a) only. The validity of this development with reference to phenomena (b) and (c) would appear to constitute an important assumption requiring some justification.

The data of figure 13 would simply, regardless of the scaling characteristics of phenomena (b) and (c) that first, equation (14) requires an additional term representative of approach flow turbulence characteristics, and second that the data of figure 7 is applicable only to installations having approach flow turbulence characteristics similar to the authors' experimental channel.

The difficulty in establishing a model law for the square edge inlet without full consideration and control of turbulence level in the approach flow is illustrated by the data of figure 14, in which a portion of the authors' data of figure 7, together with the writer's data of figure 13 are plotted in accordance with the relation

$$\frac{H}{D} = f \left(\frac{L}{D} \frac{n^2}{D^{1/3}}, \frac{SD^{1/3}}{n^2} \right), \quad (26)$$

which follows directly, of course, from the authors' equation (14). In the case of the writer's data the value of $D^{1/3}/n^2$ used was 1.24×10^4 which was computed from a full flow, Darcy-Weisbach resistance coefficient determination of 0.0149 for the zone of established flow at a Reynolds number of 2.90×10^5 , which in the writer's tests corresponded to a value of $Q/D^{5/2}$ of 8. If it were assumed that the difference in test results between the two sets of data in figure 14 were due only to difference in turbulence level between the two channels it would follow that the turbulence level in the authors' channel was

lower than in the writer's. The difficulty in accepting this interpretation of the data of figure 14 stems from two facts. First, as noted in figure 13 the writer's tests with screens in the approach channel consisted of two series of data. In the first series, one double insect wire screen was used, and in the second series, two double insect wire screens were used. As indicated in figure 13 no consistent difference in results was noted between the two series of data and it is to be inferred that the turbulence level in the writer's tests with two double sets of screens was sufficiently low so that any further reduction in approach flow turbulence level would have no effect upon the filling mechanism, and hence that the difference in test results is not attributable to the possibility of a lower turbulence level in the authors' channel than in the writer's.

This conclusion would appear to be further reinforced by the fact that the authors' gravel stilling baffle was located (as determined by scaling from figure 1) approximately 8 barrel diameters from the inlet while in the writer's setup the gravel baffle was located 16.4 diameters from the inlet, which from consideration of the work of Baines and Peterson¹⁰ with grids of high solidity ratio, would lead to the conclusion that perhaps the turbulence level in the authors' channel was higher than in the writer's, rather than the reverse.

However, the dangers of drawing general conclusions from the apparent conflict of the two sets of data in figure 14, plotted in accordance with equation (26) (or equation 14) are obvious. First, the authors' tests are for a non-supported efflux jet, while in the writer's tests an apron support was used. Secondly, the writer's data were obtained with a headwall $1.33D$ high with modeled spill cones and with a modeled embankment slope, while in the authors' tests, referring to the data of figure 7, spill cones were not used and the headwall was the full depth of the water in the upstream pool, without any modeled embankment slope. Third, the method used by the authors in determining $n^2/D^{1/3}$ is unknown. If the authors' determination was computed on the basis of including the pressure drop in the zone of flow establishment, their computed value will not, of course, be directly comparable to the writer's value for the zone of established flow.

It can only be concluded that further consideration of the problem is desirable.

The writer's comments have stemmed principally from the experimental data given in figure 13 on the effect of turbulence level on the filling or priming phenomena in a culvert barrel, larger in diameter and appreciably longer than any used by the authors. The purpose of these comments has been to further illustrate the complexity of a flow problem, which from its boundary geometry could be assumed to be simple.

10. An Investigation of Flow Through Screens, by W. D. Baines and E. G. Peterson, Transactions of the American Society of Civil Engineers, July 1951.

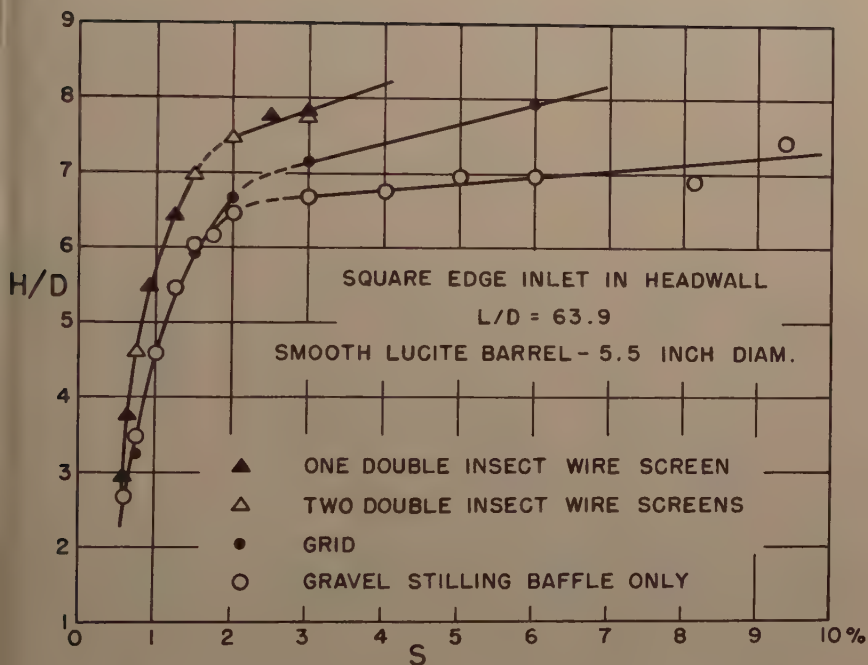


FIGURE 13

VALUES OF H/D PRODUCING REGIME CHANGE
FROM SLUICE TO FULL CONDUIT FLOW

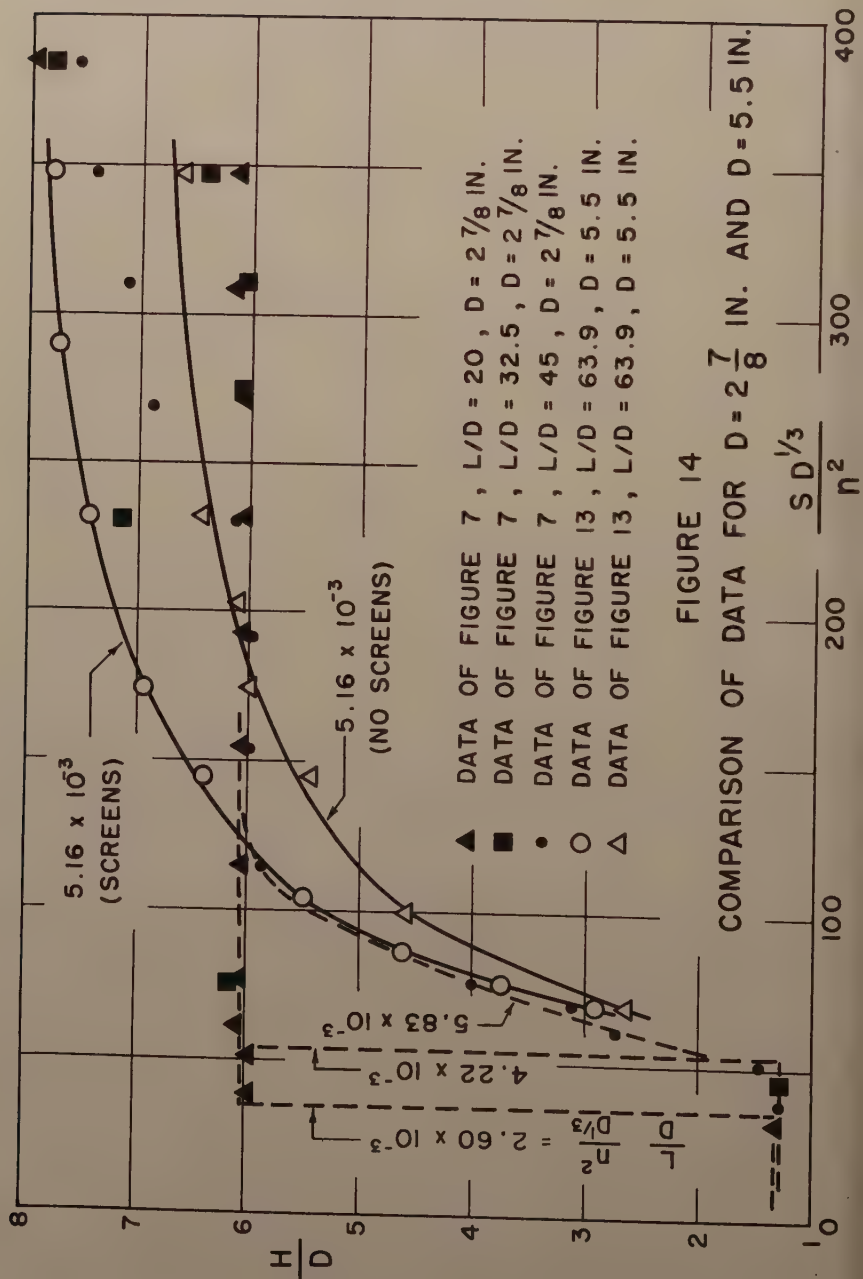


FIGURE 14

COMPARISON OF DATA FOR $D = 2 \frac{7}{8}$ IN. AND $D = 5.5$ IN.

Discussion of
 "PROPORTIONAL WEIRS FOR SEDIMENTATION TANKS"

by J. C. Stevens
 (Proc. Paper 1015)

GUIDO DI RICCO.¹—The problem considered by the author is part of the more general problem of finding the profile equation $x = f(y)$ for a weir, in which the discharge equation $Q = F(h)$ is given. This general problem is expressed by the equation

$$Q = c \sqrt{2g} \int_0^h (h - y)^{1/2} x \, dy \quad (1)$$

in which c is the discharge coefficient, either previously known or unknown, and is either a constant or a function of h .

Such a problem has been solved² and the following general formula was obtained:

$$x(y) = \frac{2}{\pi \sqrt{2g}} \frac{d}{dy} \int_0^h \frac{\frac{d}{dh} \frac{Q}{c}}{\sqrt{y - h}} \, dh \quad (2)$$

There were also shown² the particular derivations of known equations such as the Pratt formula for a linear or proportional weir (a formula established by Pratt in a different and rather complicated way, i.e., with a series expansion), the exponential-equation weir, and others.

In this manner, for example, for weirs with a given equation,

$$Q = c \sqrt{2g} a h^m \quad m > 1/2 ; c, a = \text{const.} \quad (3)$$

the following expression was obtained from (2):

$$x = \frac{m(2m + 1) \Gamma(m)}{\sqrt{\pi} \Gamma(m + 1/2)} a y^{m - 3/2} \quad (4)$$

from which one obtains, for $m = 1$, the proportional weir of Rother.

Moreover there also was derived from (2) the profile equation for a weir having a fixed percentage error for a fixed head; the "exponential" weir of Staus and Standen was thus derived.

¹ Prof. of Hydraulics, Univ. of Rome, Italy.

² G. Di Ricco—Equazione di forma di uno stramazzo dedotta dalla sua equazione di portata—L'Energia Elettrica, ottobre 1956.

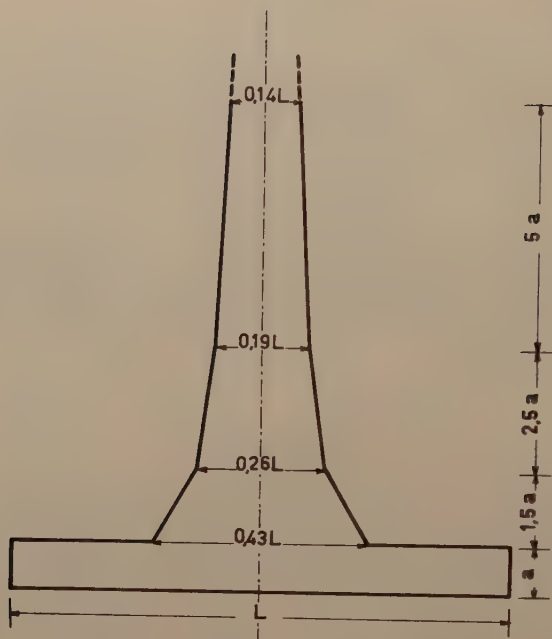


fig. 1



Fig. 2

It was also shown³ that one could determine the profile of a weir with a given discharge equation, where the dependence of the discharge coefficient on h head is unknown, by (2) and experimental tests. Practical examples were then solved. It appears as though such studies are unknown to the author inasmuch as no mention of them is made.

However, much more work does exist. Weir profiles with a polygonal contour which were easier to construct than those with a curvilinear contour were also considered. These weirs were analytically treated as the sum or difference of either triangular or rectangular notches, and the research was applied for the design of a semi-module for irrigation-flow measurements, similar to the cone module, but with a linear discharge equation.⁴

The weir under consideration was placed at the end of a rectangular flume with a horizontal bottom of width L and shape as shown in Fig. 1; its discharge equation for head ranging from $2a$ to $10a$ and for $\pm 2\%$ precision was expressed by

$$Q = 2L\sqrt{a}(h + \frac{5}{8}a) \quad (5)^5$$

Q in wm^3/sec ; L , a , and h in meters). This weir was also examined while submerged and its discharge equation which was a hyperbolic type⁶ was given.

The polygonal contour of weirs was applied to the design of a hydrometric device for flow measurements with linear discharge equation $Q = h - 1$; such a device is now being used at the Istituto di Idraulica dell'Università di Roma⁷ (Fig. 3).

Recently, the general problem considered herein has been treated in an easier way by the use of polygonal-profile weirs which could fit to any form of the discharge equation, given either analytically or graphically, upon heads in the arithmetic progression $a, 2a, 3a, \dots$; the value a represents the lower limit of validity of the equation.⁸

That is, given the value of Q for $a, 2a, \dots, na$, and letting $Q_r = Q(ra)$, the profile of the weir is defined by the following width L_r at the variable level $r = ra$:

$$L_r = \sum_{i=0}^{r-1} b_i q_{r-i} + d_r L_0, \quad (6)$$

in which

1. G. Di Ricco—Stramazzi con data equazione di portata—L'Energia Elettrica, febbraio 1939.
2. G. Di Ricco—Edificio di misura ad equazione di portata lineare—Rivista del Catasto, 1940, n° 3 e 4.
3. For $L = 0,5$ meters and $a = 0,04$ m., (5) becomes $Q = 0,2 h + 0,005$.
4. G. Di Ricco—Edificio di misura ad equazione di portata lineare. Funzionamento sotto rigurgito—Rivista del Catasto, 1949, n° 1.
5. B. Gaddini—Costruzione di uno stramazzo ad equazione lineare di portata—Rivista del Catasto, 1951, n° 3.
6. G. Di Ricco—Stramazzi a contorno poligonale—Rivista del Catasto, 1954, n° 2.

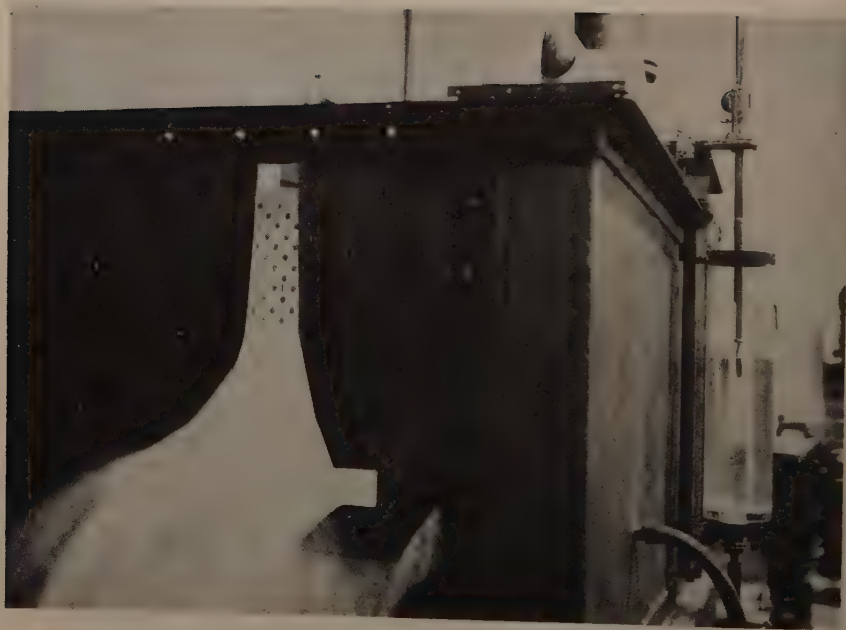


Fig. 3

$$q_r = \frac{15}{4 \sqrt{2g} a^{3/2}} \frac{Q_r}{d_r} \quad (7)$$

The values, b_r , d_r are tabulated in Table I.

Table I

| r | b_r | d_r | r | b_r | d_r |
|-----|-----------|-----------|-----|-------------|------------|
| 0 | 1,- | - | 6 | 150,8654 | 57,2270 |
| 1 | - 3,6569 | - 1,5000 | 7 | - 313,5023 | - 118,9206 |
| 2 | 8,0978 | 3,0711 | 8 | 651,4728 | 247,1334 |
| 3 | - 16,8034 | - 6,3771 | 9 | - 1353,7864 | - 513,5292 |
| 4 | 34,9397 | 13,2524 | 10 | - | 1067,1408 |
| 5 | - 72,5965 | - 27,5386 | | | |

If $c_r = c(ra)$ is either a known constant or a known function, the problem is immediately solved; if such is not the case, the profile must be found by a "trial and error" method, first assuming approximate values of c_r and testing these on the corresponding weir.

In (6) the value L_0 of the base width is arbitrary; such freedom is useful to give the weir an aesthetic shape.

Two examples of weirs, designed by use of the foregoing, are reported on herein.

The first concerns a cylindrical channel with a given trapezoidal cross-section and bottom slope where uniform flow is wanted, whatever the discharge may be.

The discharge equation was taken in the Bazin form (metrical system);

$$Q = \frac{87}{1 + \frac{0,85}{\sqrt{x}}} A \sqrt{rs}$$

The cross-section is shown in Fig. 4, where the discharge equation and the weir profile, too, are indicated.

The channel was 6 meters wide at the bottom, the slope of sides was 2 : 3. The average loss of head was $S = 0,0003$, c was assumed to be 0,6, and $a = 0,5$ meters.

The second example considers a weir suggested for model studies of the Tiber River. The discharge equation $Q(h)$ was numerically known (data of "Ripetta" Hydrometer in Roma), and it was assumed that $c = 0,6$ $a = 2$ meters.

Figs. 4 and 5 show the contours (to a distorted scale) of the two examples summarized herein. It should be noted that all measurements are in meters.

The computation of the last shown method is not difficult or impossible, regardless of the given equation, either $Q(h)$ or $V(h)$, and is resolved in a few minutes only by the use of Table I. This allows one to work with contours in number of 10 linear reaches for each side; usually, however, 4 or 5 reaches shall be sufficient, due to the allowance that the weir might not reproduce its equation at lowest heads.

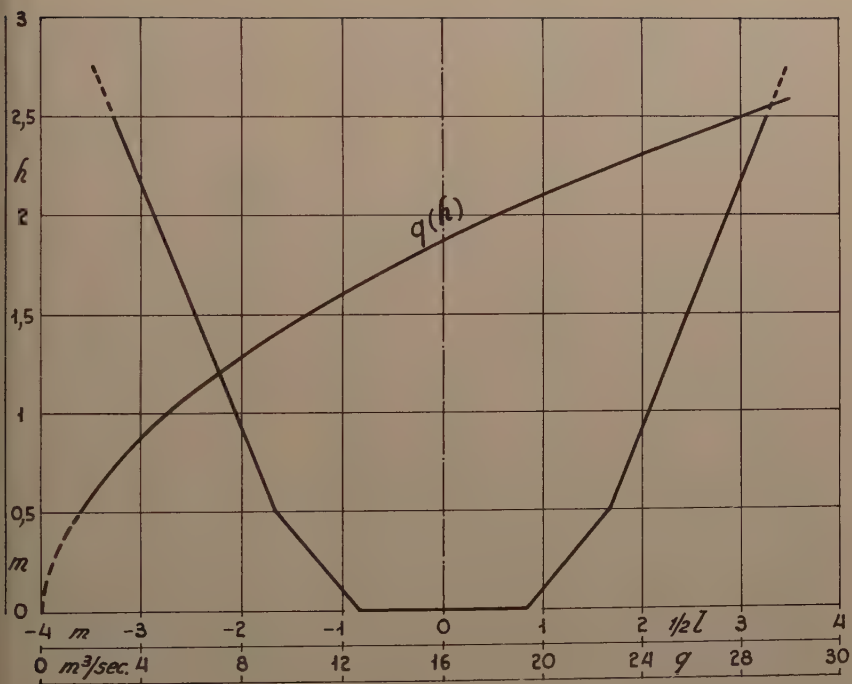


fig. 4

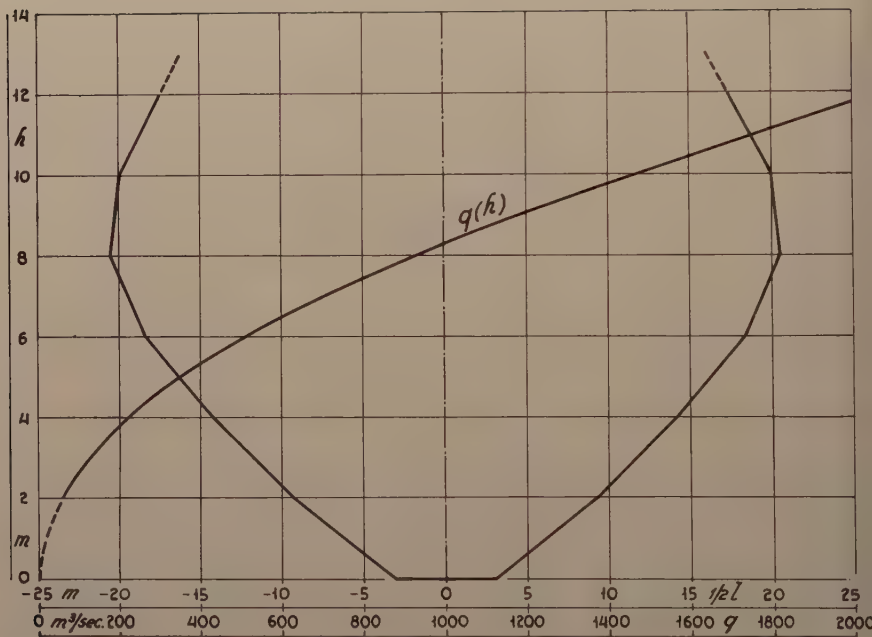


fig. 5

Discussion of
 "THE APPLICATION OF SEDIMENT-TRANSPORT
 MECHANICS TO STABLE-CHANNEL DESIGN"

by Emmett M. Laursen
 (Proc. Paper 1034)

SAM SHULITS,¹ M. ASCE.—Mr. Laursen summarizes compactly, carefully, completely and in an illuminating manner just how a hydraulic engineer should proceed to design a stable channel with the knowledge of today. At the same time his cogent comparison of available methods and formulas shows clearly and precisely the difficulties and uncertainties with which stable-channel design is beset.

In the last quarter-century, circa 1930 to the present, research in sediment-transportation has been increasingly active and inspired. Particularly true has this been in the United States in the last 10 to 15 years. It is then startling to be reminded by the author, first, that substitution of the velocity at the edge of the laminar sublayer (v_g) for the velocity at the level of the moving grain (v_g) is tantamount to the 1879 deduction of P. duBoys, that q_s is a function of τ ; and second, that transformation of the duBoys bed-load formula yields the 1926 permissible canal velocities of Fortier and Scobey. To many hydraulic engineers, it may be a strained application to apply at the open-channel bed the laminar sub-layer velocity equation based on smooth pipe experiments, whether or not the laminar sub-layer is actually existent. The only conclusion is that research in open-channel hydraulics and in sediment-transport still has not found, perhaps has not sought enough, the appropriate fundamental concepts of fluid mechanics. Until more particularized facts for open channels are available, one can only use, in the analytical process of fluid mechanics, what is on hand from the fields of aerodynamics and pipe turbulence. Unfortunately, the results are occasionally the old tools with new handles, at least in the two instances just cited.

Comparative studies of bed-load formulas have been made at the Hydraulics Laboratory of The Pennsylvania State University. One result from this work (reference A)* is presented in Table A, to illustrate the author's statement that the difficulties in stable-channel design lie in "assigning numerical values to coefficients and even in choosing a formal equation." In addition to the tabulated formulas, there exist today at least two more, the Meyer-Peter and Mueller formula (B) and a modified Einstein procedure (C,D). This jungle of formulas is so confusing that the engineer confronted with a sediment-transportation problem usually resorts to the choice of one or two of the most widely quoted in the publications crossing his desk, accompanied by gnawing uncertainties.

In the table X and Y are coefficients varying from formula to formula, and sometimes within one formula; T is the tractive force and T_0 the

¹ Associate Prof., Dept. of Civ. Eng., Pennsylvania State Univ., University Park, Pa.

* To avoid confusion in the reference numbering scheme, the writer's additions are marked A, B, C, etc.

BED-LOAD PER UNIT WIDTH (G_i)

$$\text{DUBOYS} \text{ _____ } X T (T - T_o) \\ \left(\begin{array}{l} \text{STRAUB} \\ \text{SCHAFFERNAK} \end{array} \right)$$

$$\text{CHANG} \text{ _____ } \frac{X_n}{10^2} T (T - T_o)$$

$$\text{USWES} \text{ _____ } \frac{X}{n} (T - T_o)^m$$

$$\text{CHYN} \text{ _____ } X V^m (T - T_o)$$

$$\text{SHIELDS} \text{ _____ } X \frac{q S}{d} (T - T_o)$$

$$\text{SCHOKLITSCH (OLD)} \text{ _____ } \frac{X}{d^{0.5}} S^{1.5} (q - q_o)$$

$$\text{SCHOKLITSCH (NEW)} \text{ _____ } X S^{1.5} (q - q_o)$$

$$\text{MAC DOUGALL} \text{ _____ } X S^m (q - q_o)$$

$$\text{CASEY} \text{ _____ } X S^m (q - q_o)$$

$$\text{GILBERT} \text{ _____ } X (q - q_o)$$

$$\text{FABRE} \text{ _____ } X S^{1.5} q - Y d$$

BED-LOAD PER UNIT WIDTH (G.)

$$\text{MEYER-PETER} \quad \left\{ \begin{array}{l} X(Sq^{0.67} - Y_d)^{1.5} \\ X S^{1.5} (q^{0.67} - q_o^{0.67})^{1.5} \end{array} \right.$$

$$\text{HAYWOOD} \quad X d^{1.5} m \left(\frac{S q^{0.67}}{d^{0.33}} - Y \right)^{1.5}$$

$$\text{NAKAYAMA} \quad (X + YS) q (V^2 - V_o^2)$$

$$\text{O'BRIEN} \quad X \left(\frac{V}{R^{0.33}} \right)^m$$

$$\text{EINSTEIN} \quad \frac{G_i}{\sigma_B g} \left(\frac{\sigma_F}{\sigma_B - \sigma_F} \right)^{0.5} \left(\frac{1}{g d^3} \right)^{0.5} = f \left(\frac{\sigma_B - \sigma_F}{\sigma_F} \right) \frac{d}{R^1 S}$$

$$\text{KALINSKE} \quad \frac{G_i}{d T^{0.5}} = X f \left(\frac{T_o}{T} \right)$$

inceptive or critical tractive force; n the Manning or Ganguillet and Kutter roughness coefficient; V the mean velocity and V_o the critical mean velocity; m an exponent varying from formula to formula; q the discharge and q_o the critical discharge, both per unit width; S the slope; d the grain diameter; R the hydraulic radius; γ_B and γ_F the densities of bed material and fluid (water), respectively while f is the mathematical symbol for "a function of."

Though Table A does incorporate an attempt to demonstrate similarities, these resemblances in no way imply even a similar range of quantitative results. Some of the formulas contain unsuspected sensitivities which vitiate simplifying assumptions. For example, a cursory glance at the Schoklitsch formula for the inceptive tractive force for sand (E),

$$q_o = 0.6 \frac{d^{3/2}}{S^{7/6}}$$

might lead to the conjecture that the $7/6$ power of S is an exaggerated refinement—that is, that the 1st power might be an adequate approximation. Yet there is an appreciable difference between $S^{7/6}$ and S : at $S = 0.00001$, $S^{7/6} = 0.146S$ and at $S = 0.01$, $S^{7/6} = 0.464S$.

Even for those bed-load formulas where the basic data, usually from flume tests, cover the same range, the computed results may be one to two hundred percent or more apart. These remarks pertain particularly to the DuBoys-Straub, Waterways Experiment Station, Schoklitsch, Casey, Haywood and Meyer-Peter formulas in the comparisons made at the Pennsylvania State University. Though the occurrence of such disagreements is well-known, the array of formulas in the author's Tables I and II and the writer's Table A underlines the difficulties of the formula dilemma.

REFERENCES

- A. Shulits, Sam; Sims, C. D. Jr.; and Stull, D. J., "The Dilemma of Bed-Load Formulas," Paper presented at 36th Annual Meeting, Am. Geophys. Union, Washington, D. C., May 1956.
- B. Meyer-Peter, E. and Mueller, R., "Formulas for Bed-Load Transport," International Association for Hydraulic Structures Research, Report on the Second Meeting, Stockholm, 1948, p. 39-64.
- C. Colby, B. R. and Hembree, C. H., "Computations of Total Sediment Discharge, Niobrara River near Cody, Nebraska," U.S.G.S Water Supply Paper 1357, 1955.
- D. Schroeder, K. B. and Hembree, C. H., "Application of the Modified Einstein Procedure for Computation of Total Sediment Load," Trans. Am. Geophys. Union, vol. 37, No. 2, April 1956, p. 197-212.
- E. Schoklitsch, A., "Handbook des Wasserbaues," 2d Ed., 1950, vol. 1, p. 17; Springer-Verlag, Vienna.

PROCEEDINGS PAPERS

The technical papers published in the past year are identified by number below. Technical-division sponsorship is indicated by an abbreviation at the end of each Paper Number, the symbols referring to: Air Transport (AT), City Planning (CP), Construction (CO), Engineering Mechanics (EM), Highway (HW), Hydraulics (HY), Irrigation and Drainage (IR), Power (PO), Military Engineering (SA), Soil Mechanics and Foundations (SM), Structural (ST), Surveying and Mapping (SU), and Waterways and Harbors (WW) divisions. Papers sponsored by the Board of Education are identified by the symbols (BD). For titles and order coupons, refer to the appropriate issue of "Civil Engineering." Beginning with Volume 82 (January 1956) papers were published in Journals of the various Technical Divisions. To locate papers in the Journals, the symbols after the paper numbers are followed by a numeral designating the issue of a particular Journal in which the paper appeared. For example, Paper 1113 is identified as 1113 (HY6) which indicates that the paper is contained in issue 6 of the Journal of the Hydraulics Division.

VOLUME 82 (1956)

FEBRUARY: 879(CP1), 880(HY1), 881(HY1)^c, 882(HY1), 883(HY1), 884(IR1), 885(SA1), 886(CP1), 887(SA1), 888(SA1), 889(SA1), 890(SA1), 891(SA1), 892(SA1), 893(CP1), 894(CP1), 895(PO1), 896(PO1), 897(PO1), 898(PO1), 899(PO1), 900(PO1), 901(PO1), 902(AT1)^c, 903(IR1)^c, 904(PO1)^c, 905(SA1)^c.

MARCH: 906(WW1), 907(WW1), 908(WW1), 909(WW1), 910(WW1), 911(WW1), 912(WW1), 913(WW1)^c, 914(ST2), 915(ST2), 916(ST2), 917(ST2), 918(ST2), 919(ST2), 920(ST2), 921(SU1), 922(SU1), 923(SU1), 924(ST2)^c.

APRIL: 925(WW2), 926(WW2), 927(WW2), 928(SA2), 929(SA2), 930(SA2), 931(SA2), 932(SA2)^c, 933(SM2), 934(SM2), 935(WW2), 936(WW2), 937(WW2), 938(WW2), 939(WW2), 940(SM2), 941(SM2), 942(SM2)^c, 943(EM2), 944(EM2), 945(EM2), 946(EM2)^c, 947(PO2), 948(PO2), 949(PO2), 950(PO2), 951(PO2), 952(PO2)^c, 953(HY2), 954(HY2), 955(HY2)^c, 956(HY2), 957(HY2), 958(SA2), 959(PO2), 960(PO2).

MAY: 961(IR2), 962(IR2), 963(CP2), 964(CP2), 965(WW3), 966(WW3), 967(WW3), 968(WW3), 969(WW3), 970(ST3), 971(ST3), 972(ST3)^c, 973(ST3), 974(ST3), 975(WW3), 976(WW3), 977(IR2), 978(AT2), 979(AT2), 980(AT2), 981(IR2), 982(IR2)^c, 983(HW2), 984(HW2), 985(HW2)^c, 986(ST3), 987(AT2), 988(CP2), 989(AT2).

JUNE: 990(PO3), 991(PO3), 992(PO3), 993(PO3), 994(PO3), 995(PO3), 996(PO3), 997(PO3), 998(SA3), 999(SA3), 1000(SA3), 1001(SA3), 1002(SA3), 1003(SA3)^c, 1004(HY3), 1005(HY3), 1006(HY3), 1007(HY3), 1008(HY3), 1009(HY3), 1010(HY3)^c, 1011(PO3)^c, 1012(SA3), 1013(SA3), 1014(SA3), 1015(HY3), 1016(SA3), 1017(PO3), 1018(PO3).

JULY: 1019(ST4), 1020(ST4), 1021(ST4), 1022(ST4), 1023(ST4), 1024(ST4)^c, 1025(SM3), 1026(SM3), 1027(SM3), 1028(SM3)^c, 1029(EM3), 1030(EM3), 1031(EM3), 1032(EM3), 1033(EM3)^c.

AUGUST: 1034(HY4), 1035(HY4), 1036(HY4), 1037(HY4), 1038(HY4), 1039(HY4), 1040(HY4), 1041(HY4)^c, 1042(PO4), 1043(PO4), 1044(PO4), 1045(PO4), 1046(PO4)^c, 1047(SA4), 1048(SA4)^c, 1049(SA4), 1050(SA4), 1051(SA4), 1052(HY4), 1053(SA4).

SEPTEMBER: 1054(ST5), 1055(ST5), 1056(ST5), 1057(ST5), 1058(ST5), 1059(WW4), 1060(WW4), 1061(WW4), 1062(WW4), 1063(WW4), 1064(SU2), 1065(SU2), 1066(SU2)^c, 1067(ST5)^c, 1068(WW4)^c, 1069(WW4).

OCTOBER: 1070(EM4), 1071(EM4), 1072(EM4), 1073(EM4), 1074(HW3), 1075(HW3), 1076(HW3), 1077(HY5), 1078(SA5), 1079(SM4), 1080(SM4), 1081(SM4), 1082(HY5), 1083(SA5), 1084(SA5), 1085(SA5), 1086(PO5), 1087(SA5), 1088(SA5), 1089(SA5), 1090(HW3), 1091(EM4)^c, 1092(HY5)^c, 1093(HW3)^c, 1094(PO5)^c, 1095(SM4)^c.

NOVEMBER: 1096(ST6), 1097(ST6), 1098(ST6), 1099(ST6), 1100(ST6), 1101(ST6), 1102(IR3), 1103(IR3), 1104(IR3), 1105(IR3), 1106(ST6), 1107(ST6), 1108(ST6), 1109(AT3), 1110(AT3)^c, 1111(IR3)^c, 1112(ST6)^c.

DECEMBER: 1113(HY6), 1114(HY6), 1115(SA6), 1116(SA6), 1117(SU3), 1118(SU3), 1119(WW5), 1120(WW5), 1121(WW5), 1122(WW5), 1123(WW5), 1124(WW5)^c, 1125(BD1)^c, 1126(SA6), 1127(SA6), 1128(WW5), 1129(SA6)^c, 1130(PO6)^c, 1131(HY6)^c, 1132(PO6), 1133(PO6), 1134(PO6), 1135(BD1).

VOLUME 83 (1957)

JANUARY: 1136(CP1), 1137(CP1), 1138(EM1), 1139(EM1), 1140(EM1), 1141(EM1), 1142(SM1), 1143(SM1), 1144(SM1), 1145(SM1), 1146(ST1), 1147(ST1), 1148(ST1), 1149(ST1), 1150(ST1), 1151(ST1), 1152(CP1)^c, 1153(HW1), 1154(EM1)^c, 1155(SM1)^c, 1156(ST1)^c, 1157(EM1), 1158(EM1), 1159(SM1), 1160(SM1), 1161(SM1).

FEBRUARY: 1162(HY1), 1163(HY1), 1164(HY1), 1165(HY1), 1166(HY1), 1167(HY1), 1168(SA1), 1169(SA1), 1170(SA1), 1171(SA1), 1172(SA1), 1173(SA1), 1174(SA1), 1175(SA1), 1176(SA1), 1177(HY1)^c, 1178(SA1), 1179(SA1), 1180(SA1), 1181(SA1), 1182(PO1), 1183(PO1), 1184(PO1), 1185(PO1)^c.

Discussion of several papers, grouped by Divisions.

AMERICAN SOCIETY OF CIVIL ENGINEERS

OFFICERS FOR 1957

PRESIDENT

MASON GRAVES LOCKWOOD

VICE-PRESIDENTS

Term expires October, 1957:

FRANK A. MARSTON
GLENN W. HOLCOMB

Term expires October, 1958:

FRANCIS S. FRIEL
NORMAN R. MOORE

DIRECTORS

Term expires October, 1957:

JEWELL M. GARRELTS
FREDERICK H. PAULSON
GEORGE S. RICHARDSON
DON M. CORBETT
GRAHAM P. WILLOUGHBY
LAWRENCE A. ELSENER

Term expires October, 1958:

JOHN P. RILEY
CAREY H. BROWN
MASON C. PRICHARD
ROBERT H. SHERLOCK
R. ROBINSON ROWE
LOUIS E. RYDELL
CLARENCE L. ECKEL

Term expires October, 1959:

CLINTON D. HANOVER,
E. LELAND DURKEE
HOWARD F. PECKWORTH
FINLEY B. LAVERTY
WILLIAM J. HEDLEY
RANDLE B. ALEXANDER

PAST-PRESIDENTS

Members of the Board

WILLIAM R. GLIDDEN

ENOCH R. NEEDLE

EXECUTIVE SECRETARY

WILLIAM H. WISELY

TREASURER

CHARLES E. TROUT

ASSISTANT SECRETARY

E. L. CHANDLER

ASSISTANT TREASURER

CARLTON S. PROCTOR

PROCEEDINGS OF THE SOCIETY

HAROLD T. LARSEN

Manager of Technical Publications

PAUL A. PARISI

Editor of Technical Publications

DANIEL GOTTHELF

Asst. Editor of Technical Publications

COMMITTEE ON PUBLICATIONS

JEWELL M. GARRELTS, *Chairman*

HOWARD F. PECKWORTH, *Vice-Chairman*

E. LELAND DURKEE

R. ROBINSON ROWE

MASON C. PRICHARD

LOUIS E. RYDELL